**UNIVERSIDADE ESTADUAL DE
CAMPINAS
Instituto de Biologia**

LUCIANO PEREIRA

**EMBOLISMO EM PLANTAS: NOVAS TÉCNICAS DE MEDIÇÃO E A RELAÇÃO
COM A LIGNIFICAÇÃO DO XILEMA**

**PLANT EMBOLISM: NEW TECHNIQUES OF MEASUREMENT AND THE
RELATIONSHIP WITH THE XYLEM LIGNIFICATION**

**CAMPINAS
2016**

LUCIANO PEREIRA

EMBOLISMO EM PLANTAS: NOVAS TÉCNICAS DE MEDIÇÃO E A RELAÇÃO COM A LIGNIFICAÇÃO DO XILEMA

PLANT EMBOLISM: NEW TECHNIQUES OF MEASUREMENT AND THE RELATIONSHIP WITH THE XYLEM LIGNIFICATION

Tese apresentada ao Instituto de Biologia da Universidade Estadual de Campinas como parte dos requisitos para a obtenção do Título de Doutor em Biologia Vegetal.

Thesis presented to the Institute of Biology in partial fulfillment of the requirements for the degree of Doctor in the area of Plant Biology

ORIENTADOR: PROF. DR. PAULO MAZZAFERA

ESTE EXEMPLAR CORRESPONDE À VERSÃO FINAL DA TESE DEFENDIDA PELO ALUNO LUCIANO PEREIRA, E ORIENTADA PELO PROF. DR. PAULO MAZZAFERA

CAMPINAS
2016

COMISSÃO EXAMINADORA

Prof. Dr. Paulo Mazzafera

Prof. Dr. Emerson Alves da Silva

Prof. Dr. Gustavo Habermann

Prof. Dr. Fernando Roberto Martins

Prof. Dr. Rafael Vasconcelos Ribeiro

Os membros da Comissão Examinadora acima assinaram a Ata de Defesa, que se encontra no processo de vida acadêmica do aluno.

Agradecimentos

Aprendi que ciência se faz, obrigatoriamente, de forma coletiva. Tenho muito a agradecer:

À Unicamp, ao Instituto de Biologia e ao Departamento de Biologia Vegetal, que tem sido meu porto seguro há mais de 10 anos, como aluno, estagiário ou funcionário técnico.

Ao Prof. Paulo Mazzafera, que acreditou em ideias pouco sólidas e foi, e é, o maior incentivador empolgado de todos os projetos. Obrigado pela confiança e por me ensinar o que acredito ser o verdadeiro espírito da investigação científica.

Aos professores Rafael Vasconcelos Ribeiro e Rafael Silva Oliveira, sempre presentes para sanar minhas deficiências. Obrigado pelas inúmeras orientações, sempre solícitos e incentivarores. Obrigado Prof. Rafael Oliveira, por me apresentar e "militar" em favor dos nossos trabalhos junto aos pares internacionais.

Aos professores Steven Jansen e Brendan Choat, por confiarem o uso do Xylem Functional Traits database, para a elaboração do capítulo 3 e pela correção do manuscrito.

Ao Paulo Bittencourt, que foi um grande parceiro e co-autor das presentes e futuras ideias. Obrigado pela dedicação e disponibilidade, mesmo tendo que dividir seu tempo com os seus próprios trabalhos de tese.

À Fernanda Barros e Mauro Brum, que acreditaram e se dispuseram a realizar experimentos para fortalecer o método pneumático. Obrigado por ceder a experiência e tempo de vocês.

Aos amigos e parceiros Flávia Schimpl e Pedro Araújo, que prepararam o terreno para interessantes futuros trabalhos conjuntos relacionando lignina e embolia. Obrigado pela dedicação de vocês.

Ao amigo Eduardo Kyiota, pelas consultorias de química e tantos assuntos gerais que ajudaram a melhorar as ideias, e ao amigo Adilson Pereira, pelas análises dos bancos de dados de hidráulica e lignina. Ambos ajudaram muito a desenvolver o capítulo 3.

Ao amigo Felipe Tolentino, pelas várias revisões do inglês, sempre acompanhada de uma excelente aula.

Aos amigos do Lafimp, antigos e novos, incentivadores que tornaram os dias muito mais agradáveis: Adriana, Alexandra, Igor, Milton, Pedro, Adilson, Eduardo, Sarah, Laerte, Luana, Flávia, Mariana, Felipe, Rafaela, Vanessa, Nathalia, Daniela, Ilse, Juan, Dimitry, Tatiane, Uiara, Letícia e Caio. Muito obrigado por serem tão legais!

Aos amigos do Laboratório de Ecologia Funcional, sempre importunados com minhas visitas, mas sempre solícitos e parceiros: Mauro, Grazielle, Caroline, Patrícia, Paulo, Fernanda Barros, Fernanda Piccolo e André.

Aos amigos do Laboratório do Prof. Rafael Ribeiro, pela troca de ideias, constantes ou eventuais, e as diversas ajudas: Marcela, Fernanda, Melissa, Simone, Neidiquele, Paulo e José.

À toda minha família, tão importante em tudo.

À minha amada Adriana, tão presente e, juntamente com meu filho Lucas, fazem tudo valer a pena...

Resumo

A formação de bolhas - embolia - nos conduítes do xilema tem ganho crescente interesse científico, considerando sua importância nas estratégias de plantas na resistência à seca. No entanto, continua a ser desconhecida a forma como os componentes químicos das paredes dos conduítes estão relacionados com a resistência à embolia. A lignina, o segundo composto mais abundante nas plantas depois da celulose, é essencial para o transporte de água e deve ter algum papel na resistência à embolia. A essência do presente trabalho foi criar condições (estabelecer métodos) e apontar evidências de que o conteúdo e/ou tipos de lignina estão relacionados com a resistência à embolia. A estimativa correta da embolia tem sido um desafio, principalmente devido à alta tensão nos conduítes e às estruturas microscópicas ou nanoscópicas do sistema de transporte de água, além dos artefatos em que os métodos disponíveis estão propensos. Assim, nos capítulos 1 e 2 são apresentados novos métodos e aparatos para se estudar o sistema hidráulico de plantas, procurando principalmente eliminar os artefatos que os métodos disponíveis possuem. No capítulo 1: "A low cost apparatus for measuring the xylem hydraulic conductance in plants", publicado em Bragantia, foi descrita a montagem de um aparato e a sua calibração, bem como adaptações de baixo custo que tornam o equipamento acessível. O aparato permite medir a condutância em partes de raízes ou ramos, ou em todo o sistema, no caso de pequenas plantas ou mudas. O aparato também pode ser utilizado para se estimar embolia. No capítulo 2: "Plant pneumatics: stem air flow is related to embolism – new perspectives on methods in plant hydraulics", publicado em New Phytologist, nós descrevemos um novo método para se estimar embolia, baseado em medições de fluxo de ar de ramos inteiros. Para calcular a quantidade de ar que flui para fora do ramo, um vácuo é aplicado aos ramos cortados, que são submetidos à diferentes potenciais hídricos. Propusemos um novo método para se estimar embolia, que é simples, eficaz, rápido e barato e permite várias medições no mesmo ramo, abrindo novas possibilidades para se estudar hidráulica de plantas. No capítulo 3: "Is embolism resistance in plant xylem associated with quantity and characteristics of lignin?", nós sugerimos que há relação entre conteúdo de lignina na madeira e resistência ao embolismo. Para chegar a isto, reunimos dados de conteúdo total de lignina na madeira e potencial de água em que 50% da condutividade no xilema de 99 espécies. Essas análises indicam uma relação limítrofe entre a resistência à embolia e o conteúdo de lignina. Nossas conclusões são que espécies com baixo conteúdo de lignina parecem ser mais vulneráveis à embolia, ao passo que espécies com maior conteúdo demonstram grande variabilidade de resistência. A lignina pode desempenhar algum papel indireto na resistência à embolia, uma vez que o maior conteúdo total de lignina está relacionado com paredes celulares mais espessas. Discutimos também neste capítulo, funções de diferentes tipos de lignina, diferenciando gimnospermas e angiospermas, e o desempenho de plantas transgênicas (com teor de lignina modificado) e sua relação com a vulnerabilidade à embolia. Os aparatos e os métodos aqui descritos, além das análises dos dados de literatura, permitirão futuros estudos experimentais para confirmar os modelos sobre lignina e embolia aqui propostos.

Abstract

Embolism formation in the xylem conduits has gained increased interest, considering its importance on the strategies of drought resistance in plants. However, remains unknown how the chemical components of conduits wall are related to embolism resistance. The lignin, the second most abundant compound of the plants, is essential to water transport and must have some role in the embolism resistance. The main objective of the present work was to evaluate whether content and/or types of lignin are related to embolism resistance. However, the correct estimative o embolism has been a challenge, mainly due to the high tension in xylem conduits and the microscopic or nanoscopic structures of water transport system, and the available methods are prone to several artifacts. Thus, in the chapter 1 and 2 we developed apparatus and methods as alternatives to study plant hydraulics. In the chapter 1: "A low cost apparatus for measuring the xylem hydraulic conductance in plants" we described the assembling of an apparatus and its calibration, as well as low cost adaptations that make the equipment accessible. The apparatus allows measuring the conductance in parts of roots or shoots, or in the whole system, in the case of small plants or seedlings. The apparatus can also be used to estimate embolism formation. In the chapter 2: "Plant pneumatics: stem air flow is related to embolism – new perspectives on methods in plant hydraulics", we describe a new method for estimating estimate embolisms that is based on air flow measurements of entire branches. To calculate the amount of air flowing out of the branch, a vacuum was applied to the cut bases of branches under different water potentials. We proposed a new embolism-measurement method that is simple, effective, rapid, and inexpensive and allows several measurements on the same branch, opening new possibilities to study plant hydraulic. In the chapter 3: "Is embolism resistance in plant xylem associated with more, less, or different types of lignin?", we suggest, based on data available for lignin content and Ψ_{50} (the water potential when 50% of conductivity in the xylem is lost), a boundary relationship between embolism resistance and lignin content across various groups of seed plants. Species with low lignin content seem to be more vulnerable to embolism, whereas species with higher content show wide variability in embolism resistance. Lignin content may play some indirect role in the embolism resistance, since higher total lignin content is related to thicker cell walls. We also discuss several possible functions of lignin with different composition between gymnosperms and angiosperms and the performance of transgenic plants with modified lignin content and composition regarding vulnerability to embolism. The apparatus and methods here described and the analysis from literature data will allow further experimental studies to confirm the models of lignin and embolism here proposed.

SUMÁRIO

Introdução Geral

O transporte de água nas plantas ocorre por uma diferença de pressão da água, captada no solo, conduzida pelo xilema e evaporada para a atmosfera. Dessa forma ocorre um tensionamento da coluna de água, que é gerado pela evaporação nas câmaras estomáticas e transmitido para o xilema (Zimmermann, 1983). Embora existam forças de adesão-coesão que mantém as moléculas de água juntas no interior desta coluna, a tensão que é gerada pode sugar nanobolhas de ar para dentro dos conduítes do xilema, através de poros existentes entre esses conduítes. Essas nanobolhas podem ficar instáveis em certas condições e causar embolia, interrompendo o transporte de água (Schenk *et al.*, 2015). A formação de embolia reduz a capacidade de fornecimento de água para os tecidos da parte aérea, limitando a abertura dos estômatos e assim também a fotossíntese (Brodribb *et al.*, 2005; Brodribb & Holbrook, 2007).

Esforços consideráveis foram feitos na última década para se entender a condutividade hidráulica e a formação de embolia em plantas (Rockwell *et al.*, 2014), considerando que a capacidade de transporte e a vulnerabilidade ao embolismo provavelmente determinam a distribuição global de espécies de árvores (Kursar *et al.*, 2009; Poorter *et al.*, 2010; Blackman *et al.*, 2012, 2014; Gleason *et al.*, 2012). Na verdade, a disfunção hidráulica é a principal causa de mortalidade de árvores e há uma forte demanda conflitante entre crescimento, consumo de água e propriedades hidráulicas do xilema (Zhang & Cao, 2009; Smith & Sperry, 2014; Rowland *et al.*, 2015).

A existência de altas tensões no xilema dificulta a correta estimativa da embolia, já que para medir quase sempre é necessário a destruição do material, o que altera a tensão interna e o estado da água nos conduítes. Os métodos existentes são sujeitos ao "efeito do observador", ou seja, artefatos gerados pela necessária manipulação do material (Jansen *et al.*, 2015), o que tem gerado um número bastante grande de resultados contaminados por artefatos de técnica (Cochard *et al.*, 2013) . Por exemplo, bolhas podem ser dissolvidas na manipulação do ramo durante as medições ou ainda pode ocorrer o reenchimento dos conduítes passivamente pela pressão capilar (Cochard *et al.*, 2013). Há também uma subestimação da condutividade hidráulica por diferentes motivos, como a absorção passiva de água (Torres-Ruiz *et al.*, 2012), fluxos basais (Hacke *et al.*, 2015), a reativação de conduítes inativos (Sperry *et al.*, 2012) além de diferentes protocolos usados para remoção da embolia para se

obter a condutância máxima (Hietz *et al.*, 2008). O comprimento do segmento de ramo também pode afetar as medições, devido à resistência dos poros (Cochard *et al.*, 2013).

Dentro desse contexto, para o início de nossos estudos foi necessário o domínio dos métodos para se induzir embolia e de aparatos hidráulicos para medí-los o mais corretamente possível. Como principal resultado dessa etapa inicial, nós desenvolvemos um aparato de baixo custo e de precisão, para a medição da condutância hidráulica e embolia, descrito no capítulo 1 (*A low cost apparatus for measuring the xylem hydraulic conductance in plants*) e já publicado (Pereira & Mazzafera, 2012). Posteriormente, devido a dificuldades encontradas com os métodos para se estimar embolia, nós desenvolvemos um método mais fácil, rápido e com menor manipulação do material vegetal, baseado em medições pneumáticas, que está detalhado no capítulo 2 (*Plant pneumatics: stem air flow is related to embolism – new perspectives on methods in plant hydraulics*) e já aceito para publicação (Pereira *et al.*, 2016). Esse método não apresenta os mesmos artefatos das medições hidráulicas, já que não é dependente de propriedades hidráulicas e sim pneumáticas, e também é pouco destrutivo, o que evita a modificação artificial da tensão do xilema, abrindo novas possibilidades de estudo.

Como visto, embora resistência à embolia seja fundamental para se compreender as respostas à limitação de água, as características que conferem maior ou menor resistência à embolia não estão totalmente esclarecidas, principalmente em relação a composição química da parede celular dos vasos do xilema. A lignina é o composto mais abundante das plantas depois da celulose (Donaldson, 2001) e sua presença coincide com a colonização do ambiente terrestre pelas plantas, possivelmente devido a papéis fundamentais no suporte mecânico e transporte de água (Niklas, 1992; Pittermann, 2010). A lignina quando extraída é hidrofóbica (Laschimke, 1989) e pouco resistente ao tracionamento, mas revestindo as microfibrilas de celulose confere maior rigidez à parede celular (Niklas, 1992). A tensão gerada no transporte de água pode atingir valores menores do que -10 MPa e gerar a implosão dos conduítes do xilema (Hacke *et al.*, 2001). Neste cenário, a lignina desempenha um papel importante evitando a implosão. A lignina também pode ter algum papel na resistência à embolia, já que confere impermeabilidade aos conduítes evitando, assim, a entrada de pequenas porções de ar que poderia resultar na formação de embolia (Zimmermann, 1983; Lens *et al.*, 2013). Corroborando com essa hipótese, alguns trabalhos já demonstraram que mutantes deficientes em lignina são mais vulneráveis ao embolismo (Coleman *et al.*, 2008; Voelker *et al.*, 2011; Awad *et al.*, 2012). Vários mutantes, com teor reduzido de lignina, demonstram fenótipo anão e uma capacidade deficiente para o transporte de água (Anterola & Lewis, 2002; Bonawitz *et al.*, 2014). Por outro lado, várias plantas com uma composição de lignina modificada não

apresentaram crescimento reduzido ou outros problemas funcionais aparentes (Bonawitz *et al.*, 2014; Wilkerson *et al.*, 2014; Wagner *et al.*, 2015), considerando, porém, que essas plantas ainda não tenham sido testadas em condições estressantes e que estudos funcionais apontam para papéis importantes e surpreendentes da lignina no transporte de água e resistência à embolia (Herbette *et al.*, 2014).

Aqui nosso principal objetivo foi avaliar se há relação entre o conteúdo, bem como tipo de lignina, e a resistência à embolia. Para isso nós utilizamos dados de literatura sobre composição química da madeira para avaliar possíveis relações entre o conteúdo de lignina e resistência à embolia em plantas. O resultados dessas análises, bem como uma discussão sobre os tipos de lignina e as possíveis consequências para as características hidráulicas das plantas, estão detalhados no capítulo 3 (*Is embolism resistance in plant xylem associated with more, less, or different types of lignin?*). Esse trabalho está em fase de preparação para publicação.

Referências

Anterola AM, Lewis NG. **2002**. Trends in lignin modification: a comprehensive analysis of the effects of genetic manipulations/mutations on lignification and vascular integrity. *Phytochemistry* **61**: 221–294.

Awad H, Herbette S, Brunel N, Tixier A, Pilate G, Cochard H, Badel E. **2012**. No trade-off between hydraulic and mechanical properties in several transgenic poplars modified for lignins metabolism. *Environmental and Experimental Botany* **77**: 185–195.

Blackman CJ, Brodribb TJ, Jordan GJ. **2012**. Leaf hydraulic vulnerability influences species' bioclimatic limits in a diverse group of woody angiosperms. *Oecologia* **168**: 1–10.

Blackman CJ, Gleason SM, Chang Y, Cook AM, Laws C, Westoby M. **2014**. Leaf hydraulic vulnerability to drought is linked to site water availability across a broad range of species and climates. *Annals of Botany* **114**: 435–440.

Bonawitz ND, Kim JI, Tobimatsu Y, Ciesielski PN, Anderson NA, Ximenes E, Maeda J, Ralph J, Donohoe BS, Ladisch M, *et al.* 2014. Disruption of Mediator rescues the stunted growth of a lignin-deficient Arabidopsis mutant. *Nature* **509**: 376–380.

Brodribb TJ, Holbrook NM. **2007**. Forced depression of leaf hydraulic conductance in situ: effects on the leaf gas exchange of forest trees. *Functional Ecology* **21**: 705–712.

Brodribb TJ, Holbrook NM, Zwieniecki MA, Palma B. **2005**. Leaf hydraulic capacity in ferns, conifers and angiosperms: impacts on photosynthetic maxima. *New Phytologist* **165**: 839–846.

Cochard H, Badel E, Herbette S, Delzon S, Choat B, Jansen S. **2013**. Methods for measuring plant vulnerability to cavitation: a critical review. *Journal of Experimental Botany* **64**: 4779–4791.

Coleman HD, Samuels AL, Guy RD, Mansfield SD. **2008**. Perturbed lignification impacts tree growth in hybrid poplar - A function of sink strength, vascular integrity, and photosynthetic assimilation. *Plant Physiology* **148**: 1229–1237.

Donaldson LA. **2001**. Lignification and lignin topochemistry - an ultrastructural view. *Phytochemistry* **57**: 859–873.

Gleason SM, Butler DW, Ziemińska K, Waryszak P, Westoby M. **2012**. Stem xylem conductivity is key to plant water balance across Australian angiosperm species. *Functional Ecology* **26**: 343–352.

Hacke UG, Sperry JS, Pockman WT, Davis SD, McCulloh KA. **2001**. Trends in wood density and structure are linked to prevention of xylem implosion by negative pressure. *Oecologia* **126**: 457–461.

Hacke UG, Venturas MD, MacKinnon ED, Jacobsen AL, Sperry JS, Pratt RB. **2015**. The standard centrifuge method accurately measures vulnerability curves of long-vesselled olive stems. *New Phytologist* **205**: 116–127.

Herbette S, Bouchet B, Brunel N, Bonnin E, Cochard H, Guillon F. **2014**. Immunolabelling of intervessel pits for polysaccharides and lignin helps in understanding their hydraulic properties in Populus tremula × alba. *Annals of Botany* **115**: 187–199.

Hietz P, Rosner S, Sorz J, Mayr S. **2008**. Comparison of methods to quantify loss of hydraulic conductivity in Norway spruce. *Annals of Forest Science* **65**.

Jansen S, Schuldt B, Choat B. **2015**. Current controversies and challenges in applying plant hydraulic techniques. *New Phytologist* **205**: 961–964.

Kursar TA, Engelbrecht BMJ, Burke A, Tyree MT, EI Omari B, Giraldo JP. **2009**. Tolerance to low leaf water status of tropical tree seedlings is related to drought performance and distribution. *Functional Ecology* **23**: 93–102.

Laschimke R. **1989**. Investigation of the wetting behaviour of natural lignin — a contribution to the cohesion of water transport in plants. *Thermochimica Acta* **151**: 35–56.

Lens F, Tixier A, Cochard H, Sperry JS, Jansen S, Herbette S. **2013**. Embolism resistance as a key mechanism to understand adaptive plant strategies. *Current Opinion in Plant Biology* **16**: 287–292.

Niklas K. **1992**. *Plant biomechanics: an engineering approach to plant form and function*. Chicago: University of Chicago Press.

Pereira L, Bittencourt P, Oliveira R, Monteiro-Junior M, Barros F, Ribeiro R, Mazzafera P. **2016**. Plant pneumatics: stem air flow is related to embolism – new perspectives on methods in plant hydraulics. *New Phytologist*.

Pereira L, Mazzafera P. **2012**. A low cost apparatus for measuring of xylem hydraulic conductance in plants. *Bragantia* **71**: 583–587.

Pittermann J. **2010**. The evolution of water transport in plants: an integrated approach. *Geobiology* **8**: 112–39.

Poorter L, McDonald I, Alarcón A, Fichtler E, Licona JC, Peña-Claros M, Sterck F, Villegas Z, Sass-Klaassen U. **2010**. The importance of wood traits and hydraulic conductance for the performance and life history strategies of 42 rainforest tree species. *New Phytologist* **185**: 481–492.

Rockwell FE, Wheeler JK, Holbrook NM. **2014**. Cavitation and its discontents: opportunities for resolving current controversies. *Plant Physiology* **164**: 1649–1660.

Rowland L, da Costa ACL, Galbraith DR, Oliveira RS, Binks OJ, Oliveira AAR, Pullen AM, Doughty CE, Metcalfe DB, Vasconcelos SS, *et al.* 2015. Death from drought in tropical forests is triggered by hydraulics not carbon starvation. *Nature*.

Schenk HJ, Steppe K, Jansen S. **2015**. Nanobubbles: a new paradigm for air-seeding in xylem. *Trends in Plant Science* **20**: 199–205.

Smith DD, Sperry JS. **2014**. Coordination between water transport capacity, biomass growth, metabolic scaling and species stature in co-occurring shrub and tree species. *Plant, Cell & Environment* **37**: 2679–2690.

Sperry JS, Christman MA, Torres-Ruiz JM, Taneda H, Smith DD. **2012**. Vulnerability curves by centrifugation: is there an open vessel artefact, and are 'r' shaped curves necessarily invalid? *Plant, Cell & Environment* **35**: 601–10.

Torres-Ruiz JM, Sperry JS, Fernández JE. **2012**. Improving xylem hydraulic conductivity measurements by correcting the error caused by passive water uptake. *Physiologia Plantarum* **146**: 129–135.

Voelker SL, Lachenbruch B, Meinzer FC, Kitin P, Strauss SH. **2011**. Transgenic poplars with reduced lignin show impaired xylem conductivity, growth efficiency and survival. *Plant, Cell and Environment* **34**: 655–68.

Wagner A, Tobimatsu Y, Phillips L, Flint H, Geddes B, Lu F, Ralph J. **2015**. Syringyl lignin production in conifers: Proof of concept in a Pine tracheary element system. *Proceedings of the National Academy of Sciences* **112**: 6218–6223.

Wilkerson CG, Mansfield SD, Lu F, Withers S, Park J-Y, Karlen SD, Gonzales-Vigil E,

Padmakshan D, Unda F, Rencoret J, *et al.* **2014**. Monolignol ferulate transferase introduces chemically labile linkages into the lignin backbone. *Science* **344**: 90–93.

Zhang JL, Cao KF. **2009**. Stem hydraulics mediates leaf water status, carbon gain, nutrient use efficiencies and plant growth rates across dipterocarp species. *Functional Ecology* **23**: 658–667.

Zimmermann MH. **1983**. *Xylem structure and the ascent of sap*. Springer-Verlag.

CAPÍTULO 1

Pereira, L, Mazzafera, P. 2012. **A low cost apparatus for measuring the xylem hydraulic conductance in plants.** Bragantia, 71 (4): 583-587.

Abstract

Plant yield and resistance to drought are directly related to the efficiency of the xylem hydraulic conductance and the ability of this system to avoid interrupting the flow of water. In this paper we described in detail the assembling of an apparatus proposed by TYREE et al. (2002) and its calibration, as well as low cost adaptations that make the equipment accessible for everyone working in this research area. The apparatus allows measuring the conductance in parts of roots or shoots (root ramifications or branches), or in the whole system, in the case of small plants or seedlings. The apparatus can also be used to measure the reduction of conductance by embolism of the xylem vessels. Data on the hydraulic conductance of eucalyptus seedlings obtained here and other reports in the literature confirm the applicability of the apparatus in physiological studies on the relationship between productivity and water stress.

Key words: water, conductivity, cavitation, embolism.

Um aparato de baixo custo para medição da condutância hidráulica do xilema em plantas

Resumo

A produtividade das plantas e a capacidade de resistência à seca estão diretamente relacionadas com a eficiência da condutância hidráulica do xilema e a capacidade desse sistema evitar a interrupção do fluxo de água. No presente trabalho detalhamos a montagem de um aparato proposto por TYREE et al. (2002) e sua calibração, bem como adaptações com peças de menor custo que tornam o aparelho acessível a qualquer um trabalhando nesta linha de pesquisa. Esse aparato possibilita medir a condutância de partes do sistema radicular ou da parte aérea (ramificações radiculares ou ramos), ou em todo o sistema, no caso de plantas de porte pequeno ou plântulas. O aparato também pode ser usado para medir a redução da condutância pela embolização dos vasos do xilema. Medições de condutância hidráulica feitas em plântulas de eucalipto e outros trabalhos encontrados na literatura confirmaram a aplicabilidade desse aparato em estudos fisiológicos de produtividade relacionada ao estresse hídrico.

Palavras chave: água, condutividade, cavitação, embolia.

The productivity of plants is directly related to the efficiency of their xylem conduit network to transport water and nutrients (BRODRIBB, 2009). However, for more efficient hydraulic conductance, carbon investments are required for the hydraulic system formation, which can reduce growth rates (MAHERALI et al., 2004). Moreover, the development of highly negative water potentials increases the probability of bubble formation in the xylem, which interrupts the flow through vessels and may reduce the rate of photosynthesis and, consequently, growth (TYREE and SPERRY, 1989). To avoid this problem, the hydraulic system can be more resistant to cavitation, and greater resistance is associated with lower porosity of the membrane between xylem vessels, which, in turn, reduces water flow efficiency (HACKE et al., 2006).

One basic attribute used to evaluate these complex relationships between efficiency and safety is the measurement of the hydraulic conductance (mmol s^{-1} MPa^{-1}) or conductivity (mmol m s^{-1} MPa^{-1}) of the xylem. A direct estimate of conductance can be obtained by measuring the flow of a solution through a segment of the plant, which is caused by a pressure difference (ΔP), from 3-10 kPa, between the "inlet" and "outlet" of the branch or root (SPERRY et al., 1988). This pressure difference can be applied using the height of the water column connected to the plant segment. The flow can be measured using a digital balance (accuracy of 0.1 mg) coupled to the outlet of the plant segment, measuring the mass of solution that emerges per second.

An apparatus for measuring the xylem hydraulic conductance of the entire shoot or root was proposed by KOLB et al. (1996), which uses a suction tube via a vacuum pump to generate ΔP. This vacuum tube applies suction to the entire shoot system with its various "outlets" (the leaves and branches cut), whereas the "inlet" (the trunk base) is connected to the solution arranged on a balance. Conversely, the flow direction is reversed for the roots, in which the radicular branches are suctioned as "outlets" and the "inlet" is the connection with the stem. Thus, this apparatus is inverted compared with the apparatus proposed by SPERRY et al. (1988), which considers the mass of the solution suctioned through the branch or root. The reverse flow, in relation to the flow in intact plant, has no effect on the conductance (SPERRY et al., 1988; KOLB et al., 1996).

To eliminate bubbles in the xylem, thus enabling the maximum conductance to be measured, KOLB et al. (1996) proposed a system connected to the apparatus by a three-way valve near the connection with the plant, consisting of a cylinder of compressed air that provides 100 to 175 kPa pressure on a bladder containing the solution used in the apparatus.

The air pressure on the bladder propels the solution through the plant vessels without allowing air to enter into the system. Using such relatively high pressure, this treatment eliminates xylem bubbles when applied for defined periods of time and pressures, previously tested for each plant organ and species.

The entire plant parts (whole root or shoot system, or root ramifications and branches) have a degree of conductance even without applying ΔP (KOLB et al., 1996). This requires that the mass suctioned under different ΔPs be measured to find the linear relationship between the mass and the pressure. The conductance at ΔP = zero is given by the point at which the line crosses the ordinate axis. The conductance is the slope of this line. Five or more partial vacuum tension between 0 and 70 kPa are applied.

The need to measure the conductance at a variety of vacuum tension increases the time required to acquire the measurements for each plant. When also considering the time required to stabilise the balance, each point on the curve can require 3-5 minutes, which makes experiment with use a large number of replicates or treatments unfeasible. To overcome this, TYREE et al. (2002) proposed the use of a Ultra-Low Flowmeter to decrease the time required for each measurement. By measuring the ΔP of a capillary tube using a pressure difference sensor, it is possible to estimate the flow, F, because the relationship between flow and ΔP of capillaries is calculated while calibrating the apparatus (see below the details of calibration). This sensor enables stable readings in only 4 seconds per point. The conductance is calculated as follows: k= $\Delta F/\Delta P$, where ΔF is the flow variation in relation to the variation of the vacuum pressure along the plant segment ΔP.

TYREE et al. (2002) recommend assembling the apparatus using eight-way valves (U-06473-12, Cole-Parmer). With these valves, it is possible to connect three capillaries with different sizes and internal diameters (ID), R1 = 0.13 mm ID (718765, Macherey-Nagel) by 28 cm long; R2 = 0.18 mm ID (718760, Macherey-Nagel) by 28 cm; R3 = 0.18 mm ID by 9.5 cm. These different capillaries enable the measurement of different ranges of flow. Pressure difference sensors (PX26-005DV, Omega Engineering) and a tube with an internal diameter greater than 1.5 mm are installed between the valves for rapid adjustments of the zero pressure (Figure 1).

These eight-way valves allow each of the individual components of the apparatus to be opened and closed, which facilitates switching among capillaries, making zero pressure adjustments without detaching the plant. There are also special adapters for fixing the capillary tubes and rubber seals that prevent air from entering into the system.

Figure 1 - Apparatus for measuring the hydraulic conductance of xylem. In the picture the Ultra-low Flowmeter (ULFM), the capillaries (R1, R2 and R3) and Pressure difference sensor (dP).
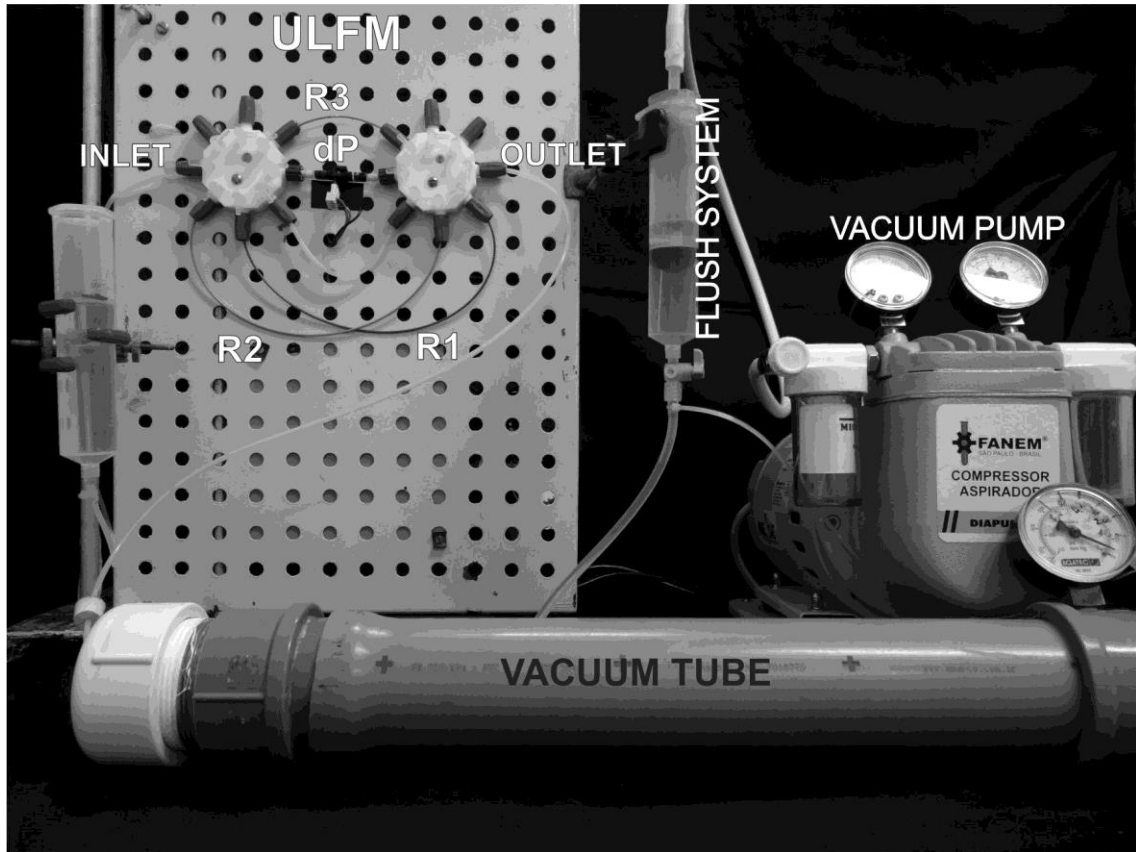
The differential pressure sensor can be connected to a datalogger to record the data (OM-CP-VOLT101A-160MV, Omega Engineering). An interface and specific software (OM-CP-IFC200, Omega Engineering) are also necessary to connect the apparatus directly to the computer, which allows real time readings.

The sensor requires between 10-16 volts to operate. Given that 5 mV V^{-1} in the sensor corresponds to 34.47 kPa, the software should be adjusted if the power is greater than 10 volts. If 12 V is used, 60 mV will return for 34.47 KPa. It is important the power source stability since the percentage of the voltage variation will be the percentage of the variation of the measurements, interfering in the apparatus precision.

TYREE et al. (2002) suggest a compression fitting (U-06473-07, Cole-Parmer) to connect the apparatus to the plant. Thus, the plant is placed within a tube with the outlet positioned towards the vacuum pump. The inlet and outlet of the apparatus are connected via stiff plastic tubing that is at least 1 mm in internal diameter.

The apparatus is calibrated using a digital balance (accuracy of 0.1 mg). Water, or any other solution, is placed in a vial on the balance and in contact with the inlet tube from the apparatus. The outlet tube from the apparatus is coupled to the vacuum pipe. The valves are opened only for the flow to pass through one of the capillaries. The vacuum pump is adjusted to a given pressure, and the mass suctioned in a given period is measured. The vacuum tension should be checked by a precision vacuum gauge during this phase of the calibration. Using the various ΔP measurements, it is possible to generate a linear relationship between mass and pressure for each capillary. For example, Figure 2 shows the calibration performed for our apparatus.

During the calibration and use of the apparatus, the levelness between the inlets, i.e., the level of the solution, and the outlet, where the plant is attached, should also be examined. A siphoning effect can occur with a ΔP of 1 kPa for each 0.1 m of height difference. The levelness can be checked by stabilising the balance or leaving the "bypass" tube open.

Although laborious, it is possible to assemble a less expensive apparatus. We estimate a cost of U$ 480.00 to mount this apparatus, versus U$ 1600.00 without the replacement of parts. Not including the pump pressure and the balance. To do so, we replaced the two eight-way valves with eight three-way valves (three-way stopcock, Embramed) commonly used in hospitals for intravenous therapy. These valves have a quick "luer-lok" connection, which enables sequential assembly (Figure 3).

Figure 2 – An example of the calibration performed for our "ultra-low" flowmeter for the three capillaries (R1 = 0.13 mm ID by 28 cm long; R2 = 0.18 mm ID by 28 cm; R3 = 0.18 mm ID by 9.5 cm) measured using a digital balance.
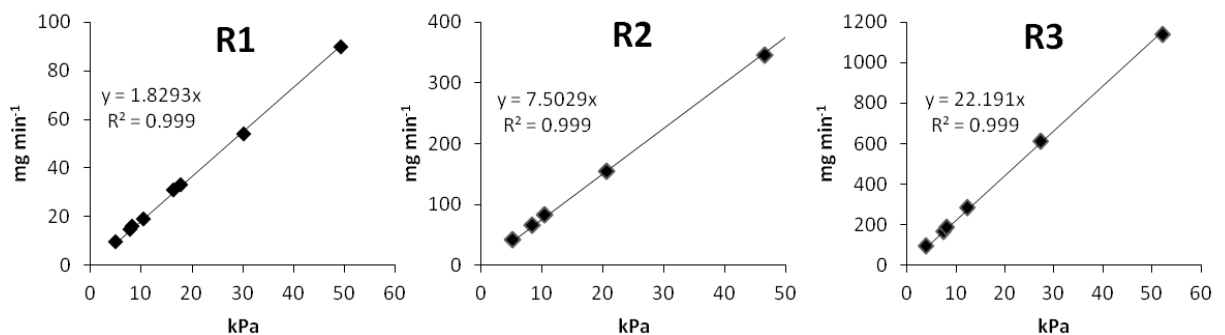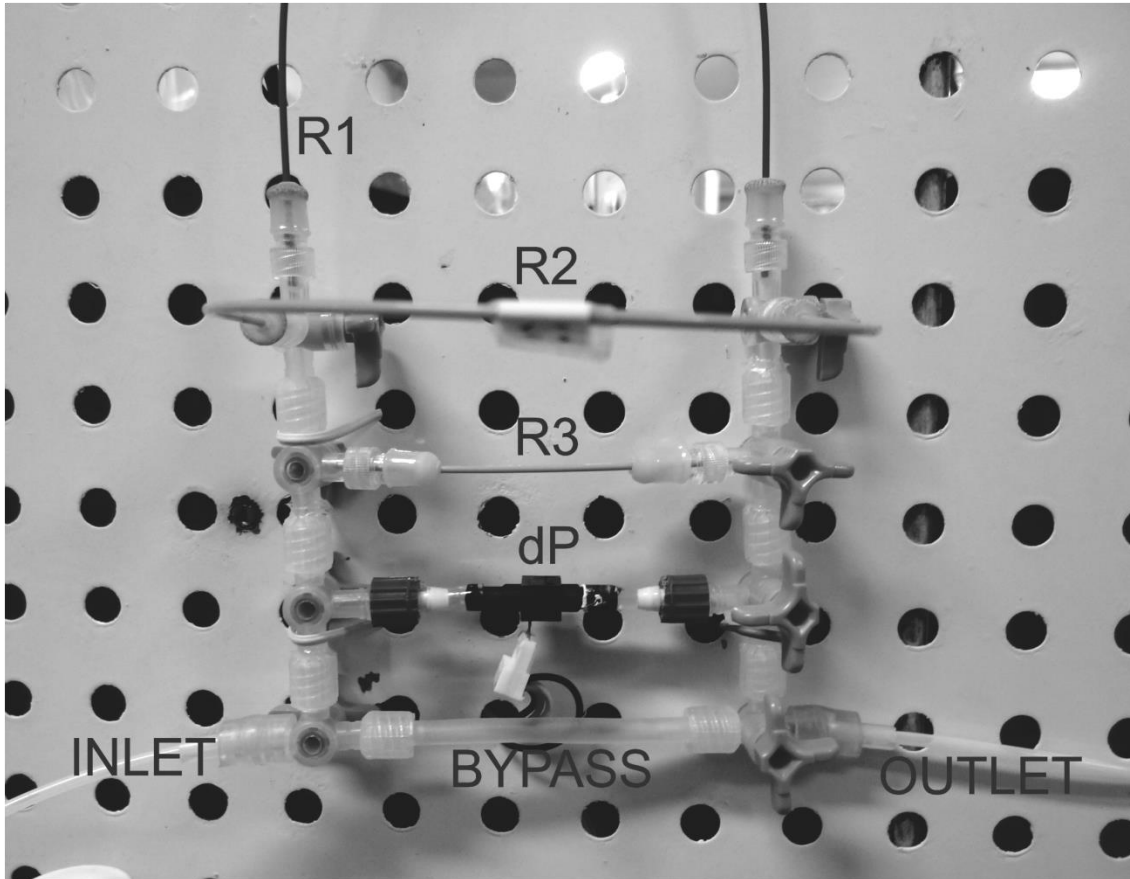
Figure 3 - Alternative assembly for an "ultra-low" flowmeter using valves with a quick "luer-lok" connection. In the picture the capillaries (R1, R2 and R3) and Pressure difference sensor (dP).

To connect the capillary tubes, we used "luer-lok" adapters with silicon stops, which are also used in hospitals for intermittent injections (385111, Becton Dickison Infusion Therapy Systems, Inc.). We filled these adapters with a silicone gel to ensure that they were sealed. The inlet, outlet and "bypass" (stiff tubing: 2.2-mm inside diameter [ID] and 3.1-mm outer diameter [OD]) tubes were connected using sections of flexible silicon tubing (3-mm ID and 5.2-mm OD).

To connect the apparatus to the plants, we used the same flexible silicone tubing described above, although the diameters of the seedlings used in our experiments were slightly larger than the tubing. To ensure a proper seal, we used sections of longitudinally matched silicone tubing (4.9-mm ID and 9.7-mm OD) and fasteners with removable plastic clamps (RZ-06832-02, Cole-Parmer). Depending on the size of the plants and type of clamp used to ensure a proper seal, tubing with different diameters can be adapted for use.

For the system to remove bubbles from the xylem, the compressed air cylinder and bladder compression system were replaced with a syringe coupled to an air compressor. The pressure was verified in the manometer of the air compressor (Figure 4).

The syringe plunger was cut to reduce its length and allow connection with air compressor (see detail in Figure 4). The 60 mL syringe barrel (309663, Becton Dickison Infusion Therapy Systems, Inc.) was connected to a tube coming from the air compressor enabling us to regulate the pressure on the solution to be injected into the plant. A three-way valve was connected to replenish the syringe with the solution as needed. This system was connected to the apparatus near the connection with the plant via another three-way valve.

The use of this apparatus and its conductance measurements enables us to compare the different characteristics of the plant with its hydraulic system. With few adaptations in the apparatus, the method with vacuum can be applied to measure the root conductance, stem and leaves, as shown by several authors (KOLB et al., 1996; SACK et al., 2002; TYREE et al., 2002; TYREE et al., 2003; KURSAR et al., 2009; MELCHER et al., 2012). We have also successfully used our assembled apparatus to determine the conductance in stems, roots and leaves of other species like coffee and citrus (unpublished data). As an example, we measured the conductance in *Eucalyptus* sp. (n=7, 120 days old seedlings, length 39 ± 4 cm), and regressed it against the leaf area (Figure 5). All leaves of each seedlings were cut in the petiole portion and measure of the total area was made with area meter (3100, Li-cor, Inc.). In this case the solution used was a 10 mM KCl, which was previously degasified and filtered in 0.22 µm filters.

Figure 4 – A simplified apparatus for applying the solution under pressure. The tubing is connected to an air compressor with a manometer to regulate the pressure. The picture shows the apparatus assembled for disconnected use of the flowmeter.

Figure 5 - Hydraulic conductance (K) relative to leaf area of *Eucalyptus* sp. seedlings.
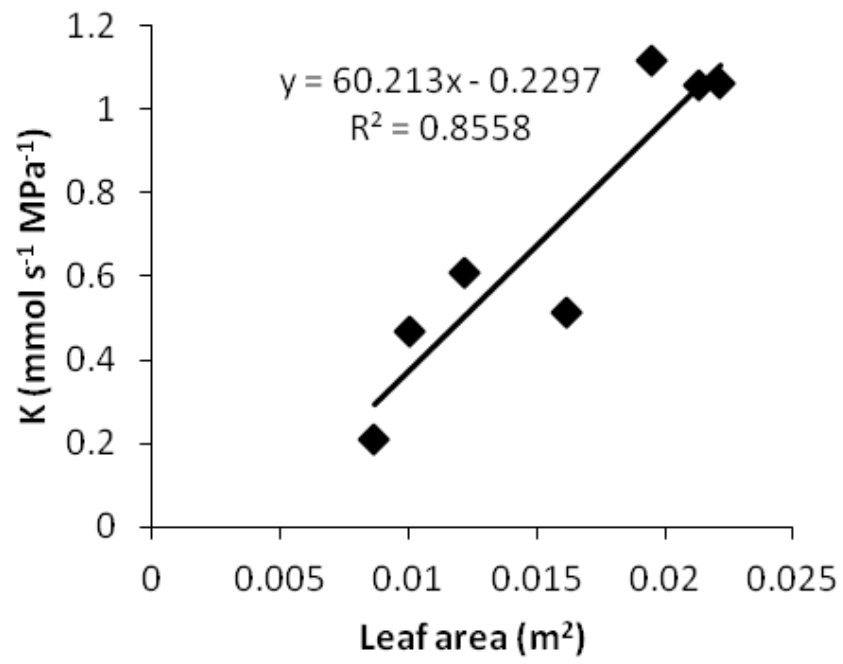
In another example, we evaluated the loss of conductance due to the cavitation of vessels. Cavitation resistance can be evaluated by comparing the conductance measurements of a desiccated plant at different water potentials in xylem and measurements after the treatment to remove bubbles from the xylem (SPERRY et al., 1988). The difference between the maximum conductance (after treatment) and conductance of the desiccated plant (initial) can be represented as the percentage loss of conductance. In Figure 6, we show the measurements in a *Eucalyptus* sp. plant that exhibited an approximately 60% loss of conductance under a leaf water potential of -2.5 MPa, measured with a pressure chamber (PMS 1000, PMS Instrument Company). We used a degasified and filtered 10 mM KCl solution.

Figure 6 - Flow rates at different vacuum pressures in *Eucalyptus* sp. seedling. The open symbols represent measurements at -2.5 MPa of plants dehydrated on the bench. The filled symbols represent measurements following the treatment to remove bubbles from the xylem. The conductance is calculated from the slope of the curves.
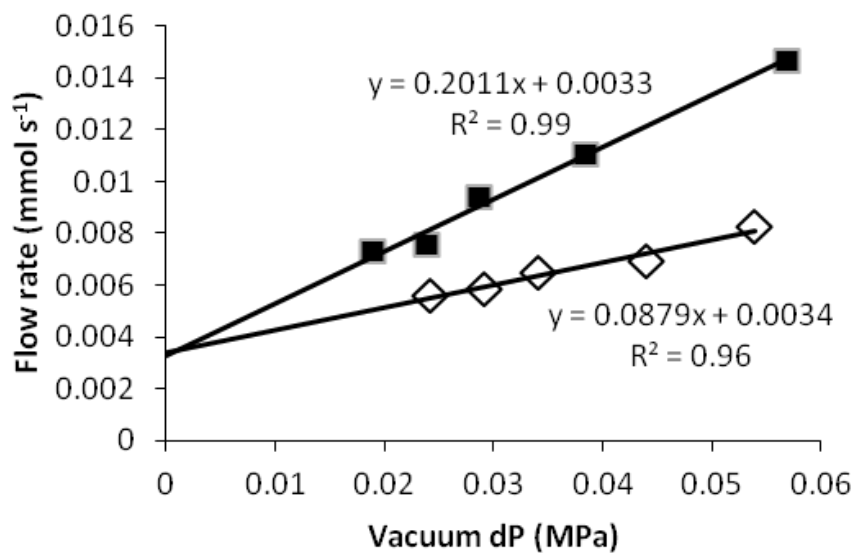
$y = 0.2011x + 0.0033$
$R^2 = 0.99$

$y = 0.0879x + 0.0034$
$R^2 = 0.96$

References

BRODRIBB, T.J. Xylem hydraulic physiology: The functional backbone of terrestrial plant productivity. **Plant Science**, v.177, p.245-251, 2009.

HACKE, U.G.; SPERRY, J.S.; WHEELER, J.K.; CASTRO, L. Scaling of angiosperm xylem structure with safety and efficiency. **Tree Physiology**, v.26, p.689-701, 2006.

KOLB, K.J.; SPERRY, J.S.; LAMONT, B.B. A method for measuring xylem hydraulic conductance and embolism in entire root and shoot systems. **Journal of Experimental Botany**, v.47, p.1805-1810, 1996.

KURSAR, T.A.; ENGELBRECHT, B.M.; BURKE, A.; TYREE, M.T.; EL OMARI, B.; GIRALDO, J.P. Tolerance to low leaf water status of tropical tree seedlings is related to drought performance and distribution. **Functional Ecology**, v.23, p.93-102, 2009.

MAHERALI, H.; POCKMAN, W.T.; JACKSON, R.B. Adaptive variation in the vulnerability of woody plants to xylem cavitation. **Ecology**, v.85, p.2184-2199, 2004.

MELCHER, P.J.; HOLBROOK, N.M.; BURNS, M.J.; ZWIENIECKI, M.A.; COBB, A.R.; BRODRIBB, T.J.; CHOAT, B.; SACK, L. Measurements of stem xylem hydraulic conductivity in the laboratory and field. **Methods in Ecology and Evolution,** v.3, p.685–694, 2012.

SACK, L.; MELCHER, P.J.; ZWIENIECKI, M.A.; HOLBROOK, N.M. The hydraulic conductance of the angiosperm leaf lamina: a comparison of three measurement methods. **Journal of Experimental Botany**, v.53, p.2177-2184, 2002.

SPERRY, J.S.; DONNELLY, J.R.; TYREE, M.T. A method for measuring hydraulic conductivity and embolism in xylem. **Plant, Cell and Environment**, v.11, p.35-40, 1988.

TYREE, M.T.; SPERRY, J.S. Vulnerability of xylem to cavitation and embolism. **Annual Review of Plant Physiology and Plant Molecular Biology**, v.40, p.19-38, 1989.

TYREE, M.T.; VARGAS, G.; ENGELBRECHT, B.M.J.; KURSAR, T.A. Drought until death do us part: a case study of the desiccation-tolerance of a tropical moist forest seedling-tree, *Licania platypus* (Hemsl.) Fritsch. **Journal of Experimental Botany**, v.53, p.2239-2247, 2002.

TYREE, M.T.; ENGELBRECHT, B.M.J.; VARGAS, G.; KURSAR, T.A. Desiccation tolerance of five tropical seedlings in Panama. Relationship to a field assessment of drought performance. **Plant Physiology**, v.132, p.1439-1447, 2003.

CAPÍTULO 2

Pereira, L, Bittencourt, PRL, Oliveira, RS, Monteiro-Junior, MB, Barros, FV, Ribeiro, RV and Mazzafera, P. 2016. **Plant pneumatics: stem air flow is related to embolism – new perspectives on methods in plant hydraulics**. New Phytologist. *Online first.*

Summary

- Wood contains a large amount of air, even in functional xylem. Air embolisms in the xylem affects water transport and can determine plant growth and survival. Embolisms are usually estimated with laborious hydraulic methods, which can be prone to several artefacts.
- Here, we describe a new method for estimating estimate embolisms that is based on air flow measurements of entire branches. To calculate the amount of air flowing out of the branch, a vacuum was applied to the cut bases of branches under different water potentials.
- We first investigated the source of air by determining whether it came from inside or outside the branch. Second, we compared embolism curves according to air flow or hydraulic measurements in fifteen vessel- and tracheid-bearing species to test the hypothesis that the air flow is related to embolism.
- Air flow came almost exclusively from air inside the branch during the 2.5 min of measurements and was strongly related to embolism. We propose a new embolism-measurement method that is simple, effective, rapid, and inexpensive and allows several measurements on the same branch, opening new possibilities to study plant hydraulic.

Keywords: Cavitation, drought, plant hydraulics, water transport, xylem

Introduction

Plants supply water to their tissues by a complex mechanism. The evaporative force at the water-air interface generates tension in the water column of the plant-soil continuum (Zimmermann, 1983). While adhesion-cohesion forces hold water molecules together inside this column, the tension that is generated at evaporative sites forces water to a metastable state in which air bubbles can be pulled inside the vessel through pores in the pit membrane. These nanobubbles might become unstable under certain conditions and cause embolisms, which disrupt water transport (Schenk et al., 2015). Embolism formation reduces the capacity of plants to supply water to aboveground tissues, limiting stomata opening and thereby limiting photosynthesis and all energy-requiring processes over the long term (Brodribb et al., 2005; Brodribb & Holbrook, 2007). This embolism formation is dependent on xylem negative pressure and on the hydraulic architecture of the given plant species (Cruiziat et al., 2002).

Considerable efforts have been made over the last decade to understand hydraulic conductance and embolism formation in plants (Rockwell et al., 2014). Water transport ability and embolism sensitivity likely determine the global distribution of tree species (Kursar et al., 2009; Poorter et al., 2010; Blackman et al., 2012, 2014; Gleason et al., 2012). In fact, hydraulic dysfunction is the major cause of tree mortality, and there is a strong trade-off between growth, water consumption and xylem hydraulic properties (Zhang & Cao, 2009; Smith & Sperry, 2014; Rowland et al., 2015).

The relation between embolism formation and xylem pressure can be described by the vulnerability curve (VC), which relates changes in hydraulic conductance to changes in the xylem water potential. According to most methods, the VC is created by inducing embolism in a branch or in another plant organ and then measuring the resulting hydraulic conductance (Cochard et al., 2013). The embolism is induced by leaving entire branches to dehydrate in the air (Sperry et al., 1988), by centrifugation (Alder et al., 1997) or by pressurizing the air in stem segments (Cochard et al., 1992). The stem hydraulic conductance (K) is commonly measured by applying a water pressure difference through a stem segment and then measuring the resulting water flow (Sperry et al., 1988). Embolisms are then typically quantified as a percentage loss of conductance (PLC), which is the ratio between the conductance of the embolized stem segment (K_{min}) and the conductance of the non-embolized stem segment (K_{max}).

The presence of air inside the xylem as a consequence of the embolisms is often overlooked. Although interesting studies on plant pneumatics had been performed in the past (e.g., MacDougal, 1932, 1936, Hook *et al.*, 1972), to our knowledge, very few studies have directly examined the air in the xylem by using several methods. Visualization methods such as classical anatomy, high-resolution magnetic resonance and X-ray microtomography have been used to quantify hydraulic conductance by counting the number of air- and water-filled vessels (Hacke & Sperry, 2001; Cochard *et al.*, 2015). The air-injection technique proposed by Ennajeh *et al.* (2011a) is based on air conductance and relates the PLC to the bubble production that is generated by air pressurization; the authors found that estimating the VCs based on quantifying the air conductance was more reliable than the original air pressurization method with hydraulic measurements. Franks *et al.* (1995) froze stem samples (20 mm) from *Eucalyptus camaldulensis* at different water potentials, measured the xylem air conductance in the frozen samples and then used the measurements to estimate their xylem water conductance and VCs. These authors proposed the use of air in frozen samples as a way to prevent some of the artefacts caused by conventional hydraulic methods.

While experimentally sucking air from a cut branch with a syringe, we noticed that the applied tension decreased after a period of time had passed. We questioned whether the air that was being sucked from the branch should be proportional to the air volume inside the branch and whether this air volume should be proportional to the embolism quantity inside the plant. A direct, though not necessarily linear relation between the air volume inside the plant and the plant conductance is expected because both the vessel conductance and embolized vessel volume are functions of the vessel length and diameter. Assuming a branch segment with n vessels of equal length L (m), diameter D (m) and e embolized vessels, the branch segment conductance K (kg MPa^{-1} s^{-1})equals the sum of each remaining vessel conductance K_i as follows (Tyree & Ewers, 1991):

$$K = \sum K_i = (n\text{-}e)Ki = (n\text{-}e)\alpha D^4 L^{-1} \qquad\qquad (1)$$

where α is a constant related to the water dynamic viscosity and density (kg s m^{-3} MPa^{-1}) and the vessel morphology and chemistry according to Poiseuille's law. In considering non-vessel air volume as negligible, the same segment air volume V will be the sum of each embolized vessel volume V_i as follows:

$$V = \sum V_i = eV_i = e\pi(0.5D)^2 L \qquad\qquad (2)$$

In this case, a clear relation between V and K can be expected, and the actual conductances could be calculated from the air volume (although pit membranes and non-vessel air volumes can cause this relation to become more complex). If we consider that the number of embolized vessels e is a function of the xylem water potential (Fig. 1a), then the percentage of V and K at a given water potential should be strongly related through e (Fig. 1b, continuous red line). Even if we consider V not only as a function of the number of embolized vessels but also of the air from non-vessel tissues, V and K should still be correlated, and the embolism formation signal should still be visible (Fig. 1b, dashed red lines).

Here, we studied the air dynamics of entire branches because we believe that this information can be useful for understanding the mechanisms of plant hydraulics and for developing new methods to study plant hydraulics. By measuring the air flow that comes out of branches when applying a vacuum to the cut base of the branches, we aimed to address the following questions.

(1) Where does the air that is leaving the branch come from? Can this air be used as an indicator of the branch air volume? We tested the following possibilities: (i) the air comes from air spaces inside the plant only; (ii) the air comes from outside the plant only; and (iii) the air comes from both inside and outside the plant. Independent of the air origin, the term "air flow" (AF) will be used throughout this text as the sum of its origins, i.e., air from inside and outside the branch.

(2) Can the plant air volume be used to estimate plant embolisms? We test the hypothesis that the branch air volume increases when the branch dries in proportion to embolism formation. We predict (i) that the AF increases when the xylem water potential of the branch decreases and (ii) that the AF is correlated to the PLC.

Based on our findings, we propose a pneumatic method for studying plant hydraulics, and this method is simple, effective, rapid, and inexpensive and opens new possibilities for understanding water and embolism dynamics in plants.

Fig. 1 Relation between the embolized vessels, hydraulic conductance, vessel plus non-vessel air volume (branch air volume; graph b) and xylem water potential (Ψ_x) of a branch segment with all vessels of the same length, diameter and with the same morphology and chemistry. If the non-vessel air volume is negligible (continuous line), then the relation between the branch air volume and the Ψ_x should correspond exactly to the relation between the hydraulic conductance and Ψ_x. When the non-vessel air is significant (dashed lines), then the air volume can still be used to predict Ψ_{50}. The Ψ_{88} can be predicted accurately for species with small amounts of non-vessel air or when this effect is discounted. a) Hydraulic conductance and embolized vessels as functions of the xylem water potential. b) Branch air volume as function of xylem water potential. Ψ_{50} and Ψ_{88} are the Ψ_x when hydraulic conductance is 50% and 88%, respectively. The percentage values are the relative amount of non-vessel air volume at $\Psi_x = -8$ MPa for each curve. The non-vessel air volume is considered here as a linear function of Ψ_x with different slopes for each curve. The circles and triangles are the Ψ_x values in which the branch air volume is 50% and 88% of the branch air volume at -8 MPa.
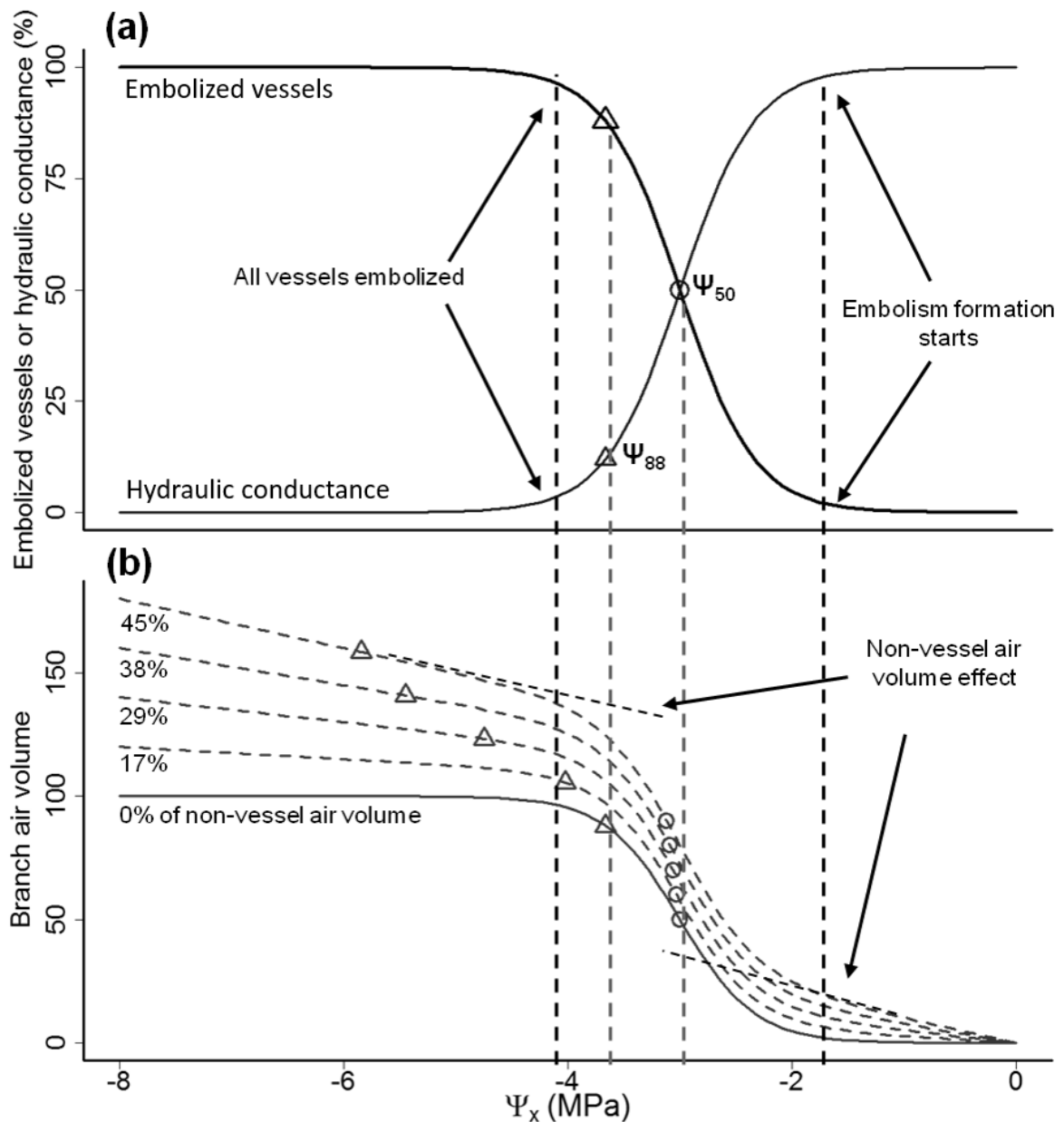
Materials and Methods

Pneumatic apparatus - The air (the correct term is gas, but we use "air" throughout the text because it is a more commonly used term in the literature) that was exiting the branch samples was estimated by monitoring pressure changes in a vacuum reservoir that was connected to the base of each branch (Fig. 2). The pressure changes were measured with a vacuum meter connected to the vacuum reservoir. A common syringe was used as the vacuum source. The syringe and vacuum meter were connected to the vacuum reservoir through a three-way stopcock. The branch sample was connected to the vacuum reservoir with a second three-way stopcock by a silicon tube and a plastic clamp. Plastic film and latex-based glue were used to improve the fitting and to avoid leakage through the branch connection. One exit from the second three-way stopcock was left empty and was used to apply atmospheric pressure to the apparatus. The vacuum was monitored with a millivoltmeter or a voltage logger with a precision of 0.01 kPa. Based on the detailed specifications of each component, the vacuum reservoir volume was 3.9 mL (Fig. 2), which allowed the apparatus to operate within the precision limits of the vacuum meter.

Air flow measurements - A pressure of 35–40 kPa was applied to the vacuum reservoir by pulling the syringe plunger, and then the syringe path was closed to the vacuum reservoir. To avoid possible misinterpretation, we will use the absolute vacuum as a reference throughout the text, i.e. -10 kPa is negative pressure and not vacuum pressure. The vacuum reservoir was then opened to the branch, and the initial pressure was measured (P_i, kPa). The discharged air from the branch to the vacuum reservoir lasted 2.5 min, and then the final pressure was measured in the vacuum reservoir (P_f, kPa; see Fig. 3). We defined 2.5 min as the discharge time because we wanted to evaluate a rapid method, and our initial tests showed that this period of time was sufficient for obtaining a good air flow signal. The increased in moles of air in the vacuum reservoir (Δn, mol) were calculated according to the ideal gas law as follows:

$$\Delta n = n_f - n_i = P_i V_r / RT - P_f V_r / RT \qquad\qquad (3)$$

where n_i (mol) is the number of moles of air in the vacuum reservoir before it was connected to the branch and n_f (mol) is the number after being connecting to the branch. R is the gas

constant (8.314 kPa L mol^{-1} K^{-1}), T is the temperature (the room temperature was maintained at 20º C by air conditioning), and V_r is the vacuum reservoir volume (L). We considered the ideal gas law to be valid because atmospheric air behaves essentially as an ideal gas under low pressure and room temperature (Barton, 2012). Even if the xylem concentrations of O_2, N_2 and CO_2 were different from the concentrations in atmospheric air, our assumption remains valid, because those gases behave in a ideal manner (MacDougal, 1936).

Fig. 2 Schematic representation of the apparatus for measuring air inside branches. The branch is connected to a section of silicone tubing [1] (3.0 mm ID and 5.2 mm OD or 4.9 mm ID and 9.7 mm OD), which is attached with plastic clamps (RZ-06832-02, Cole-Parmer, USA). Adapter luers (EW-30800-06, Cole-Parmer, USA) connect the branch to PVC tubing [2] (EW-30600-62, Cole-Parmer, USA) and then to a three-way stopcock [3] (EW-30600-04, Cole-Parmer, USA). A vacuum meter transducer (PX141-015V5V, Omega Engineering, USA) is connected to the three-way stopcock, and the output signal is detected with a voltage meter or a data logger. The vacuum is created with a syringe that is directly connected to the tube, as shown in the scheme. The vacuum reservoir (a 1 L Kitasato flask connected to a vacuum pump) may be used to produce a vacuum rapidly in the tubes. The scheme shows the stopcocks in the measurements positions, i.e., they are closed to the vacuum reservoir and open to the branch and vacuum meter.
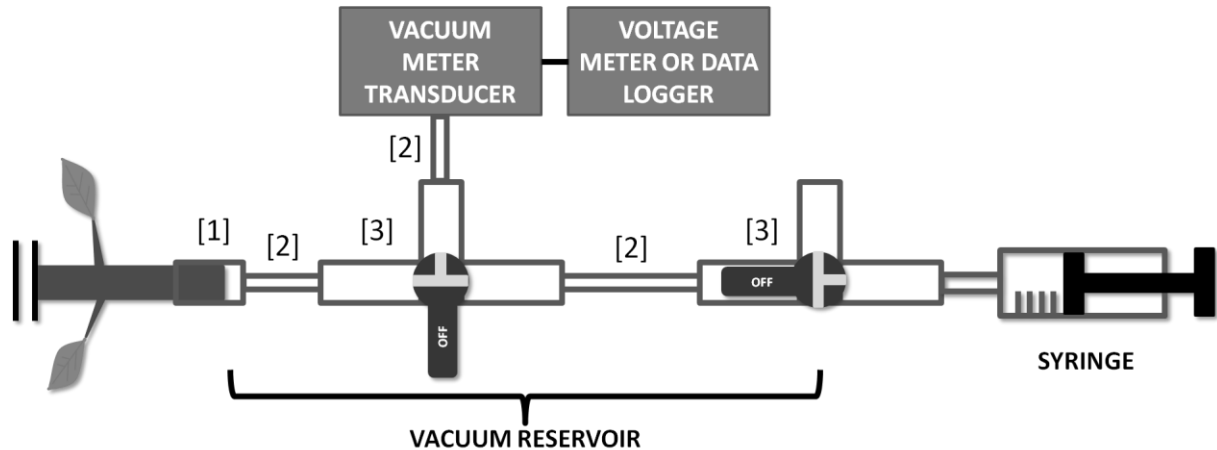
By transforming the Δn to an equivalent volume of air at atmospheric pressure (P_{atm}, 98 kPa at 700 m, the altitude of Campinas SP, Brazil), the total air flow out of the branch was calculated as the volume of air that was discharged into the vacuum reservoir (AD; μL) according to the ideal gas law as follows:

$$AD = (\Delta nRT/P_{atm})*10^6 \tag{4}$$

The leakage from the apparatus was much lower than the lowest amount of air that was discharged from the samples (Fig. 3). This air leakage was calculated as the air that was discharged from the vacuum reservoir by using a branch with a glue-sealed cut. To correct the AD, the leakage was subtracted from the AD (See Methods S1). The samples were open to the atmosphere when not subject to measurement to ensure that no vacuum remained inside the samples before beginning the next measurement. During the measurements, the samples were bagged to ensure that there was no transpiration or other changes in the xylem water potential.

The vacuum reservoir pressures were also measured at 15, 30, 60, 90 and 120 s to test possible variations over the 2.5 min measurements. The AD was calculated in the same manner as described above for each partial measurement, by considering either the cumulative AD (from 0 to 90 s, for example) or the AD at intervals (from 61 to 90 s, for example). To calculate the AD at intervals, the P_i was considered as the vacuum reservoir pressure at the beginning of the interval. The P_f, for cumulative and interval measurements, was defined as the vacuum reservoir pressure at the end of the cumulative or partial measurements. Unless stated, AD will refer to the full 2.5 min measurement (i.e. the cumulative AD from 0 to 150 s) throughout the text. We also evaluated the effects of the measuring time, as described in the Methods S1.

Xylem water potential - The leaves were bagged in black plastic bags for one hour before measurement to create equilibrium between the leaf and xylem water potential (Ψ_x). The leaf water potential was measured with a pressure chamber (PMS 1000; PMS Instruments Company, Albany, OR, USA) and was used as the Ψ_x of the sample. The leaf cuts were sealed with latex-based glue (seven leaves per branch, on average). The application of glue to the leaf cut was sufficient to prevent air leaks (Fig. 3).

Fig. 3 Pressure and air discharged from the vacuum reservoir during several air discharge measurements in a *E. camaldulensis* branch as an intact sample and after removing the basal, apical and all other leaves. Glue was applied at the leaf insertion position after removal. The grey line is the apparatus leakage with a glass bar instead of the branch. The black line is the leakage from the system when the branch sample is cut to 1–2 cm and sealed with glue. Ψ_x is the water potential of the branch. P_i and P_f are the initial and final pressures in the vacuum reservoir respectively. The atmospheric pressure was 98 kPa. Data were sampled every second.
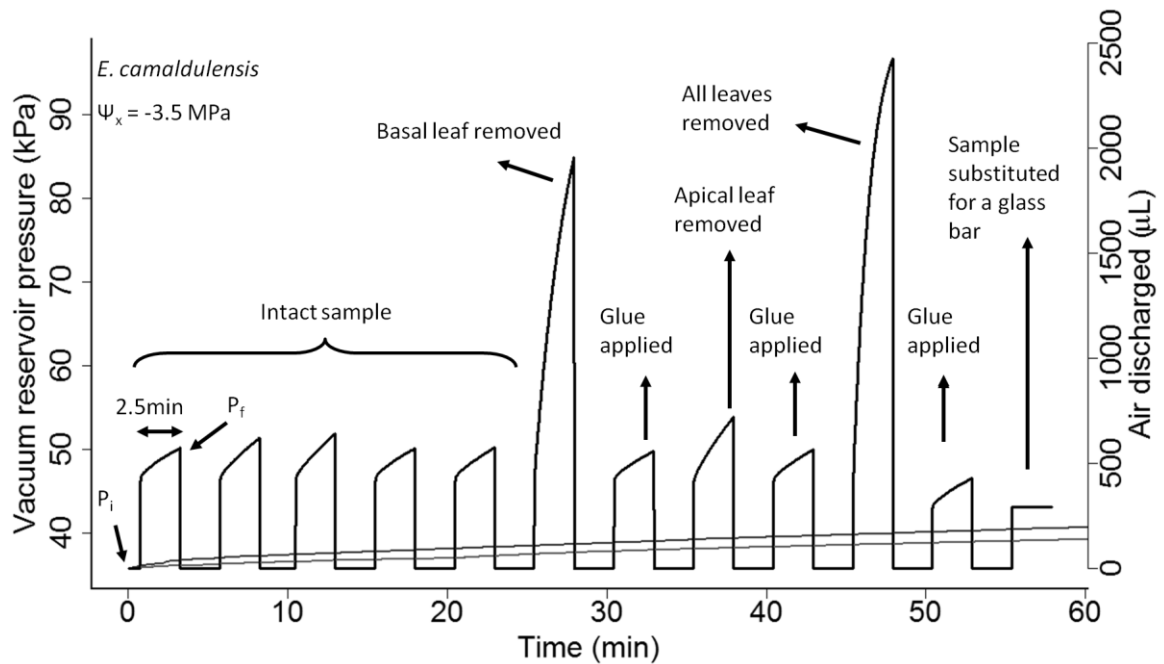
Plant material – branches from saplings and trees of 12 vessel-bearing species and three tracheid-bearing species (Table 1) were used to test the pneumatic method. The plant species and sampling description are detailed in the Methods S1.

Evaluation of air origin - To identify the origin of air for the AD measurements, entire branches (leaves and stems) from *E. camaldulensis* were connected to a chamber and the basal cut was connected to the vacuum reservoir of the pneumatic apparatus (Fig. 4). The chamber was made with a PVC tube (55 cm length $\times$ 6 cm diameter), which was connected to a vacuum meter and a vacuum pump. The chamber also had an aperture on one side in which the branch was placed and held by a rubber stopper and caulking mastic to prevent air leakage. The AD of each sample was then measured in two situations. Here, the AD is the absolute amount of air that is entering or exiting the vacuum reservoir within 2.5 min, depending on the situations described as follows:

(1) a normal gradient (NG), with atmospheric pressure (98 kPa) inside the chamber and a vacuum (50 kPa) in the vacuum reservoir (Fig. 4c). In this situation we expected that the

air present inside and/or outside the plant would flow to the vacuum reservoir and increase the pressure. We believe that air from the outside could pass through the bark/leaves if the plant are not well sealed; and

(2) an inverse gradient (IG), with a vacuum (50 kPa) inside the chamber and atmospheric pressure (98 kPa) in the vacuum reservoir (Fig. 4a,b). In this situation the pressure should decrease (forming a vacuum in the vacuum reservoir) only if the bark/leaves are not sealed against the outside (Fig. 4b).

In both cases, the pressure gradient for the air flow was the same, but it moved in opposite directions. For each sample, the situation that was first applied was alternated, and the Ψ_x was also measured. The following hypotheses were evaluated, as described in the Methods S1:

(i) the plants are sealed against the air from outside, and then the pressure in the vacuum reservoir remains the same, i.e., the amount of air does not decrease inside the vacuum reservoir in the IG situation;

(ii) the plants are not sealed, and the air only comes from outside. In this case, the difference between the amount of air in the vacuum reservoir at NG and IG would be zero (Fig. 4b,c), i.e., the amount of air in the vacuum reservoir would increase in the NG and decrease in the IG, but in the same absolute quantity; and

(iii) the plants are not sealed against the outside air, and the air comes from both the inside and outside. If this hypothesis is true, then the difference between the amount of air in the vacuum reservoir for NG and IG would be greater than zero (Fig. 4b,c).

Fig. 4 Schematic representation of the apparatus used to evaluate the source of air in the branches and the possible air pathways. (a) A vacuum pump was used to apply a vacuum to the chamber, whereas the vacuum reservoir was maintained at atmospheric pressure [inverse gradient (IG)]. If the branches are sealed to outside air, then the pressure in the vacuum reservoir does not change. (b) Same treatment as in (a), but in this case, the branches are supposedly not sealed. (c) A vacuum was applied to the vacuum reservoir, and the chamber was maintained at atmospheric pressure [normal gradient (NG)]. Arrows represent the air pathway under each condition.
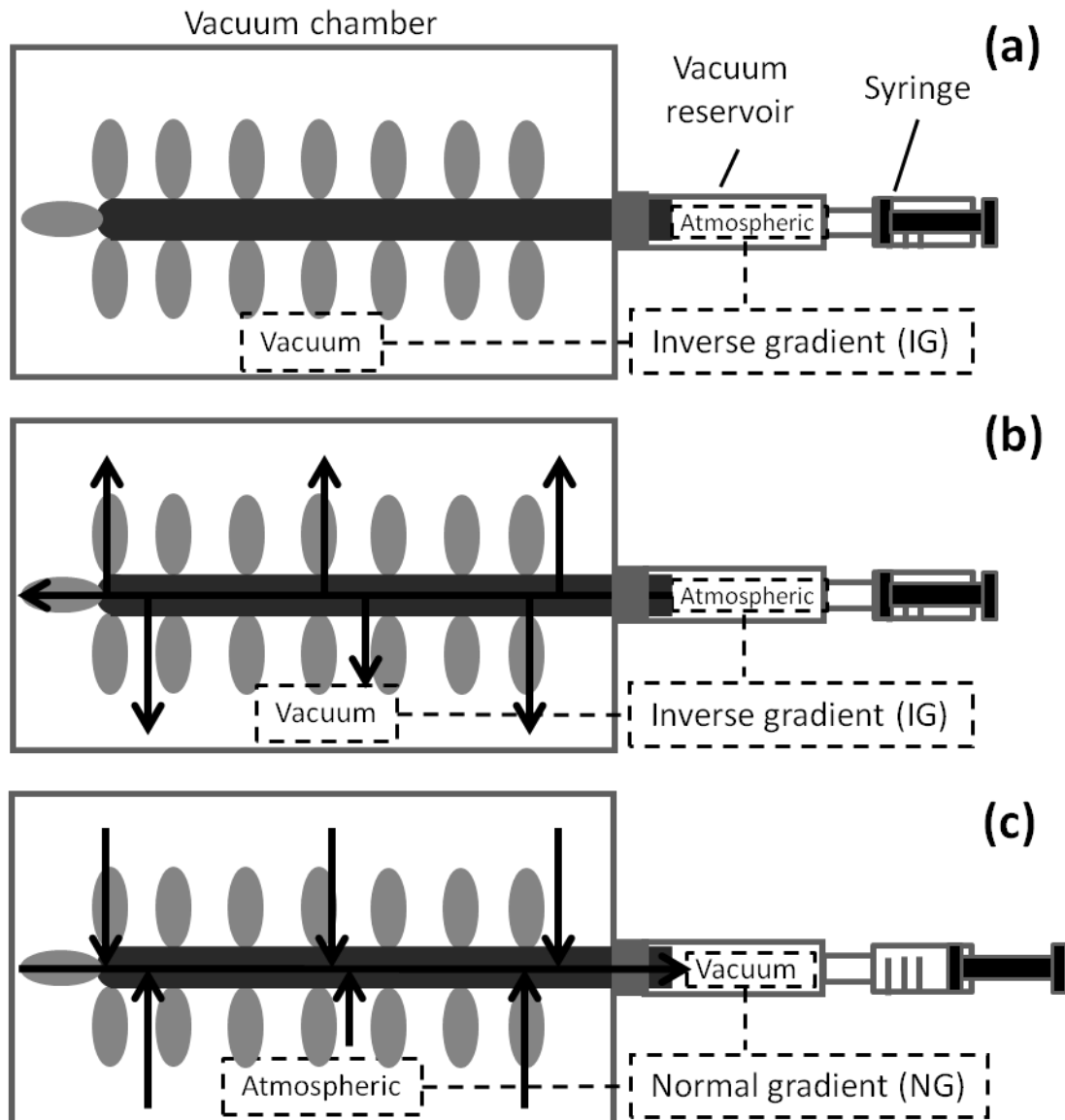
Air discharge (AD) and Ψ_x - The AD was measured in the same sample several times at different Ψ_x values. Four to seven branches from different well-watered individuals were used. An initial measurement was made with the well-hydrated branches, which were then dehydrated by bench dehydration method (Sperry *et al.*, 1988). The last measurement from each sample was recorded when the Ψ_x was lower than the maximum limit of the pressure chamber (-10 MPa) or when the branches had lost their leaves. In AD compared with Ψ_x curves, the AD data were first normalized so that the data from different samples from the same species could be pooled. The AD values were normalized by considering the AD values from well-watered and dehydrated measurements, which were transformed to percentages (PAD, percentage air discharged) according to the following equation:

$$PAD = 100*(AD - AD_{min})/(AD_{max} - AD_{min}) \tag{5}$$

where AD_{min} is the AD value that was obtained when the branch was well-hydrated (highest Ψ_x) and AD_{max} is the AD value that was obtained when the branch was the most dehydrated (lowest Ψ_x). *Erisma uncinatum* and *M. lepidota* did not have enough leaves on each branch to obtain maximum, minimum and intermediate values for the same sample. Because both species presented low intraspecific variability for a given Ψ_x and also had a low Ψ_{min} in relation to the Ψ_{max}, we normalized each sample by considering the AD_{max} of the species (and not the AD_{max} of each sample).Given that the PAD values ranged between 0 and 100, these values were fitted to the following logistic function that is commonly used in VC curves (Pammenter & Vander Willigen, 1998):

$$PAD = 100/(1 + \exp((S_p/25)(\Psi_x - \Psi_{50p})) \tag{6}$$

where Ψ_{50p} is the Ψ_x when PAD equals 50% and S_p (%PAD MPa^{-1}) is the slope of the curve. From this equation, the Ψ_x that was calculated for the PAD equal to 88% (Ψ_{88p}). The subscript annotation "p" (for pneumatic) was used with Ψ_{50p}, Ψ_{88p} and S_p to differentiate them from $\Psi_{50h,}$ Ψ_{88h} and S_h (h for hydraulic), or the Ψ_x that occurred when the plant lost 50% and 88% of its hydraulic conductance and the slope of the VC (%PLC MPa^{-1}), respectively. The goodness of fit for the logistic function in relation to a constant fitting that was equal to the mean (R^2, to differentiate it from linear regression r^2) was calculated as one minus the sum of squares for the residuals of the logistic fitting, divided by the sum of squares of the residuals for the constant fit.

Embolism vulnerability curves – The hydraulic vulnerability curves were estimated for ten species by the bench dehydration method (Sperry *et al.*, 1988), using an ultra-low flow meter as previously described by Pereira & Mazzafera (2012) [See Methods S1 for the detailed procedure]. The AD was then related to Ψ_x, embolisms and allometric relations, as described in the Methods S1.

Sample size and vessel length – Samples that were longer or shorter than the maximum vessel length may have had fewer or more open vessels, respectively. Given that the branches that were in contact with the air were used for AD measurements, we also evaluated whether the sample length affects the AD measurements and PAD curve fitting. In *S. terebinthifolius* trees, we measured the AD and water potential of branches that were shorter and longer (0.15 and 0.30 m long, respectively) than the maximum vessel length (0.25 m), which were measured by the air injection method (Zimmermann & Jeje, 1981) [see Methods S1 for sampling conditions], and the PAD curves for both branch lengths were compared. The data were analysed as described in the Methods S1.

Results

The AD values ranged from 3.74 µL in well-hydrated *C. sempervirens* to 2314.9 µL in dehydrated *M. lepidota* branches. When considering all the samples, the maximum and minimum average AD from all samples were 591.6 ± 525.1 µL and 120.8 ± 174.4 µL, respectively (Fig. S1). The air leakage that occurred when considering all measurements was 1.1 ± 0.4 µL per 2.5 minutes. The AD rate decreased exponentially during the measurement time (Fig. 5), and this pattern was consistent in all analysed species (data not shown). The maximum AD was not related to the sample length, diameter, volume, stem surface area or maximum vessel length ($p > 0.68$ for all correlations).

Fig. 5 Rate of total air discharge over 2.5 min (%AD s^{-1}) for all evaluations (610 AD measurements, 6 points for each AD measurement). The black line is the best fit for the non-linear regression of the exponential decay function $y = ax^{-1}$. The inset is the absolute (non-standardized by measurement) rate of AD (μL s^{-1}). a = 31.1 for the line in the main primary graph, and a = 77.0 in the inset.
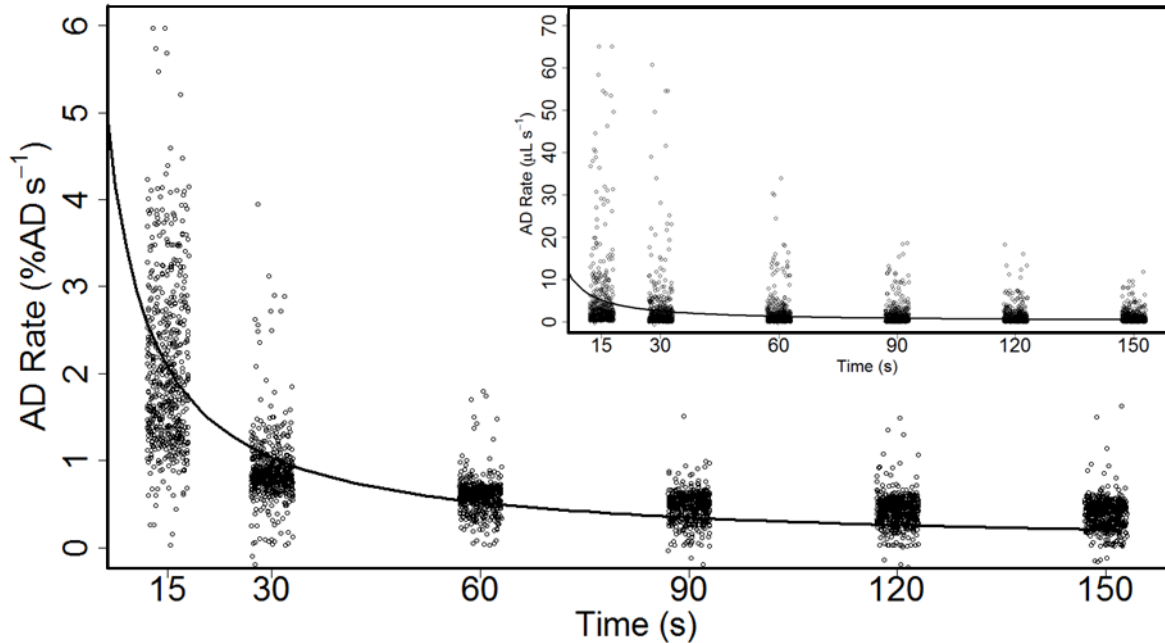
Where does the air come from?

The AD from *E. camaldulensis* that was obtained in the inverse gradient (IG) situation was higher than zero (n = 12; V = 78; p = 1). The average AD from the normal gradient (NG) situation was 224.9 ± 141.3 μL, which was higher than the AD in the IG situation (70.9 ± 108.0 μL). Therefore, the difference in the AD between the NG and IG situations was also higher than zero ($t_{(11)}$ = 5.59; p<0.0001; Fig. 6a). The AD values in the NG situation were significantly correlated with the Ψ_x ($F_{(1,10)}$ = 28.3; p = 0.0003; r^2 = 0.71), but the AD values in the IG situation were not ($F_{(1,10)}$ = 3.37; p = 0.096; r^2 = 0.18; Fig. 6b). The AD from the NG situation was marginally related to the AD from the IG situation (r^2 = 0.566; p = 0.059). In conclusion, most of the AD from the NG situation comes from branches, despite the fact that the branches were not sealed against the outside air (Fig. 6c).

How is air discharge related to embolism?

Despite the interspecific differences in branch lengths and diameters, the AD increased with Ψ_x reductions for all species (Fig. S1). The estimated parameters of the PLC and PAD curves (Fig. 7) are summarized in Table 1. The Ψ_{50p} was strongly correlated with the Ψ_{50h}

$(F_{(1,13)} = 28.6; p = 0.0001; r^2 = 0.69;$ Fig. 8a), as Ψ_{88p} and Ψ_{88h} $(F_{(1,13)} = 21.7; p = 0.0005; r^2 = 0.63;$ Fig. 8b). However, the S_p was not correlated with the S_h $(F_{(1,13)} = 0.35; p = 0.6; r^2 = 0.03;$ Fig. 8c). The relation between S_p and S_h became significant after removing the *M. acutata* outlier $(F_{(1,12)} = 5.41; p = 0.038; r^2 = 0.31)$. The same trends were observed in our randomization approach to account for uncertainty in the literature data, with the regressions between Ψ_{50} and Ψ_{88} always being significant and the regressions between S being almost always not significant. The relation between S_p and S_h without the outliers was significant only 29% of the times, suggesting that the significant, albeit weak, relationship we found for the original data $(p = 0.038, r^2 = 0.31)$ is either a false positive or very sensitive to noise (Fig. 9).

The Ψ_{50p} values that were estimated with cumulative and interval AD measurements were also strongly related to the Ψ_{50h} for all discharge durations (Fig. S3a,b). The coefficient of determination (r^2) and the p-value of the linear regressions changed abruptly during the first 60 seconds but stabilized afterwards (Fig. S3c,d).

Table 1 Summary of species air discharge (AD) and maximum vessel length (MVL), sample lengths (L) and diameters (D) and species xylem water potentials in which the PAD (Ψ_{50p} and Ψ_{88p}) and PLC (Ψ_{50h} and Ψ_{88h}) values equal 50% and 88% respectively, with references used for the PLC curves. Values are the mean ± standard deviation, for measured parameters, or mean ± standard error, for estimated parameters.

Species	Sample L (mm)	D (mm)	MVL (mm)	Maximum AD (μL)	Minimum AD (μL)	Hydraulic (MPa) Ψ_{50}	Ψ_{88}	Pneumatic (MPa) Ψ_{50}	Ψ_{88}	Hydraulic reference
Calyptranthes brasiliensis	NA	NA	474 ± 113	228.3 ± 25.2	97.2 ± 28.3	-4.9 ± 0.4	-8.5	-5.5 ± 0.3	-7.7	-
Citrus sinensis	530 ± 99	8.4 ± 0.9	362 ± 22	761.3 ± 97.6	469.0 ± 242.2	-3.7 ± 0.3	-8.7	-4.3 ± 0.2	-7.8	-
Coffea arabica	708 ± 68	6.4 ± 0.4	400 ± 30	97.5 ± 40.4	29.8 ± 27.3	-2.5 ± 0.2	-7.7	-2.9 ± 0.2	-5.3	-
Cupressus sempervirens	641 ± 65	6.8 ± 0.4	Tracheid	129.3 ± 79/9	3.3 ± 5.5	-10.4	-14.0	-8.0 ± 0.6	-14.3	[1][2]
Drimys brasiliensis	404 ± 126	5.8 ± 0.5	Tracheid	1244.6 ± 791.2	12.0 ± 8.0	-1.6 ± 0.1	-2.9	-2.2 ± 0.2	-3.3	-
Erisma uncinatum	NA	5.2 ± 1.0	410 ± 15	1981.4 ± 37.4	377.9 ± 789.4	-1.1 ± 0.1	-2.4	-2.1 ± 0.2	-3.1	-
Eucalyptus camaldulensis	763 ± 136	4.1 ± 0.5	460 ± 26	489.1 ± 202.0	21.2 ± 8.8	-3.9 ± 0.2	-7.4	-4.1 ± 0.1	-5.8	-
Hymenaea courbaril	486 ± 102	5.9 ± 0.9	0.15 ± 0.05	288.7 ± 90.0	17.9 ± 9.2	-2.8	-3.9	-1.0 ± 0.1	-1.8	[3]
Miconia lepidota	NA	6.38 ± 1.0	250 ± 100	1122.9 ± 855.6	555.7 ± 649.2	-4.6 ± 0.2	-8.4	-4.4 ± 0.3	-5.9	-
Myrceugenia acutata	450 ± 115	5.9 ± 0.9	662 ± 78	454.2 ± 141.0	94.8 ± 71.2	-4.9 ± 0.1	-5.4	-6.5 ± 0.5	-10.3	-
Olea europaea	648 ± 109	4.7 ± 0.5	293 ± 68	176.9 ± 59.8	26.8 ± 8.4	-4.0	-5.7	-2.9 ± 0.4	-6.6	[4][5]
Populus nigra	619 ± 215	4.4 ± 0.7	163 ± 67	544.7 ± 220.8	188.8 ± 114.4	-2.7	-3.6	-2.6 ± 0.2	-4.3	[6][7][8]
Schinus terebinthifolius sapling	420 ± 55	4.6 ± 0.3	187 ± 32	326.6 ± 123.6	16.4 ± 3.6	-3.1 ± 0.1	-4.6	-2.3 ± 0.2	-3.8	-
Schinus terebinthifolius tree-short	145 ± 16	3.1 ± 0.6	254 ± 114	109.2 ± 30.7	35.4 ± 12.7	-3.1 ± 0.1	-4.6	-2.3 ± 0.3	-4.3	-
Schinus terebinthifolius tree-long	338 ± 23	4.3 ± 0.6	254 ± 114	479.4 ± 184.0	46.2 ± 14.5	-3.1 ± 0.1	-4.6	-2.7 ± 0.2	-5.2	-
Thuja plicata	612 ± 98	6.4 ± 0.8	Tracheid	339.1 ± 169.1	9.0 ± 2.3	-5.0	-6.4	-7.6 ± 0.3	-10.1	[1][2][9]
Weinmannia organensis	412 ± 45	6.2 ± 1.1	497 ± 158	1283.3 ± 254.9	50.5 ± 36.1	-2.1 ± 0.1	-3.3	-2.5 ± 0.1	-4.0	-

[1] (Choat *et al.*, 2012); [2] (Delzon *et al.*, 2010); [3] (Brodribb *et al.*, 2003); [4] (Hacke *et al.*, 2015); [5] (Torres-Ruiz *et al.*, 2014)*;* [6] (Froux *et al.*, 2002); [7] (Cochard *et al.*, 2005); [8] (Guet *et al.*, 2015); [9] (Mcculloh *et al.*, 2014). NA = Not Available

Fig. 6 (a) Air discharged (µL) under vacuum or atmospheric pressure in the leaves/stem chamber and (b) the relation between the xylem water potential and the air discharged with vacuum pressure (closed circles) or with atmospheric pressure (open circles) in a chamber containing *E. camaldulensis* branches. The normal gradient (NG) is given by the atmospheric pressure inside the chamber, whereas the inverse gradient (IG) is applied by vacuum in the chamber. The continuous line is the regression curve for the measurements with a vacuum in the chamber, and the dashed line is the regression curve for the measurements with atmospheric pressure in the chamber. (c) A schematic representation of the air pathway and the large amount of air coming from inside the branches, as found experimentally.
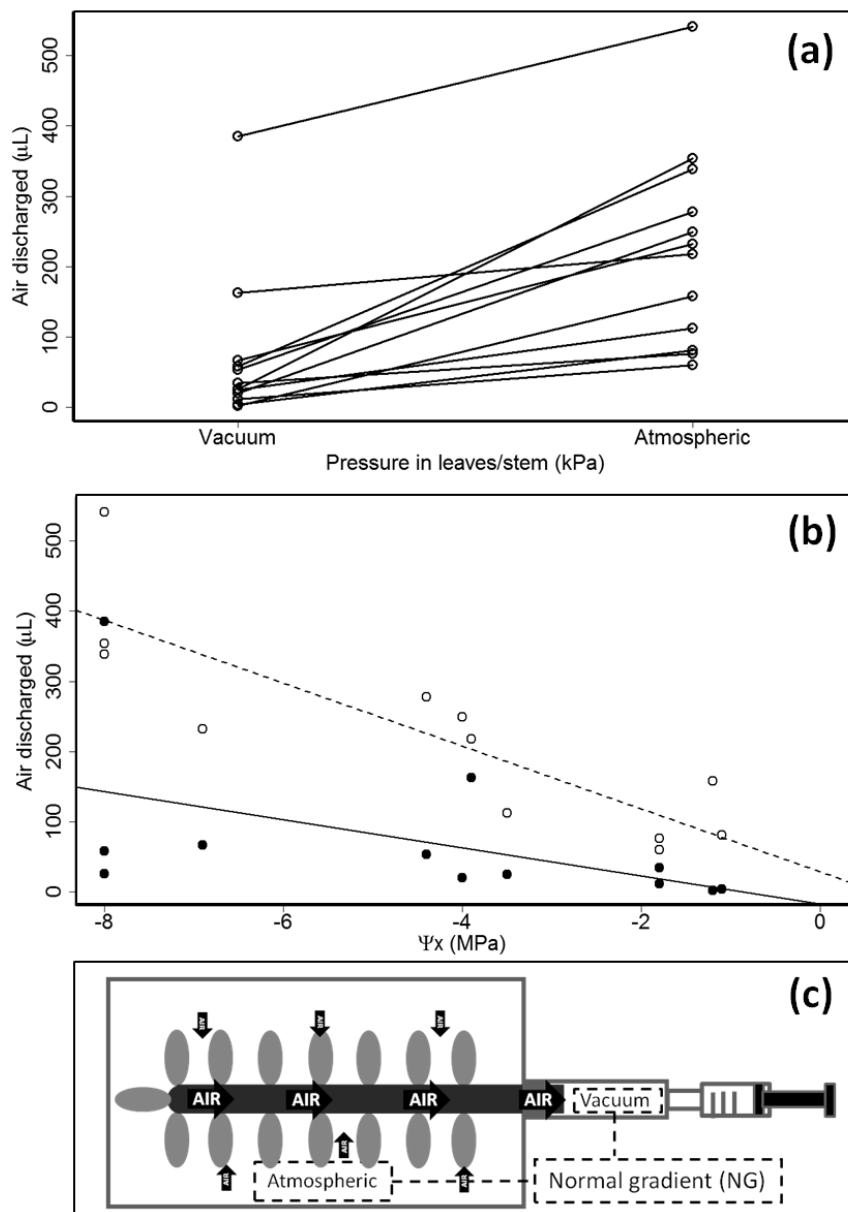
Fig. 7 Percentage of maximum air discharge (PAD) or percentage loss of conductance (PLC) as a function of the xylem water potential (Ψ_x). The different symbols are PAD data from different individuals. The red line is the regression curve obtained for the PAD values, and the blue line is the regression curve for the PLC data (shown in the Fig. S2). Full circles and triangles are the Ψ_{50} and Ψ_{88} for the PAD curve (red) and PLC curve (blue), respectively. We used Ψ_{50} and Ψ_{88} data from the literature for five species (see methods) to calculate the slope of the sigmoidal curve as $PLC = 100/(1 + \exp((S/25)S(\Psi_x - \Psi_{50p}))$ and to plot the curve. The published curves were not necessarily regressions with the same equation.
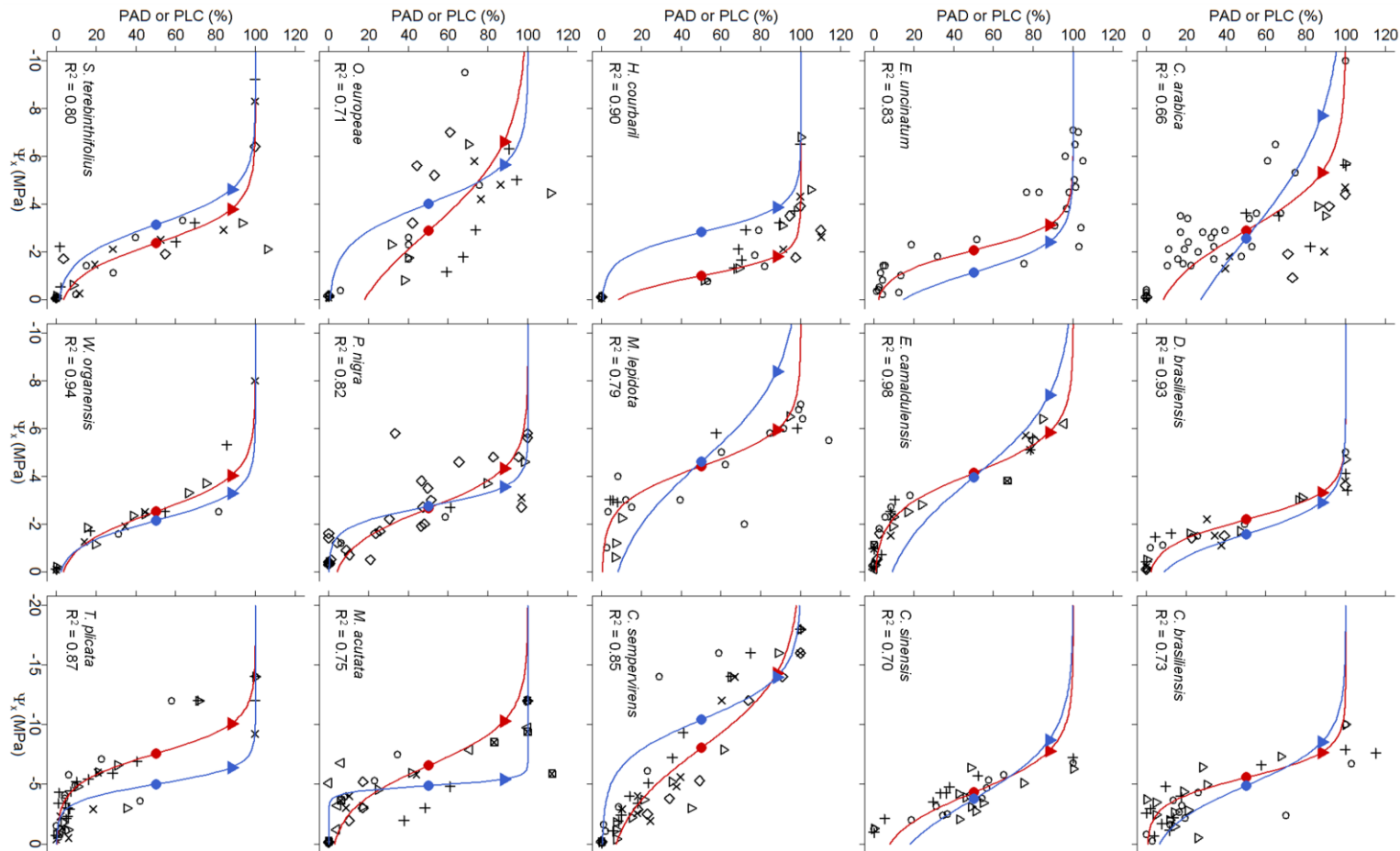
Fig. 8 Relation between Ψ_{50} (a), Ψ_{88} (b), and slope (c) of the PLC (hydraulic method) and PAD (pneumatic method) fitted curves for each studied species. Red points and lines are used for data and regression fits from species with hydraulic data from the literature, and the blue points and lines are for the others. The continuous black lines are the regression fit for the combined data, and the dotted lines indicate the 1 to 1 line. The black line in the lower panel is the regression, which is fitted without the two outliers. Regression lines are presented only when significant or marginally significant. * values for the regression of all data after removing the two outliers.
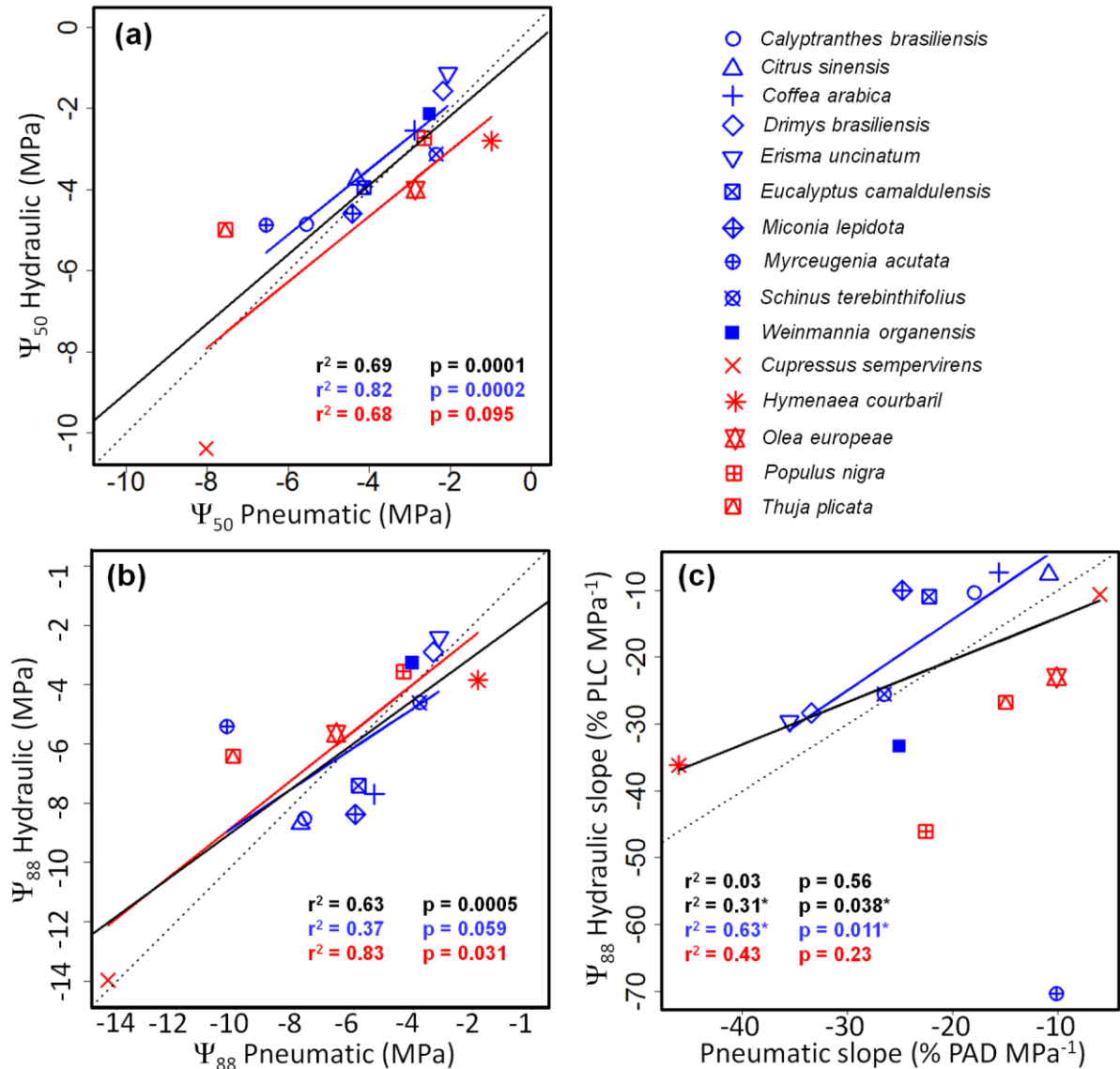
Fig. 9 Coefficient of determination (r^2; black box plots and left y-axis) and p-value (grey box plots and right y-axis) when comparing the Ψ_{50}, Ψ_{88} and S (slopes) values between the pneumatic and hydraulic methods. The continuous and dashed lines represent p-values equal to 0.05 and 0.07, respectively. A randomization approach was used to account for uncertainty in the literature data and is described in method S1. The variability was applied to the literature data, and the linear regression was analysed. We repeated this procedure 1000 times. The S* is the slope without *M. acutata* outlier.
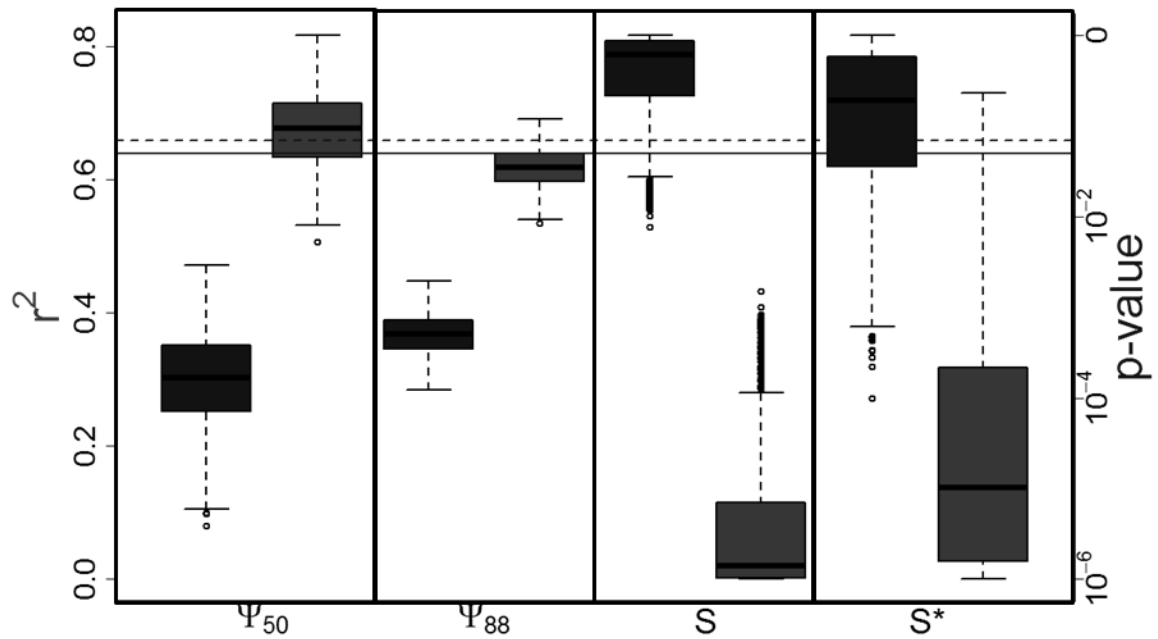
Fig. 10 (a) Air discharged and (b) percentage air discharged (PAD) or percentage loss of conductance (PLC) in *S. terebinthifolius* samples as functions of the xylem water potential (Ψ_x). Green points and lines are data for sapling samples; blue points and lines are data for trees from short branches; red points and lines are data for trees from long branches; and the black line is the hydraulic regression of the PLC as a function of Ψ_x.
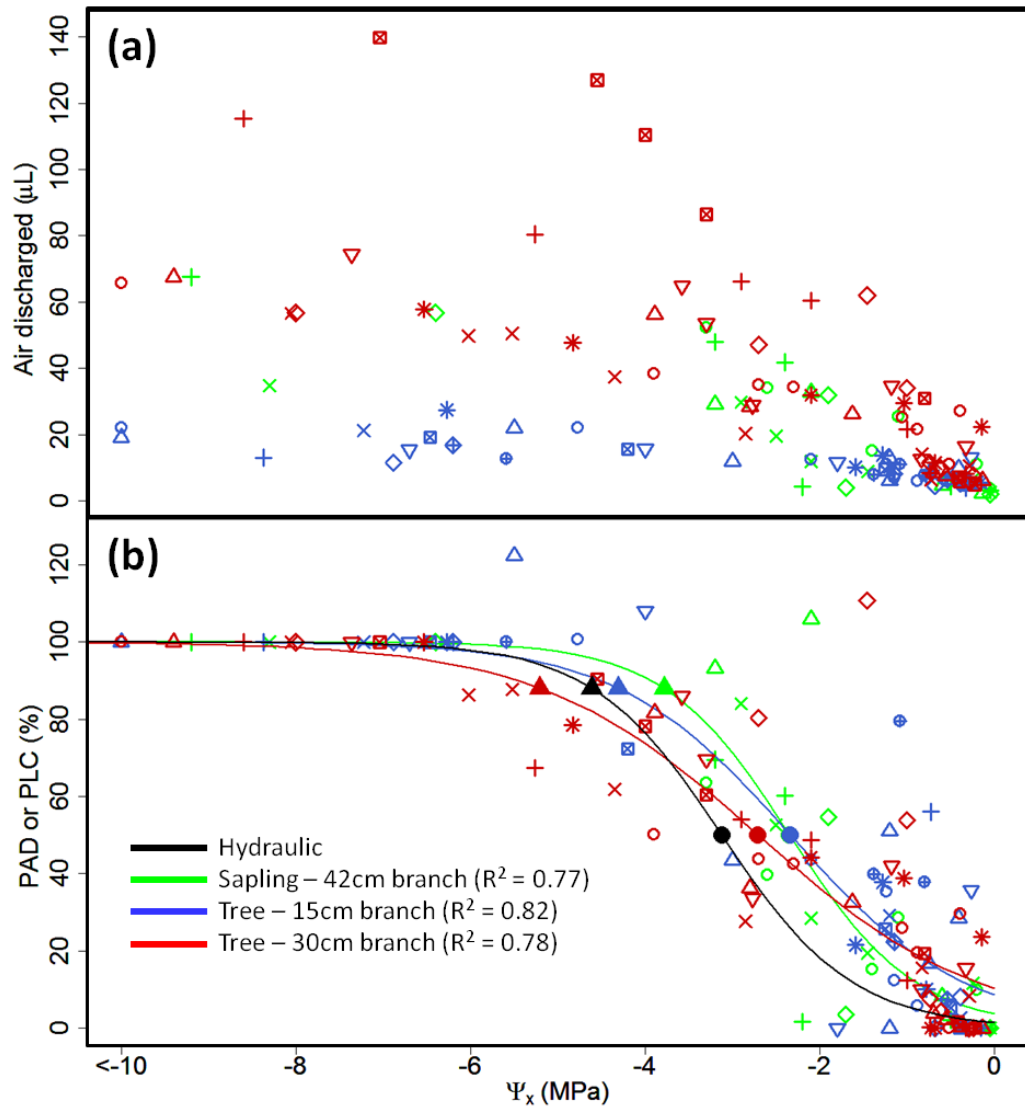
Does the vessel length affect air discharge and PAD curves?

The AD from *S. terebinthifolius* was different when comparing short and long branches (V = 491; p <0.0001, Fig. 10a), with AD values from long branches 3.5 times higher than the values from short branches. By contrast, the Ψ_{50p} and Ψ_{88p} of short branches were similar (p > 0.05) to the Ψ_{50p} and Ψ_{88p} of long branches (Fig. 10b).

Discussion

Air origin

The air flow was measured during two situations: under normal (NG; Fig. 4c) and inverse (IG; Fig. 4a,b) pressure gradients. The air flow was higher in the NG situation than in the IG situation (Fig. 6a). Thus, the hypothesis that air comes from both inside and outside the plant was confirmed, with the contribution of internal air spaces being much higher than that of external sources. Because the air flow for the IG was lower than it was for the NG condition, we may argue that the radial resistance to air flow (air that passes through the bark/leaves) is higher than the longitudinal resistance (air that flows through xylem conduits and other tissues, but in an axial direction). Thus, the air that is stored inside the plant discharged faster in the NG situation. This high radial resistance to air flow is in accordance with studies on air permeability and diffusion in wood, in which the resistance through the lumen conduits and pit membranes (axial resistances) is lower that of in the radial direction through the periderm and cambium (Comstock, 1970; Sorz & Hietz, 2006).

The air flow in the IG situation did not change significantly with the Ψ_x, but it increased in the NG situation (Fig. 6b). Because the system was the same but was operating at different rates in the NG and IG situations, the magnitude of the component that affected the air flow related to the Ψ_x was weaker in the IG situation and thus weakened the relation between the air flow and Ψ_x.

Air Discharge

The AD differed by two orders of magnitude among individuals of the same species and among different species (Table 1). The differences among species might be related to structural variations such as the presence of lenticels, intercellular spaces, heartwood, pit membranes resistance and primarily the cumulative conduit lumen area (Prak, 1970; Hansmann *et al.*, 2002). Although the AD from 0.3 m *S. terebinthifolius* branches was 3.5 times higher than that of 0.15 m branches, we did not find any significant relation between the

AD and branch allometry in the evaluated species. Therefore, our data revealed that AD differences among species are related to other structures, such as the volume of vessel lumens as it affects both air storage and air axial conductance (Hicks, 1995).

The rate of AD was not constant over time (Fig. 5). This finding is in accordance with the NG/IG tests that showed a higher contribution from air storage inside the plant than external air sources in terms of AD. The air storage adds a capacitance effect to the system, which then operates in an unsteady state (Prak, 1970). Both the non-linearity of the AD and the NG/IG gradient test suggest that AD is an indicator of plant air volume.

Air flow and embolism

We found a strong relation between the PAD and PLC, with estimations of Ψ_{50} and Ψ_{88} being very similar when the hydraulic and pneumatic methods were used, and Ψ_{50} presented a stronger relation than Ψ_{88} (Fig. 9). Our data confirm that the AD is related to the PLC, with an expected loss of accuracy from the symmetry point of the curve (Fig. 1). In comparing the hydraulic and pneumatic methods, the S slopes of fitted curves presented a weaker relation, but only after the removal of the *M. acutata* outlier (Fig. 8c). In fact, the S parameter incorporates errors for both Ψ_{50} and Ψ_{88} from the hydraulic and pneumatic methods, which doubles the degrees of freedom of its uncertainty, making it harder to detect a trend. Even when considering the uncertainty and avoiding outliers, S_h and S_p were only weakly correlated (Fig. 8c), and they were significant only 29% of the time, according to our randomization approach (Fig. 9). Thus, the hypothesis that the plant air flow and plant air volume are related to embolism is confirmed, and the AD and other measurements of air volume (or, conversely, vessel water volume changes, see Vergeynst *et al.* (2014)) can be used to estimate Ψ_{50} and Ψ_{88}, with the latter exhibiting less accuracy.

The lower accuracy for detecting Ψ_{88} may be related to the non-vessel air volume, such as dead cells in the heartwood. We did not notice an effect from the non-vessel air volume in our samples, but we also did not plan our measurements to look specifically for non-vessel air volumes. Another possibility to explain the lower accuracy for estimating the Ψ_{88} is the axial or radial air conductance, which likely changed with the Ψ_x because of changes in turbulence and branch permeability. However, our results indicate that the effects of non-vessel air volume and changes in air conductance on Ψ_{50} and Ψ_{88} estimations are small, because both can be predicted from AD measurements. Another possible bias in the estimation of Ψ_{88}, for both hydraulic and pneumatic methods, is that there are usually few data points under low Ψ_x because of the limitation of the pressure chamber to -10 MPa. Unless accounted for, this

condition forces the regression algorithm to minimize the residuals of high Ψ_x data, increasing the uncertainty of Ψ_{88}.

The relation between the pneumatic and hydraulic curves was still strong despite the fact that the hydraulic curves were built with short branches and the pneumatic ones were made from long leafy branches. We did not expect that air from the mesophyll or the spongy palisade would affect our measurements, because they would have to diffuse through the symplast to reach the xylem vessels. In fact, this diffusion is a slow process that is unlikely to affect the measurements that were taken in 2.5 minutes to a significant extent. However, we would expect that the air inside the leaf vessels could affect our measurements but our results suggest that this effect was weak. This finding indicates that the effect of leaf embolisms on the air volume was small, and our measurements actually integrated the air volume inside the branches. The presence of leaves during the pneumatic method likely affected the residuals in the hydraulic-pneumatic comparisons and caused non-significant differences between the pneumatic curves that were built with the short and long branches of *S. terebinthifolius*. It is possible that the pneumatic method can be used to evaluate leaf vulnerability curves in branches with more leaves in a proportional manner.

Plant air storage and air network

Tree wood contains a large amount of air (Zimmermann, 1983), and air permeability in dead wood increases with increasing gas volume (Sorz & Hietz, 2006). Gartner *et al.* (2004) estimated that 18% to 26% of the volume in living functional xylem could be air, and it could be up to 50% in non-functional heartwood. However, these researchers did not distinguish vessel (embolism) and non-vessel air volumes. The volume of intercellular spaces and rays is too small to contain all this air (approximately 7% of the total air volume). Thus, most of the air inside the plants must be in the cell lumens and wall pore spaces (Gartner *et al.*, 2004), which emphasizes the strong relation between air flow and embolism. It is possible that a small portion of the air measured in our samples was already inside the tissues, even in well-hydrated plants, and it was likely distributed in the fibres, pith, bark and open conduits at the base of the branch. This possibility was considered by removing the AD_{min} of well-hydrated plants from all other measurements when fitting the PAD curves (see Methods section).

In well-hydrated plants, we would expect that air only comes through the open vessels (Fig. S4a). As embolism formation begins, the network of air-filled spaces would increase progressively (Fig 12b). Whether air filled spaces would be compartmentalized and not

accessible from the initial open vessels (Fig. S4c) and the connectivity of the plant air network are issues that remain unsolved. The segmentation of air spaces could bias PLC estimations from PAD curves and affect relations between the air flow and air volume, with air flow increasing disproportionally when two unconnected air networks become connected. Hydraulic measurements could also be biased by segmentation if samples are chosen from a non-segmented branch section. Given that we have found a good correlation between the PAD and PLC curves, we may argue that segmentation is not an issue and that plant air spaces are more connected, although evidences of isolated embolized conduits (Choat *et al*. 2015)..

The arrangement of the cellulose microfibrils impregnated by lignin turns the cell wall free of water (Niklas, 1992) and it is possible consider it impermeable for models of wood permeability (Siau, 1984). For air that is sucked from embolized and closed vessels through the cut at the branch base (Fig. S4b), the pit membranes should be dry and permeable to air. Otherwise, a pressure that is much higher than the one applied in this study would be necessary to force air through the wet membranes. In fact, we do not know the water status of pit membranes in embolized vessels. Ieperen *et al.* (2002) suggest that pit membranes can dry in cut stems because they contact dry air, and their data on refilling open vessels that were immersed in water corroborated this assumption. In addition, pit membrane shrink when dry forming large pores (Pesacreta *et al.*, 2005), which may reduce the resistance to air flow. Two high-energy processes must occur in the pit membranes when embolism takes place; first, potential energy that is stored as the elastic deformation of pit membranes is suddenly released, which is one possible cause of acoustic emissions during embolism formation (Milburn, 1973). Second, the vessel has a water vapour concentration of almost zero (vacuum) in the instant after embolism formation, which would cause the water potential of the air inside the vessel to become extremely negative. Both processes, individually or together, can potentially dry the pit membrane, at least partially. Our data do suggest that the pit membranes allowed air passage and were thus dry. The air volumes measured in our experiments were strongly related to embolisms for all species, which suggests that the permeability of pit membranes of embolized vessels to air is widespread. Otherwise, although we already know that the intercellular spaces in the wood may form an air duct system, the communication that occurs among these spaces has not been clearly demonstrated (MacDougal, 1932, 1936; Zimmermann, 1983) and as we discussed before, the intercellular spaces represent a small air volume inside the wood (Gartner *et al.*, 2004) to explain our results.

Time of air discharge

The relation between Ψ_{50p} and Ψ_{50h} was significant for AD that were estimated several times, i.e., during cumulative and interval measurements (Fig. S3). The increase in the coefficient of determination for the relation between Ψ_{50p} and Ψ_{50h} (Fig. S3c,d) with increasing AD has some possible explanations as follows: (1) the initial measurements that were taken, when most of the air is discharged (see Fig. 5), are subjected to unknown interferences; (2) the effect of embolisms on AD is different after the first 30 s (weaker before and/or stronger after the first 30 s); or (3) integrating the embolism signal for AD over a long period of time reduces noise and makes the signal stronger.

The influence of open conduits on air discharge

The bench dehydration method is currently used as considered the reference method for inducing embolism formation (Sperry *et al.*, 1988). It is assumed that the open conduits that are in contact with the atmosphere are filled with air instantaneously (Cochard *et al.*, 1994), forming menisci in the pit membranes that are in contact with other water-filled conduits. Thus, the branch length in the bench dehydration method must be longer than the maximum conduit length for hydraulic measurements, and the branch can be re-cut under water until the sample only contains closed vessels. These menisci must remain until the water potential exceeds the embolism formation pressure and the nanobubbles become unstable, forming embolisms.

In using the pneumatic method, we account for the open vessel air volume (AD_{min}) and thus only measure the air from embolized closed vessels that did not embolize by artefact (Fig. S4). We do not expect that open vessels are artefacts of the pneumatic method unless these open vessels change embolism formation in the adjacent closed vessels. If they do form, then the bench dehydration method and any other destructive method will also involve artefacts. However, we do expect that the pneumatic method is effectively integrating embolisms that occur in open vessels where the branch is cut (Fig. S4, see 'pneumatic effective sample'). We did not find evidence for open vessel artefacts in our sample size experiment, and both the short and long branches of *S. terebinthifolius* showed similar Ψ_{50p} values (Fig. 10). This finding reinforces that we were able to correct the effects of open vessels by accounting for the open vessel air volume in the AD_{min}.

A pneumatic approach to plant hydraulic mechanisms

The air permeability method (Franks *et al.*, 1995) and bubble production during the air pressurization method (Ennajeh *et al.*, 2011) previously demonstrated the reliability of xylem air conductance measurements for studying the embolism phenomenon. Air is always an implicit counterpart of plant hydraulics and we have found that air flow is related to embolisms. Although many questions regarding the nature of the processes that affect air flow remain unsolved, such as air permeability of pit membrane, measurement in unsteady state or turbulent flow, we provide additional support for the effectiveness of pneumatic methods for studying plant hydraulics.

Several hydraulic methods are available to study embolism, but they are usually time-consuming and subject to various artefacts; 1) bubbles can dissolve as the branch is manipulated during the measurements, or the conduits may be passively refilled by capillary pressure (Cochard *et al.*, 2013); 2) an underestimation of K_{max} can occur for different reasons, such as passive water uptake (Torres-Ruiz *et al.*, 2012), background flow (Hacke *et al.*, 2015), the reactivation of conduits with flushing (Sperry *et al.*, 2012) and the use of different protocols for flushing (Hietz *et al.*, 2008); and 3) the branch length can affect the K_{max} measurements because of end wall resistance. Assuming that open conduits have higher conductance and are embolized first, the K_{max} can be overestimated depending on the proportion of air-filled conduits without end walls and water-filled conduits with end walls (Cochard *et al.*, 2013). Because pneumatic methods are not dependent directly on hydraulic properties, it is possible that the hydraulic-related artefacts may not affect pneumatic measurements. Consistent with this hypothesis, Ennajeh *et al.* (2011a) improved the air pressurization method with air conductance instead of hydraulic conductance.

The pneumatic method may also contribute to the current discussion regarding embolism induction when a sample is cut under tension (Wheeler *et al.*, 2013). Some hydraulic curves presented herein were obtained before the description of this artefact and the samples were not relaxed as described by Wheeler *et al.* (2013). However, care was taken to cut the sample several times under water, which may be effective for preventing embolism induction (Venturas *et al.*, 2015). During the pneumatic method, we do no cut the samples, and thus this artefact is not expected. In any case, we showed similar results between hydraulic and pneumatic methods, which indicate that: either embolism induction was prevented by cutting the samples several times under water during the hydraulic method or that the pneumatic method could overestimate embolisms. Considering that this artefact is still

a controversial issue, further studies are needed and the pneumatic method may be an alternative test.

Although we were unable to find any major disadvantage or artefact associated with the pneumatic method, we are able to highlight several advantages of this method when using vulnerability curves. We built a complete vulnerability curve with this method by using the same entire branch, and the limitation for increasing the number of data points by branch was the amount of leaves used for measuring the Ψ_x. By contrast, hydraulic measurements from the bench dehydration method only allowed the use of stem segments, with each representing one point of the curve. The pneumatic method also integrated the whole air network (Fig. S4), and hydraulic methods are usually limited to small segments because of the precision of flowmeters and flush limitations. As shown, the pneumatic method is substantially faster than the hydraulic one; i.e, most PAD curves presented in Fig. 8 were made simultaneously in two days (the time required for plant dehydration). Franks *et al*. (1995) also used the bench dehydration method to induce embolism in their pneumatic approach; however, their air conductance measurements were taken from frozen stem segments, and this method is only reliable for diffuse-porous species. In the method proposed by Ennajeh *et al.* (2011a), samples were embolized by air pressurization and may have suffered from the limitations imposed by this method (Ennajeh *et al.* 2011b). Finally, a major advantage of the pneumatic method described herein is the minimal manipulation of samples, which may limit interference or artefacts.

Despite the abundance of air in wood (Gartner *et al.*, 2004) and the fact that air conductance measurements provide the basis for our understanding of embolism formation (Sperry & Tyree, 1988), little is known about the relation of air to hydraulic properties and plant function. We showed that air flow from intact segments came primarily from air storage inside the plants. We showed that the relative amount of air in a branch is related to the embolism. To our knowledge, this study is the first to take direct measurements of air in entire branches (see MacDougal (1936) for a similar approach), which opens new possibilities to study not only xylem embolism and plant-water relations but also to address questions related to the significance of air inside plants and its role on plant anatomical and physiological responses to environmental changes and mechanical support. In addition, the pneumatic method proposed herein might increase our ability to screen for embolism resistance among genotypes and hydraulic diversity in species-rich communities such as tropical forests, providing a unique opportunity to study the impact of abiotic stresses on plant and community water relations.

Acknowledgements

References

Alder NN, Pockman WT, Sperry JS, Nuismer S. **1997**. Use of centrifugal force in the study of xylem cavitation. *Journal of Experimental Botany* **48**: 665–674.

Barton NG. **2012**. The Expansion-Cycle Evaporation Turbine. *Journal of Engineering for Gas Turbines and Power* **134**: 051702.

Blackman CJ, Brodribb TJ, Jordan GJ. **2012**. Leaf hydraulic vulnerability influences species' bioclimatic limits in a diverse group of woody angiosperms. *Oecologia* **168**: 1–10.

Blackman CJ, Gleason SM, Chang Y, Cook AM, Laws C, Westoby M. **2014**. Leaf hydraulic vulnerability to drought is linked to site water availability across a broad range of species and climates. *Annals of Botany* **114**: 435–440.

Brodribb TJ, Holbrook NM. **2007**. Forced depression of leaf hydraulic conductance in situ: effects on the leaf gas exchange of forest trees. *Functional Ecology* **21**: 705–712.

Brodribb TJ, Holbrook NM, Edwards EJ, Gutiérrez M V. **2003**. Relations between stomatal closure, leaf turgor and xylem vulnerability in eight tropical dry forest trees. *Plant, Cell & Environment* **26**: 443–450.

Brodribb TJ, Holbrook NM, Zwieniecki MA, Palma B. **2005**. Leaf hydraulic capacity in ferns, conifers and angiosperms: impacts on photosynthetic maxima. *New Phytologist* **165**: 839–846.

Choat B, Brodersen CR, Mcelrone AJ. **2015**. Synchrotron X-ray microtomography of xylem embolism in *Sequoia sempervirens* saplings during cycles of drought and recovery. *New Phytologist* **205**: 1095–1105.

Choat B, Jansen S, Brodribb TJ, Cochard H, Delzon S, Bhaskar R, Bucci SJ, Feild TS, Gleason SM, Hacke UG, *et al.* **2012**. Global convergence in the vulnerability of forests to drought. *Nature* **491**: 752–755.

Cochard H, Badel E, Herbette S, Delzon S, Choat B, Jansen S. **2013**. Methods for measuring plant vulnerability to cavitation: a critical review. *Journal of Experimental Botany* **64**: 4779–4791.

Cochard H, Cruiziat P, Tyree MT. **1992**. Use of positive pressures to establish vulnerability curves. *Plant Physiology* **100**: 205–209.

Cochard H, Damour G, Bodet C, Tharwat I, Poirier M, Améglio T. **2005**. Evaluation of a new centrifuge technique for rapid generation of xylem vulnerability curves. *Physiologia Plantarum* **124**: 410–418.

Cochard H, Delzon S, Badel E. **2015**. X-ray microtomography (micro-CT): A reference technology for high-resolution quantification of xylem embolism in trees. *Plant, Cell and Environment* **38**: 201–206.

Cochard H, Ewers FW, Tyree MT. **1994**. Water relations of a tropical vine-like bamboo (*Rhipidocladum racemiflorum*): root pressures, vulnerability to cavitation and seasonal changes in embolism. *Journal of Experimental Botany* **45**: 1085–1089.

Comstock GL. **1970**. Directional permeability of softwoods. *Wood and Fiber* **1**: 283–289.

Cruiziat P, Cochard H, Améglio T. **2002**. Hydraulic architecture of trees: main concepts and results. *Annals of Forest Science* **59**: 723–752.

Delzon S, Douthe C, Sala A, Cochard H. **2010**. Mechanism of water-stress induced cavitation in conifers: bordered pit structure and function support the hypothesis of seal capillary-seeding. *Plant, Cell & Environment* **33**: 2101–2111.

Ennajeh M, Nouiri M, Khemira H, Cochard H. **2011**. Improvement to the air-injection technique to estimate xylem vulnerability to cavitation. *Trees* **25**: 705–710.

Franks PJ, Gibson A, Bachelard EP. **1995**. Xylem Permeability and Embolism Susceptibility in Seedlings of *Eucalyptus camaldulensis* Dehnh. from Two Different Climatic Zones. *Australian Journal of Plant Physiology* **22**: 15–21.

Froux F, Huc R, Ducrey M, Dreyer E. **2002**. Xylem hydraulic efficiency versus vulnerability in seedlings of four contrasting Mediterranean tree species (Cedrus atlantica , Cupressus sempervirens , Pinus halepensis and Pinus nigra). *Annals of Forest Science* **59**: 409–418.

Gartner BL, Moore JR, Gardiner BA. **2004**. Gas in stems: abundance and potential consequences for tree biomechanics. *Tree Physiology* **24**: 1239–1250.

Gleason SM, Butler DW, Ziemińska K, Waryszak P, Westoby M. **2012**. Stem xylem conductivity is key to plant water balance across Australian angiosperm species. *Functional Ecology* **26**: 343–352.

Guet J, Fichot R, Lédée C, Laurans F, Cochard H, Delzon S, Bastien C, Brignolas F. **2015**. Stem xylem resistance to cavitation is related to xylem structure but not to growth and water-use efficiency at the within-population level in *Populus nigra* L. *Journal of Experimental Botany* **66**: 4643–4652.

Hacke UG, Sperry JS. **2001**. Functional and ecological xylem anatomy. *Perspectives in Plant Ecology, Evolution and Systematics* **4**: 97–115.

Hacke UG, Venturas MD, MacKinnon ED, Jacobsen AL, Sperry JS, Pratt RB. **2015**. The standard centrifuge method accurately measures vulnerability curves of long-vesselled olive stems. *New Phytologist* **205**: 116–127.

Hansmann C, Gindl W, Wimmer R, Teischinger A. **2002**. Permeability of wood - a review. *Wood Research* **47**: 1–16.

Hicks D. **1995**. How to blow air through sticks, or, xylem structure and function. *Bioscene* **21**: 3–6.

Hietz P, Rosner S, Sorz J, Mayr S. **2008**. Comparison of methods to quantify loss of hydraulic conductivity in Norway spruce. *Annals of Forest Science* **65**.

Hook DD, Brown CL, Wetmore RH. **1972**. Aeration in trees. *Botanical Gazette* **133**: 443–454.

Ieperen W van, Meeteren U van, Nijsse J. **2002**. Embolism repair in cut flower stems: a physical approach. *Postharvest Biology and Technology* **25**: 1–14.

Kursar TA, Engelbrecht BMJ, Burke A, Tyree MT, EI Omari B, Giraldo JP. **2009**. Tolerance to low leaf water status of tropical tree seedlings is related to drought performance and distribution. *Functional Ecology* **23**: 93–102.

MacDougal DT. 1932. The pneumatic system of trees. *Proceedings of the American Philosophical Society* **71**:299-307.

MacDougal DT. 1936. The communication of the pneumatic system of trees with the atmosphere. *Proceedings of the American Philosophical Society* **76**:823-845.

Martin-StPaul NK, Longepierre D, Huc R, Delzon S, Burlett R, Joffre R, Rambal S, Cochard H. **2014**. How reliable are methods to assess xylem vulnerability to cavitation? The issue of 'open vessel' artifact in oaks. *Tree Physiology* **34**: 894–905.

Mcculloh KA, Johnson DM, Meinzer FC, Woodruff DR. **2014**. The dynamic pipeline: Hydraulic capacitance and xylem hydraulic safety in four tall conifer species. *Plant, Cell & Environment* **37**: 1171–1183.

Milburn JA. **1973**. Cavitation in *Ricinus* by acoustic detection: induction in excised leaves by various factors. *Planta* **110**:253-265.

Niklas K. **1992**. *Plant biomechanics: an engineering approach to plant form and function*. University of Chicago Press.

Pammenter NW, Vander Willigen C. **1998**. A mathematical and statistical analysis of the curves illustrating vulnerability of xylem to cavitation. *Tree Physiology* **18**: 589–593.

Pereira L, Mazzafera P. **2012**. A low cost apparatus for measuring of xylem hydraulic conductance in plants. *Bragantia* **71**: 583–587.

Pesacreta T, Groom LH, Rials TG. **2005**. Atomic force microscopy of the intervessel pit membrane in the stem of *Sapium sebiferum* (Euphorbiaceae). *IAWA Journal* **26**: 397–426.

Poorter L, McDonald I, Alarcón A, Fichtler E, Licona JC, Peña-Claros M, Sterck F, Villegas Z, Sass-Klaassen U. **2010**. The importance of wood traits and hydraulic conductance for the performance and life history strategies of 42 rainforest tree species. *New Phytologist* **185**: 481–492.

Prak AL. **1970**. Unsteady-State gas permeability of wood. *Wood Science and Technology* **4**: 50–69.

Rockwell FE, Wheeler JK, Holbrook NM. **2014**. Cavitation and its discontents: opportunities for resolving current controversies. *Plant Physiology* **164**: 1649–1660.

Rowland L, da Costa ACL, Galbraith DR, Oliveira RS, Binks OJ, Oliveira AAR, Pullen AM, Doughty CE, Metcalfe DB, Vasconcelos SS, et al. **2015**. Death from drought in tropical forests is triggered by hydraulics not carbon starvation. *Nature*.

Schenk HJ, Steppe K, Jansen S. **2015**. Nanobubbles: a new paradigm for air-seeding in xylem. *Trends in Plant Science* **20**: 199–205.

Smith DD, Sperry JS. **2014**. Coordination between water transport capacity, biomass growth, metabolic scaling and species stature in co-occurring shrub and tree species. *Plant, Cell & Environment* **37**: 2679–2690.

Siau JF. **1984**. *Transport process in wood.* Springer-Verlag.

Sorz J, Hietz P. **2006**. Gas diffusion through wood: implications for oxygen supply. *Trees* **20**: 34–41.

Sperry JS, Christman MA, Torres-Ruiz JM, Taneda H, Smith DD. **2012**. Vulnerability curves by centrifugation: is there an open vessel artefact, and are 'r' shaped curves necessarily invalid? *Plant, Cell & Environment* **35**: 601–10.

Sperry JS, Donnelly JR, Tyree MT. **1988**. A method for measuring hydraulic conductivity and embolism in xylem. *Plant, Cell & Environment* **11**: 35–40.

Sperry JS, Tyree MT. **1988**. Mechanism of water stress-induced xylem embolism. *Plant Physiology* **88**: 581–587.

Torres-Ruiz JM, Cochard H, Mayr S, Beikircher B, Diaz-Espejo A, Rodriguez-Dominguez CM, Badel E, Fernández JE. **2014**. Vulnerability to cavitation in olea europaea current-year shoots: further evidence of an open-vessel artifact associated with centrifuge and air-injection techniques. *Physiologia Plantarum* **152**: 465–474.

Torres-Ruiz JM, Sperry JS, Fernández JE. **2012**. Improving xylem hydraulic conductivity measurements by correcting the error caused by passive water uptake. *Physiologia Plantarum* **146**: 129–135.

Tyree MT, Ewers F. **1991**. The hydraulic architecture of trees and other woody plants. *New Phytologist* **119**: 345–360.

Venturas MD, Mackinnon ED, Jacobsen AL, Pratt RB. **2015**. Excising stem samples underwater at native tension does not induce xylem cavitation: No evidence for a tension-cutting artifact. *Plant, Cell & Environment* **38**: 1060–1068.

Vergeynst LL, Dierick M, Bogaerts JAN, Cnudde V, Steppe K. **2014**. Cavitation: a blessing in disguise? New method to establish vulnerability curves and assess hydraulic capacitance of woody tissues. *Tree Physiology* **35**: 400–409.

Wheeler JK, Huggett BA, Tofte AN, Rockwell FE, Holbrook NM. **2013**. Cutting xylem under tension or supersaturated with gas can generate PLC and the appearance of rapid recovery from embolism. *Plant, Cell & Environment* **36**: 1938–1949.

Zhang JL, Cao KF. **2009**. Stem hydraulics mediates leaf water status, carbon gain, nutrient use efficiencies and plant growth rates across dipterocarp species. *Functional Ecology* **23**: 658–667.

Zimmermann MH. **1983**. *Xylem structure and the ascent of sap*. Springer-Verlag.

Zimmermann MH, Jeje AA. **1981**. Vessel-length distribution in stems of some American woody plants. *Canadian Journal of Botany* **59**: 1882–1892.

Supplemental Material

Fig. S1 Volume of air discharged from the samples as a function of xylem water potential (Ψ_x). Different symbols are data from different individuals. rho values for Spearman's correlation are presented. Note that "<-10" in some x-axis means the xylem water potential was less than -10 MPa (out of equipment scale). *** $p < 0.0001$; ** $p < 0.001$; * $p < 0.05$.

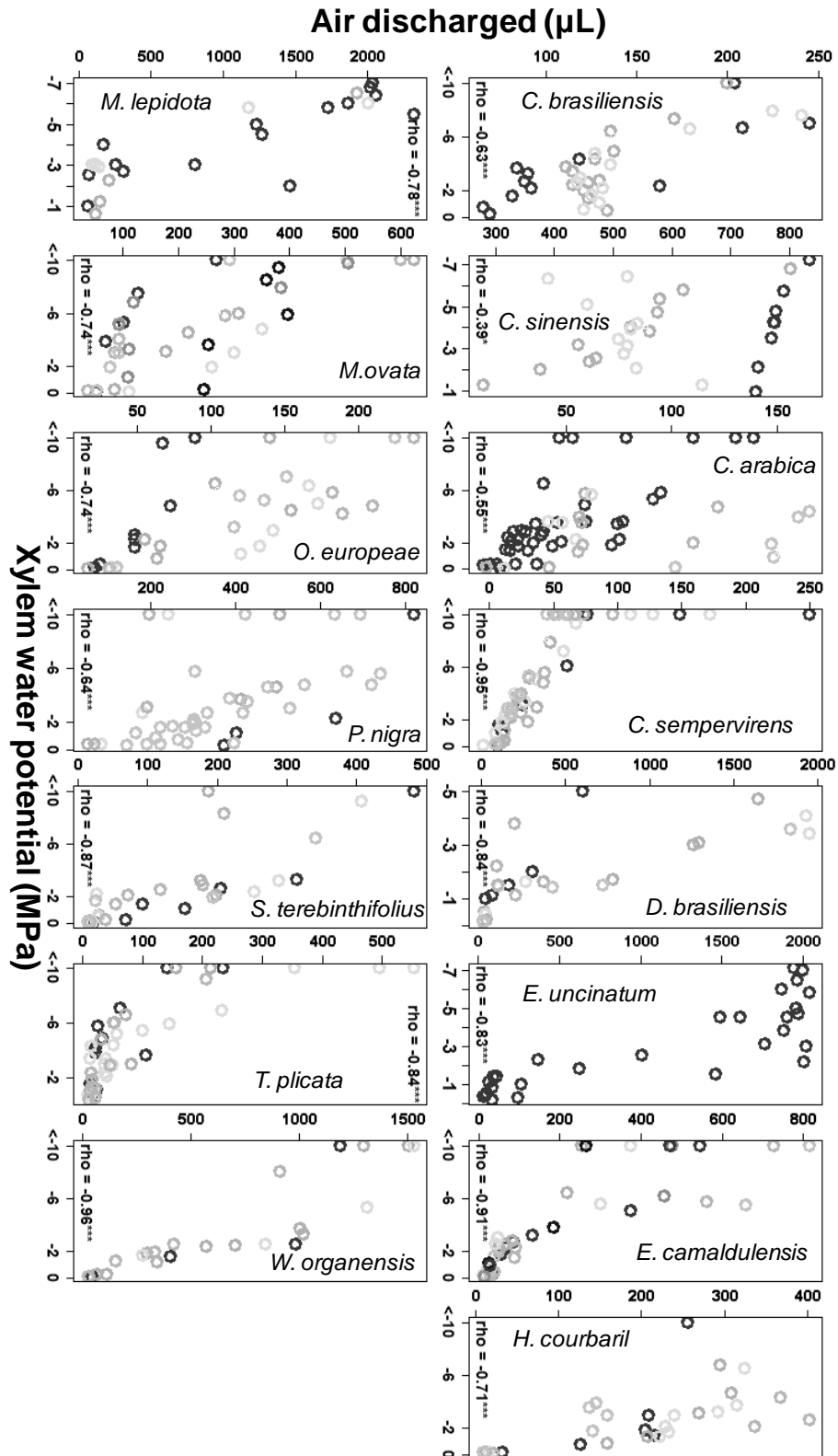**Fig. S2** Percentage of maximum air discharge (PAD) or percentage loss of conductivity (PLC) as a function of xylem water potential (Ψ_x). The red line is the regression curve obtained for the PAD values (data not shown), and the blue line is the regression curve for the PLC data (open circles). Full circles and triangles are the Ψ_{50} and Ψ_{88} for the PAD curve (black) and PLC curve (grey), respectively.
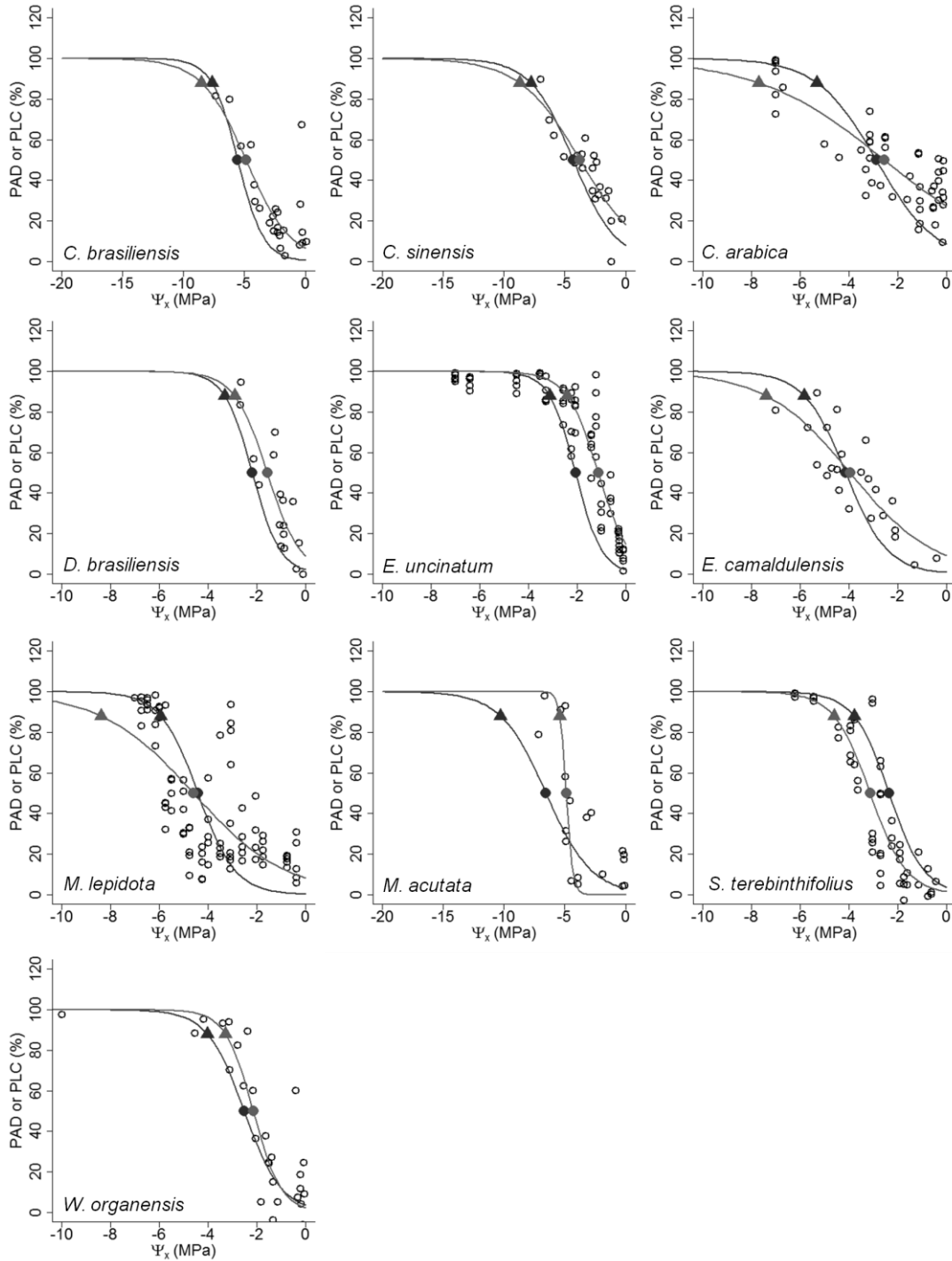
Fig. S3 Ψ_{50} estimated using partial AD measurements from (a) cumulative AD (e.g., 90 is from 0 to 90 s) and (b) the AD sampled in intervals (e.g., 90 is from 61 to 90 s). Different symbols represent different species. The coefficient of determination (r^2; closed circle and dashed line) and p-value (open circle and continuous line) for the linear regression between the Ψ_{50h} and Ψ_{50p} when estimated with the cumulative AD (c) and with the AD sampled from intervals (d). Note that the p-value axis values are on a log10 scale. The dotted horizontal line in c) and d) represents p = 0.05.
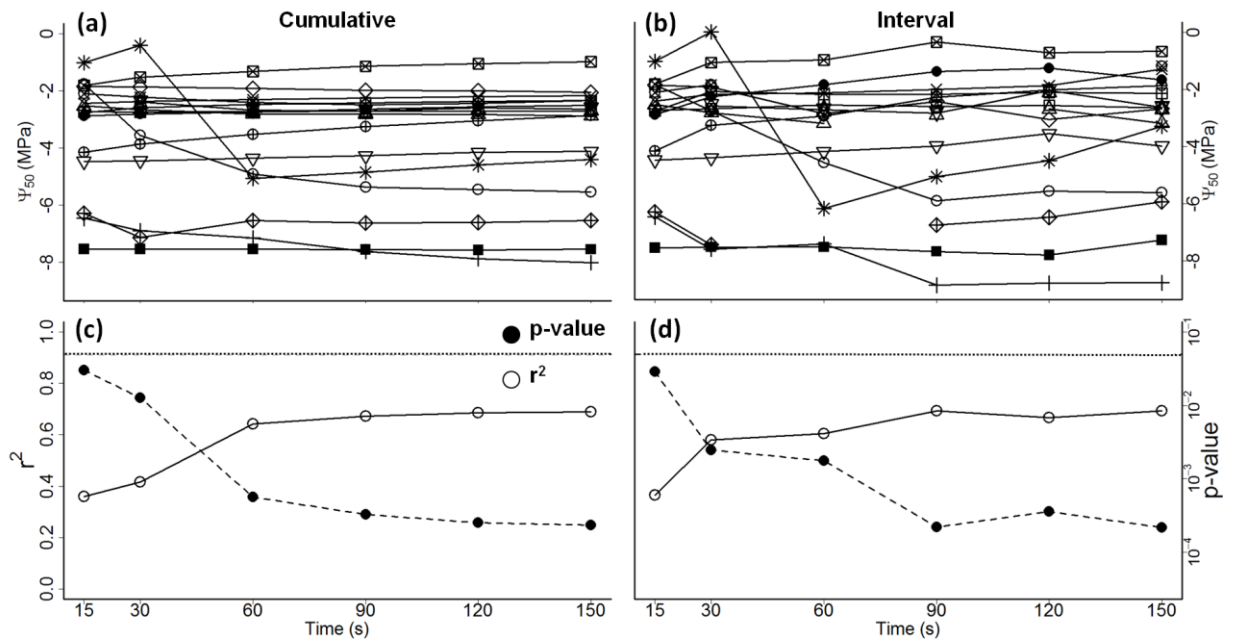
Fig. S4 Hypothetic air flow pathway in branches that were well-hydrated (a); dehydrated (b) and dehydrated with segmentation in the air flow network, with some embolized vessels not connected to the basal cut (c). Grey colours represent water whereas white ones represent air inside the vessels. Arrows represent the hypothetical air pathway during an air discharge measurement. The left side of the branch is continuous and linked to leaves (not represented). The branch length values are the usual sample size used in hydraulic measurements with bench dehydration, and the sample lengths used here are the pneumatic measurements and the effective sample length (in which the initial air discharge is not taken into account) that the pneumatic method is measuring. The pneumatic method is supposed to measure closed vessels, and thus the effective sample is smaller than the total sample length by a value that lies between the maximum and minimum vessel lengths. The pneumatic method could integrate the measurement over a much longer sample than the hydraulic method.

Table S1 Data derived from hydraulic vulnerability curves reported in literature for several species and using different methods.
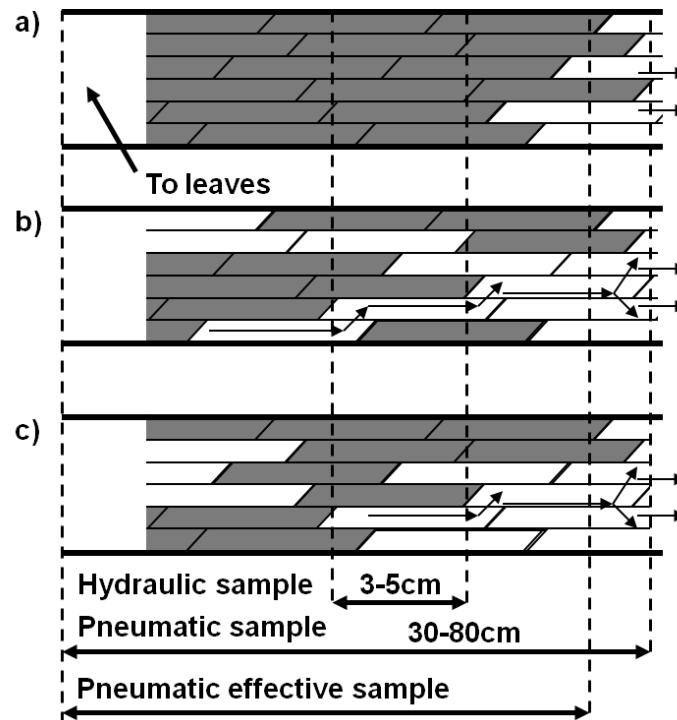
Species	Ψ_{50}	Ψ_{88}	Ψ_{12}	Method	Plant	Used in paper?	Justification	Reference*
Cupressus sempervirens L.	-10.4	-14.0	-5.4	cavitron	Adult	Yes		Choat *et al.* (2012)
Cupressus sempervirens L.	-5.8	-8.0	-5.1	air injection	Sapling	No	Both the more recent works Choat et al. (2012) and Delzon et al. (2010) found very low Ψ_{50} value for *C. sempervirens*. During measurements, *C. sempervirens* was turgid and looking really well at a xylem water potential of -5.0 MPa.	Froux *et al.* (2005)
Cupressus sempervirens L.	-4.4	-5.4	-3.5	air injection	Sapling	No		Froux *et al.* (2002)
Cupressus sempervirens L.	-4.8	-5.3	-4.3	air injection	Sapling	No		
Cupressus sempervirens L.	-10.4	-14.0	-6.8	cavitron	Adult	Yes		Delzon *et al.* (2010)
Hymenaea courbaril L.	-2.6	-3.7	-1.6	air injection	Adult	Yes		Brodribb *et al.* (2003)
Hymenaea courbaril L.	-3.0	-4.0	-2.0	air injection	Adult	Yes		
Olea europaea L. *Chemlali*	-7.1	NA	-3.7	bench dehydration	Adult	No	Authors used a particular variety	Ennajeh *et al.* (2008)
Olea europaea L. *Meski*	-7.5	NA	-2.7	bench dehydration	Adult	No		
Olea europaea L.	-1.9	-3.9	-0.6	centrifuge 27 cm	Adult	No	Authors suggest data obtained with single spin centrifuge or bench dehydration	Hacke *et al.* (2015)
Olea europaea L.	-2.2	-3.9	-1.0	centrifuge 14 cm	Adult	No		
Olea europaea L.	-3.0	-6.2	-1.0	standard centrifuge	Adult	No		
Olea europaea L.	-3.3	NA	-0.2	centrifuge single spin	Adult	Yes		
Olea europaea L.	-3.3	NA	-0.2	bench dehydration	Adult	Yes		
Olea europaea L.	-5.0	-6.1	NA	bench dehydration	Adult	Yes		
Olea europaea L.	-3.7	NA	-0.5	air injection	Adult	No	Authors suggest using data obtained with HRCT or bench dehydration	Torres-Ruiz *et al.* (2014)
Olea europaea L.	-0.9	-2.9	-0.1	static centrifuge 150 mm	Adult	No		
Olea europaea L.	-2.8	NA	-0.4	static 280 mm	Adult	No		
Olea europaea L.	-0.9	-2.0	-0.2	flow centrifuge 150 mm	adult	No		
Olea europaea L.	-1.5	-4.1	-0.2	flow centrifuge 280 mm	Adult	No		
Olea europaea L.	-1.5	-2.9	-0.6	cavitron	Adult	No		
Olea europaea L.	-4.4	-5.2	NA	HRCT	Adult	Yes		
Olea europaea L. *Dwarf*	-2.4	NA	-0.3	air injection	Adult	No	Authors used a particular variety	Trifilò *et al.* (2007)

Olea europaea L. *Minerva*	-3.6	NA	-1.7	air injection	Adult	No		
Populus nigra L.	-3.1	-4.4	-1.0	air injection	Sapling	Yes		Froux *et al.* (2002)
Populus nigra L.	-2.8	-4.0	-1.0	air injection	Sapling	Yes		
Populus nigra L.	-3	NA	NA	cavitron	Adult	Yes		Cochard *et al.* (2005)
Populus nigra L.	-0.9	-1.7	-0.5	air injection	Sapling	No	Presents a negative Ψ_{50} safety margin of -0.8 MPa.	Lambs *et al.* (2006)
Populus nigra L.	-2.0	-2.3	NA	cavitron	Adult	Yes	Mean of the maximum and minimum values found for the 33 genotypes from one population; P88 calculated from the mean of maximum and minimum slope	Guet *et al.* (2015)
Thuja plicata Donn ex D.Don	-5.3	NA	NA	NA	Adult	Yes		Choat *el al.* (2012)
Thuja plicata Donn ex D.Don	-4.6	-6.1	-3.0	air injection	Adult (small diameter branch)	Yes		Mcculloh *et al.* (2014)
Thuja plicata Donn ex D.Don	-5.9	-7.4	-3.1	air injection	Adult (large diameter branch)	Yes		
Thuja plicata Donn ex D.Don	-4.2	-5.7	-2.7	cavitron	Adult	Yes		Delzon *et al.* (2010)

* the references used were cited in the main document

References of table S1

Brodribb TJ, Holbrook NM, Edwards EJ, Gutierrez MV. 2003. Relations between stomatal closure, leaf turgor and xylem vulnerability in eight tropical dry forest trees. Plant, Cell & Environment 26: 443–450.

Choat B, Jansen S, Brodribb TJ, Cochard H, Delzon S, Bhaskar R, Bucci SJ, Feild TS, Gleason SM, Hacke UG, et al. 2012. Global convergence in the vulnerability of forests to drought. Nature 491: 752–755.

Cochard H, Damour G, Bodet C, Tharwat I, Poirier M, Améglio T. 2005. Evaluation of a new centrifuge technique for rapid generation of xylem vulnerability curves. Physiologia Plantarum 124: 410–418.

Delzon S, Douthe C, Sala A, Cochard H. 2010. Mechanism of water-stress induced cavitation in conifers: bordered pit structure and function support the hypothesis of seal capillary-seeding: Cavitation in conifers. Plant, Cell & Environment 33: 2101–2111.

Ennajeh M, Tounekti T, Vadel AM, Khemira H, Cochard H. 2008. Water relations and drought-induced embolism in olive (Olea *europaea*) varieties 'Meski' and 'Chemlali' during severe drought. Tree Physiology 28: 971–976.

Froux F, Huc R, Ducrey M, Dreyer E. 2002. Xylem hydraulic efficiency versus vulnerability in seedlings of four contrasting Mediterranean tree species (*Cedrus atlantica, Cupressus sempervirens, Pinus halepensis* and *Pinus nigra*). Annals of Forest Science 59: 409–418.

Froux F, Ducrey M, Dreyer E, Huc R. 2005. Vulnerability to embolism differs in roots and shoots and among three Mediterranean conifers: consequences for stomatal regulation of water loss? Trees 19: 137–144.

Guet J, Fichot R, Lédée C, Laurans F, Cochard H, Delzon S, Bastien C, Brignolas F. 2015. Stem xylem resistance to cavitation is related to xylem structure but not to growth and water-use efficiency at the within-population level in Populus nigra L. Journal of Experimental Botany 66: 4643–4652.

Hacke UG, Venturas MD, MacKinnon ED, Jacobsen AL, Sperry JS, Pratt RB. 2014. The standard centrifuge method accurately measures vulnerability curves of long-vesselled olive stems. New Phytologist 205: 116-127.

Lambs L, Loubiat M, Girel J, Tissier J, Peltier J-P, et al. 2006. Survival and acclimation of *Populus nigra* to drier conditions after damming of an alpine river, southeast France. Annals of Forest Science 63: 377–385.

Mcculloh KA, Johnson DM, Meinzer FC, Woodruff DR. 2014. The dynamic pipeline: hydraulic capacitance and xylem hydraulic safety in four tall conifer species: The dynamic pipeline. Plant, Cell & Environment 37: 1171–1183.

Pratt RB, Black RA. 2006. Do invasive trees have a hydraulic advantage over native trees? Biological Invasions 8: 1331-1341.

Torres-Ruiz JM, Cochard H, Mayr S, Beikircher B, Diaz-Espejo A, Rodriguez-Dominguez CM, Badel E, Fernández JE. 2014. Vulnerability to cavitation in *Olea europaea* current-year shoots: further evidence of an open-vessel artefact associated with centrifuge and air-injection techniques. Physiologia Plantarum 152: 465–474.

Trifilò P, Lo Gullo MA, Nardini A, Pernice F, Salleo S. 2007. Rootstock effects on xylem conduit dimensions and vulnerability to cavitation of *Olea europaea* L. Trees 21: 549–556.

Methods S1 Plant material, cavitation vulnerability curves, data analyses and apparatus leakage

1- Plant material

Saplings - Branches were collected from the saplings of five vessel-bearing species [*Eucalyptus camaldulensis* Dehn. (Myrtaceae), *Hymenaea courbaril* L. (Fabaceae), *Olea europaea* L. (Oleaceae), *Populus nigra* L. (Salicaceae) and *Schinus terebinthifolius* Raddi (Anacardiaceae)] and three tracheid-bearing species [(*Cupressus sempervirens* L. (Cupressaceae), *Drimys brasiliensis* Miers (Winteraceae) and *Thuja plicata* Donn ex D.Don (Cupressaceae)]. All individuals were 0.5–2 m in height, and they were all grown and maintained under greenhouse conditions. The plants were watered daily to prevent water deficits, and they were subjected to natural fluctuations in solar radiation and air temperatures. To prevent embolism formation before sampling, the plants were bagged overnight to ensure high water potential (they were always higher than -0.1 MPa at the sampling time). We used all the aerial parts of the saplings as samples, except for *P. nigra* and *T. plicata* from which lateral branches were collected (see Table 1 for detailed descriptions). We decided to use all the aerial parts to ensure that most of the vessels were entire, i.e., with end walls. The samples were collected at sunrise and immediately transported to the laboratory.

Trees – We also took measurements from the branch samples of the following eight tree species: two lowland Amazon species [(*Miconia lepidota* Schrank & Mart. ex DC. (Melastomataceae) and *Erisma uncinatum* Warm. (Vochysiaceae)], three cloud forest species from the Atlantic Forest (*Myrceugenia acutata* (D. Legrand.) O. Berg (Myrtaceae), *Calyptranthes brasiliensis* Spreng. (Myrtaceae) and *Weinmannia organensis* Gardner (Cunoniaceae). In addition, branches were also collected from a common semi-deciduous tropical forest species called *Schinus terebinthifolius* Raddi (Anacardiaceae) to test the effect of different sample sizes, as described below, and from crop species *Coffea arabica* L. (Rubiaceae) and *Citrus sinensis* (L.) Osbeck (Rutaceae). All the individuals were mature trees (2 to 30 m height), and they were sampled during the wet season at sunrise to ensure high water potential. We collected branches that were 3-4 times larger than the samples that were used in the experiments and then cut them to their sample sizes in the air. The maximum vessel lengths were measured by air injection method (Zimmermann & Jeje, 1981) in at least three branches from all the sapling and tree species. Because the saplings did not have

sufficient branches for all the measurements, the maximum vessel lengths were measured in other individuals that were grown under similar environmental conditions as the ones used for the AD evaluation.

2- Cavitation vulnerability curves

We measured the Ψ_{50h} and Ψ_{88h} for ten species with a hydraulic apparatus to measure the hydraulic conductance, and we used the bench dehydration method to induce embolism (Sperry *et al.*, 1988). A VC curve was then built, and the Ψ_{50h} and Ψ_{88h} values were estimated. The hydraulic apparatus was an ultra-low flow meter as previously described by Pereira & Mazzafera (2012) and modified to the inlet positive pressure. The water that was used in the apparatus was deionized, degassed and filtered, and a maximum pressure head of 6 kPa was used to avoid dislodging bubbles. The initial conductance (K_{ini}) was measured, the samples were flushed for 2 min (Martin-StPaul *et al.*, 2014), and then the maximum conductance (K_{max}) was measured. The PLC was calculated as a percentage of K_{ini} in relation to the K_{max} and equation 6 was fit to the data. Three-centimetre stem segments were used, and on average, three to five segments were taken from the same branch. These segments were connected to the apparatus that kept the stopcocks open to prevent any pressure that could remove the embolism from the segment. All samples were re-cut several times under water to avoid embolism artefacts (Venturas *et al.*, 2015). In addition, we obtained the mean of Ψ_{50h} and Ψ_{88h} for *C. sempervirens*, *H. courbaril*, *Olea europeae*, *P. nigra* and *T. plicata* from the literature. For reference, we used papers that presented the Ψ_{50h} and Ψ_{88h} values for those species, and unreliable values were not considered (Tables 1 and S1). Ψ_{50h} and Ψ_{88h} were used to calculate the slope parameter S_h. We also considered possible variations of Ψ_{50h} and Ψ_{88h} using a statistical procedure (see below).

3- Data analyses

Evaluation of air origin - Prediction (i) was tested with a Mann-Whitney U test, because the AD from IG was not normally distributed, with a null hypothesis of IG<0. Prediction (ii) was tested with a one-sided paired t-test between the AD in the NG situation (Fig. 4c) minus the AD in the IG situation (Fig. 4b) with the a null hypothesis of (NG-IG)>0. The absolute AD values were used to remove the effect of the different air flow directions in both situations, i.e., the AD would be negative in the IG situation (Fig. 4b), according to equation 4.

Relation between air flow and embolism –To determine whether the AD was related to the Ψ_x and to embolisms, curves AD in comparison with Ψ_x were created and compared with curves relating the hydraulic conductance to Ψ_x (VCs). We first verified whether non-standardized AD data are correlated to Ψ_x with Spearman's correlation test for each species. To test the hypothesis that air flow is related to embolisms, we tested the prediction that Ψ_{50p}, Ψ_{88p} and S_p are good predictors of Ψ_{50h}, Ψ_{88h} and S_h, respectively. We used simple linear regressions to test these correlations. To consider possible variations in the VC of species with hydraulic measurements that were not taken on the same material as the pneumatic ones (i.e., literature data), we used the randomization approach (see below).

Measuring time – We evaluated the effects of the measurement time on the relation between the AD and embolisms by calculating the Ψ_{50p} for cumulative and interval AD measurements of 15, 30, 60, 90, 120 and 150 s. The resulting Ψ_{50p} estimates were compared with the Ψ_{50h} using simple linear regressions. *C. sinensis* was not used in this analysis because we only measured the AD at 15 and 150 s.

Allometric relations and vessel length - To determine whether the size of the sample affected the AD, the maximum AD of each sample was correlated to the length, basal diameter, volume, stem surface area and maximum vessel length of the branch with Spearman's correlation.

Sample size and vessel length – We used the Mann-Whitney U test to test the hypothesis that different sample lengths produce different AD values. To test the hypothesis that the sample length affects PAD curve fittings, we tested whether the Ψ_{50p} and Ψ_{88p} parameters of curves from short (Ψ_{50ps} and Ψ_{88ps}) and long (Ψ_{50ps} and Ψ_{88pl}) branches were different by using a randomization procedure (see below)).

Randomization approach to incorporate uncertainty in literature data - To consider possible variability in VC of species in which hydraulic data was not taken from the same material as the pneumatic data (i.e., literature data), we used a randomization approach. We considered that literature data on Ψ_{50h} and Ψ_{88h} had an uncertainty of ±1 MPa and subtracted or added a random value from +1 to -1 MPa (in 0.01 intervals) to each literature value. We repeated this procedure 1,000 times for each time we tested the regression between hydraulic and pneumatic parameters using the data with added uncertainty. The p-values and r^2 of the regressions were stored and we analyzed the percentage of times the p-values were significant.

Randomization approach to test for effect of sample length on S. terebinthifolius vulnerability curve - To test the hypothesis that sample length affects PAD curve fitting, we tested if Ψ_{50p} and Ψ_{88p} estimated from short (Ψ_{50ps} and Ψ_{88ps}) and long (Ψ_{50ps} and Ψ_{88pl}) branches were different using the randomization procedure previously described. We randomly assigned the (Ψ_x, PAD) pair values either to the short or long branch samples, a procedure repeated 1,000 times. Then, we estimated Ψ_{50p} and Ψ_{88p} for short and long samples using the randomized value. We calculated the absolute difference between the parameters of each curves [abs(Ψ_{50ps}-Ψ_{50pl}) and abs(Ψ_{88ps}-Ψ_{88pl})] and used it as the test statistics. This procedure was repeated 1,000 times. We then calculated the probability that the test statistics was equal or higher than the absolute difference of the real curve parameters. If $p<0.05$, it is unlikely that the difference between Ψ_{50ps} and Ψ_{50pl} was obtained by chance and we accept the hypothesis that different sample lengths produce different PAD curves.

4- Apparatus leakage and air discharge

We evaluated the leakage of the apparatus by measuring the air discharge of the apparatus using a branch segment that was cut, sealed with glue and then connected to the apparatus. All air discharged would then be due to leakage from the atmosphere to the vacuum reservoir. We did this procedure 12 times and, as leakage was very small, we measured leakage for a period of several hours. For each measurement, we calculated the leakage conductance (K_{leak}), which is the conductance for air to leak from the atmosphere to inside the vacuum reservoir as:

$$K_{leak} = L/(t*(P_{atm}-P_r)) \quad\quad\quad\quad (1)$$

where L is the air flow leaked from atmosphere to inside the vacuum reservoir (calculated in the same way as the volume of air discharged), t is the duration of the leakage test, P_{atm} is the atmospheric pressure and P_r is the mean vacuum reservoir pressure during the test. We assumed K_{leak} was constant during the test.

We estimated the leakage L of each sample using the mean K_{leak} of the 12 measurements ($3.4*10^{-11}$ mol s^{-1} kPa^{-1}) as:

$$L = K_{leak}*t*(P_{atm}-P_{r'}) \quad\quad\quad\quad (2)$$

where $P_{r'}$ is the vacuum reservoir pressure during the air discharge measurement.

We calculated L for each time interval that air discharge was sampled and subtracted it from the total air discharge at that interval to get the actual air discharged of each sample (AD):

$$AD = AD_t - L \tag{3}$$

where AD_t is the total air discharged at that interval t.

CAPÍTULO 3

Pereira, L, Domingues-Junior, AP, Jansen, S, Choat, B, Mazzafera, P. **Is embolism resistance in plant xylem associated with quantity and characteristics of lignin?**
Submitted to Tree Physiology.

Abstract

Lignin appearance during plant evolution had a marked importance in the colonization of the terrestrial environment. Among several evolutionary advantages, lignin deposition in the xylem conferred to plants mechanical support to stand and enabled efficient water transport because of its hydrophobicity. One of the possible functions resulting from the greater lignin content in the xylem is embolism resistance mainly induced by drought. Here we suggest, based on data available for lignin content and Ψ_{50} (the water potential when 50% of conductivity in the xylem is lost), a boundary relationship between embolism resistance and lignin content across various groups of seed plants. Species with low lignin content seem to be more vulnerable to embolism, whereas species with higher content show wide variability in embolism resistance. Lignin content may play some indirect role in the embolism resistance, since higher total lignin content is related to thicker cell walls. We also discuss several possible functions of lignin with different composition between gymnosperms and angiosperms and the performance of transgenic plants with modified lignin content and composition regarding vulnerability to embolism.

Key words: embolism, plant cell wall, plant hydraulics, water transport, xylem, pit membrane

Introduction

Lignin is the most abundant compound in plants after cellulose (Donaldson 2001). The presence of lignin coincides with the colonization of the terrestrial environment by plants (Popper et al. 2011), possibly due to its fundamental roles in mechanical support and water transport (Niklas 1992, Pittermann 2010). In addition, its biosynthetic pathway may have played a role in the protection from UV radiation and microbial infection in a unicellular ancestor (Popper et al. 2011). Lignin is present in all derived land plants, except for bryophytes, but it was also found in *Calliarthron cheilosporioides,* a red algae that shared a common ancestor over 1 billion years ago (Martone et al. 2009), as well as lignin-like compounds in primitive green algae (Delwiche et al. 1989).

Extracted lignin is hydrophobic (Laschimke 1989) with low resistance to tensile stress, but in the cell wall is found coating cellulose microfibrils conferring rigidity when compared to hydrated microfibrils of the xylem tissue (Niklas 1992). Lignin is also a bulking agent, increasing the compression resistance (Niklas 1992). During transpiration the negative pressure generated in the xylem can reach values lower than -10 MPa in some cases and this high tension imposes a minimum thickness of the conduit wall to resist to stress induced by drought (Hacke et al. 2001). In this scenario, lignin could play a role in providing rigidity to the conduit cell wall, avoiding implosion. The strength of the conduit is proportional to the ratio between the wall thickness and lumen diameter, which shows the necessary investment needed to avoid implosion, particularly in vessels, which are close to the limit of implosion (Hacke et al. 2001, Sperry et al. 2006). In tracheids, however, the ratio of the wall thickness to lumen diameter is higher than in vessels, which might be an evolutionary consequence of the combined function of water transport and mechanical support (Hacke et al. 2001, Sperry et al. 2006, Bouche et al. 2014).

As xylem sap is typically transported under tension, gas emboli can form in conduits, which interrupts the water transport to shoots. Depending on the number of conduits embolised and the degree to which water transport is impaired, this can have lethal consequences (Choat et al. 2012). Several hypotheses have been developed to explain embolism formation and some are related to the characteristics of the conduit walls, such as 1) the "air-seeding" mechanism, which means that air-water menisci will penetrate through the cellulose microfibrils of bordered pit membranes between two neighbouring vessels (Zimmermann 1983, Sperry and Tyree 1988, Brodersen et al. 2013, Lens et al. 2013, Schenk et al. 2015); 2) heterogeneous nucleation from surface bubbles that are associated with a hydrophobic conduit wall (Tyree et al. 1994, Zwieniecki and Secchi 2015); or 3) surfactant

coated nanobubbles in xylem sap may become unstable under certain conditions of gas concentration, temperature, or pressure (Jansen and Schenk 2015, Schenk et al. 2015). It is known that lignin confers to conduits relative hydrophobicity and rigidity and it may thus also be arguable that it has a role in embolism resistance. There is evidence that thicker conduit walls have confer greater resistance to xylem embolism (Hacke et al. 2001, Cochard et al. 2008).

A strong line of evidence that lignin influences embolism resistance comes from work with mutants and transgenic plants. It has been shown that mutants deficient in lignin can have increased embolism vulnerability (Coleman et al. 2008, Voelker et al. 2011, Awad et al. 2012). Several mutants for reduced lignin content with a dwarf phenotype showed a deficient capacity to transport water (Anterola and Lewis 2002, Bonawitz et al. 2014). On the other hand, several plants with a modified lignin composition do not have reduced growth or other apparent functional problems (Bonawitz et al. 2014, Wilkerson et al. 2014, Wagner et al. 2015). It was recently shown in *Arabidopsis thaliana* that the dwarf phenotype seems to be caused by the disruption of the transcription factor Mediator, which rescues the stunted growth of a lignin-deficient mutant (Bonawitz et al. 2014).

Here we discuss the role of lignin content, distribution and composition to embolism resistance, analyze the different patterns of lignin investment in gymnosperms and angiosperms, and propose that this polymer plays an important functional role in plant hydraulics.

Lignin distribution and lignin types

Lignin in the cell wall forms chemical bonds with hemicellulose, which in turn adheres to cellulose microfibrills (Donaldson 2001), but the concentration of these components varies widely. According to Donaldson (2001), the middle lamella and primary wall are composed of more than 50% of lignin in both angiosperms and gymnosperms, whereas about 20% is found in the secondary wall, depending on the cell type. However, the secondary wall contains most of the total lignin content by virtue of its greater volume. A hypothetical model of the contribution of the middle lamella region (including the primary wall) and secondary wall to the total lignin content is shown in figure 1 A. It was considered that the middle lamella region represents 10%, and the secondary wall 90% of the cell wall volume (Fergus et al. 1969). In this situation the contribution of the middle lamella to the total lignin content is about 17%. Alternatively, the amount of lignin content in the middle lamella and secondary wall could be 85% and 15%, respectively (Fergus et al. 1969, Donaldson

2001). An implication of this different concentration of lignin is that the proportion of the middle lamella to total lignin content might be greater when the wood contains a lower amount of total lignin.

Fig. 1 – Hypothetical contribution of cell wall region and cell type to wood lignin content. A) Contribution of middle lamella (grey lines) and secondary wall (black lines) considering that the volume of the cell wall occupied by the middle lamella is 10% and by the secondary wall is 90%. It was also considered that lignin content in the middle lamella is 50% and in the secondary wall is 20%. An alternative situation is represented by dashed lines, with 85% of lignin in the middle lamella and 15% in the secondary wall. B) Contribution of vessels (grey lines) and fibers (black lines), in angiosperms, considering that the cell wall of vessels represents up to 30% and fibers up to 70% of the total cell wall in wood. The middle lamella and the secondary wall correspond to 10% and 90% of the cell wall volume and they are composed by 50% and 20% of lignin, respectively. The continuous, dashed and dotted lines represent the total lignin content, lignin present in the secondary walls, and middle lamellas, respectively.
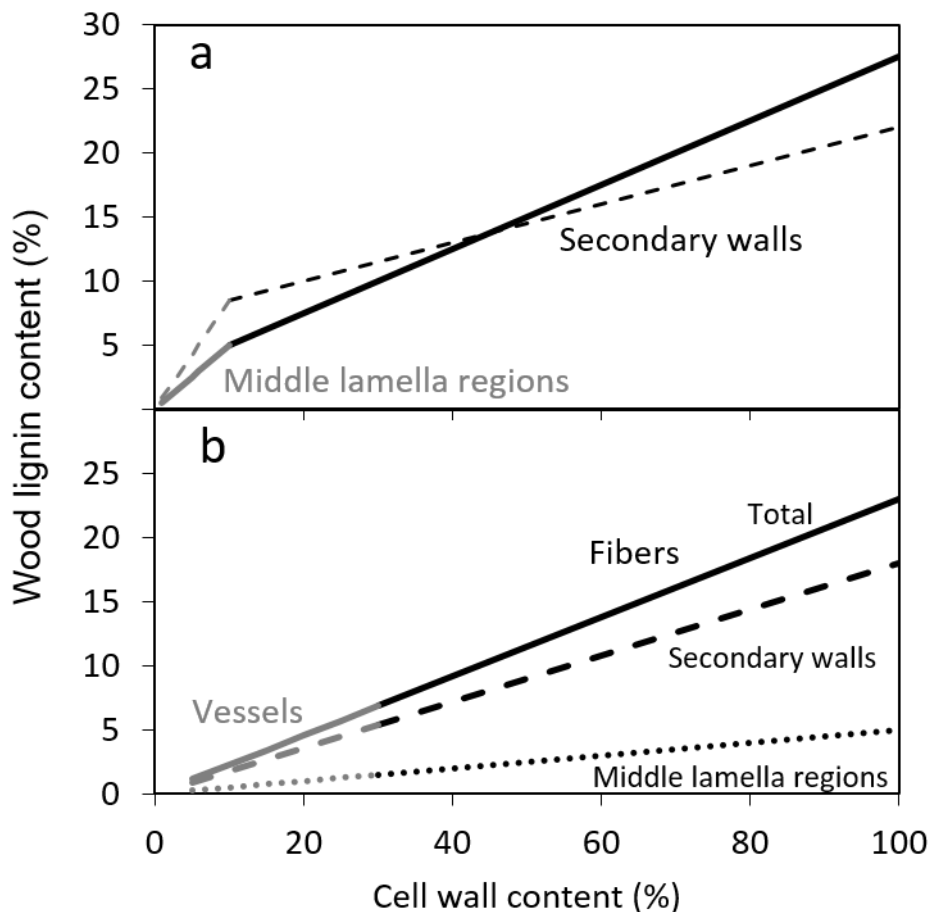
Lignin is also heterogeneously distributed in wood because of the different cell types in angiosperm xylem. Secondary walls of vessels and fibers are composed of roughly 20% of lignin and ray cells about 44%, when the latter are lignified (Donaldson 2001). Wood is composed by up to 70% of fiber walls and up to 15% of vessel walls (Jacobsen et al. 2007,

Pratt et al. 2007, Zanne et al. 2010, Martínez-Cabrera et al. 2011, Ziemińska et al. 2013, Morris et al. 2016). If we consider only cell walls of these two tissues, since the cell wall of the parenchyma may not be lignified in some cases, 70% and 30% of the lignin in wood should be present in fibers and vessels, respectively (Fig. 1 B).

The biosynthesis of lignin in plants is carefully controlled spatially and temporally (Ralph et al. 2004). Lignin composition varies in gymnosperms and angiosperms. Three canonical precursors produced in the phenylpropanoids pathway are involved in the biosynthesis of lignin - *p*-coumaryl, coniferyl and sinapyl alcohols, which after incorporation into lignin are referred to as *p*-hydroxyphenyl (H), guaiacyl (G) and syringyl (S) units, respectively (Bonawitz and Chapple 2010, Cesarino et al. 2012). Their proportion varies among cell types, taxa and between tissues in the same plant, but other phenylpropanoids may also be part of the lignin and are incorporated at varying levels (Raes et al. 2003). The incorporation of H and G units into lignin starts during early phases of the primary cell wall formation, but are only incorporated in the actual cell wall after initiation of the secondary wall (Grabber 2005). The lignin of angiosperms is mainly composed of G and S units and has traces of H units, while the lignin of gymnosperms is mostly composed of G units with small amounts of H units (Vanholme et al. 2010).

Although it is generally accepted that angiosperm vessels are composed mostly of G units and minor part of S units, variation exists among species (Takabe et al. 1992, Wu et al. 1992, Watanabe and Fukazawa 1993).

Embolism resistance

The interruption of the water column by the occurrence of embolism in tracheids and vessels is a major problem associated with long distance water transport (Tyree and Sperry 1989). This is particularly important when water stress is developed as greater negatives pressures may develop in the conduits, increasing the probability of embolism formation.

Understanding embolism resistance is a key factor to understand plant response to drought and adaptive strategies in both dry and wet environments (Choat et al. 2012, Lens et al. 2013, Anderegg et al. 2016). A key feature that contributes to embolism resistance seems to be pit membrane thickness (Choat et al. 2008, Jansen et al. 2009, Li et al. 2016). Reduced diameter of the pores confers a greater capillary resistance to air entry (Zimmermann 1983, Choat et al. 2008). Although most papers suggest that lignin does not occur in the pit membrane (Bamber 1961, Bauch and Berndt 1973, Sano and Fukuzawa 1994, Fineran 1997, Donaldson 2001), there are some papers suggesting that cellulose microfibrils in the pit

membrane are impregnated with lignin ((Bauch and Berndt 1973; Fromm *et al.* 2003; Boyce *et al.* 2004; Schmitz *et al.* 2008; Herbette *et al.* 2015). Since bordered pit development is controlled by microtubules before secondary wall formation and lignin impregnation of the wall, it seems unlikely from a developmental point of view that lignin is deposited in developing pit membranes and perforation sites of vessel elements (Czaninski 1973, O'Brien 1981, Chaffey et al. 1997). Lignification of the pit membrane, however usually takes place during deposition of polyphenolic compounds in heartwood or during wound response (Bauch and Berndt 1973, Fromm et al. 2003, Boyce et al. 2004, Schmitz et al. 2008, Herbette et al. 2015).

Other anatomical traits that have been indirectly related to embolism resistance include conduit wall thickness (Hacke et al. 2001, Cochard et al. 2008) and fibre wall thickness (Jacobsen et al. 2005, Cochard et al. 2007). Thickening of secondary wall of the conduits is directly related to implosion resistance (Hacke et al. 2001, Jacobsen et al. 2005, Sperry et al. 2006). Due to a correlation between vessel wall thickness and pit membrane thickness (Jansen et al. 2009, Li et al. 2016), wall thickness is indirectly correlated with air-seeding via pit membranes. It is possible that reinforced walls of conduits, neighbouring fibers, or parenchyma cells surrounding vessels, avoid micro-cracks through which air could be sucked (Jacobsen et al. 2005, Kedrov 2013). Another possibility is that the conduit lumen is reduced when walls are thick, with consequent low conductivity, and it is known that species resistant to embolism show low conductivity (Gleason et al. 2015).

Embolism resistance and lignin content

Considering the fundamental importance of lignin for the development of an efficient water transport system in plants due to mechanical strength and impermeability of the conduits, we may assume that a greater lignin deposition increases embolism resistance. Although lignin deficient mutants show greater embolism vulnerability (Coleman et al. 2008, Voelker et al. 2011, Awad et al. 2012), the functional effects of natural variation in lignin content are not known.

Total wood lignin content of plants is available for many species (Fengel and Grosser 1975, Pettersen 1984), and allows direct and/or simple comparison with hydraulic traits. Embolism can be estimated by vulnerability curves (VC), which is the relationship between water potential and loss of conductivity; a useful parameter to compare different species is the water potential in which occurs 50% loss of conductivity (Ψ_{50}, MPa). Thus, to assess a possible relationship between lignin content and embolism resistance, we used the Ψ_{50} values

from the Xylem Functional Traits (XFT) database (Choat et al. 2012) and the lignin content of angiosperms and conifers (Fengel and Grosser 1975, Pettersen 1984). We did not consider Ψ_{50} values from "r" shaped vulnerability curves, which may be prone to artifacts associated with open vessels (Cochard et al. 2013). Data of lignin (% of total dry mass) extracted according to the Klason method was published by Pettersen (1984) - 695 entries of 589 species - and Fengel & Grosser (1975) - 153 species. We used average values for species for which various values of lignin content were available. Based on this database it was possible to compare Ψ_{50} and lignin content for 91 species (54 angiosperms and 37 gymnosperms). Some species had more than one Ψ_{50} value in the XFT database, but no mean Ψ_{50} values were used, resulting in a total of 294 specimens. The data were analysed by quantile regression (Cade and Noon 2003) using the 95th quantile (corresponding to the 5th quantile for a negative parameter such as Ψ_{50}). We found in this analysis a significant boundary relationship between lignin content and Ψ_{50} (Fig. 2 [τ=0.05; t= -3.57; P<0.001]). When analysed separately, gymnosperms also showed a boundary relationship (τ=0.05; t= -2.97; P=0.003), but with a greater slope, while there was no significant relation for the angiosperms (τ=0.05; t= 0.33; P=0.74). Considering all species, low lignin content was strongly related with high Ψ_{50}, i.e., with low resistance to embolism. Species with greater lignin content exhibited greater variation in Ψ_{50}, i.e. they were not constrained to high or low embolism resistance.

We also tested our dataset to verify that it was not biased by methodology used to estimate the Ψ_{50}, i.e., if more vulnerable species were obtained using a centrifuge or air pressurization method, which may overestimate the Ψ_{50} (Cochard et al. 2013). However, we did not find any trend associated with the vulnerability curve method that was applied (Fig. 3; N=259).

The greater lignin content may be evolutionary related to other functions in addition to water transport, such as UV tolerance and protection to pests and pathogens. It is important also to consider that Ψ_{50} values used in our analysis were based on terminal branches, whereas the lignin content was extracted from mature wood, which could be more embolism resistant than terminal branches (Pivovaroff et al. 2014). This may partially explain the occurrence of the species with high lignin content but low resistance to embolism in our analyses.

The boundary relationship considering all species may indicate a biophysical limitation by the embolism formation related to lignin content in the cell wall, i.e., plants have to have a certain amount of lignin to avoid embolism regardless of species groups (angiosperms or gymnosperms) considering that there were few species beyond this limit. The

investment of 1% of lignin in wood may result in a reduction of Ψ_{50} by approximately -0.3 MPa (Fig. 2).

Fig. 2 – Lignin content and Ψ_{50} to gymnosperms (black points) and angiosperms (grey points). The solid line represents the boundary relationship considering all species and dashed line only to gymnosperms. There was no significant relationship considering only angiosperms. As Ψ_{50} is a negative variable, the lines represent 5% quantile regression (p< 0.05), which is equivalent to the 95% quantile for a positive response variable.
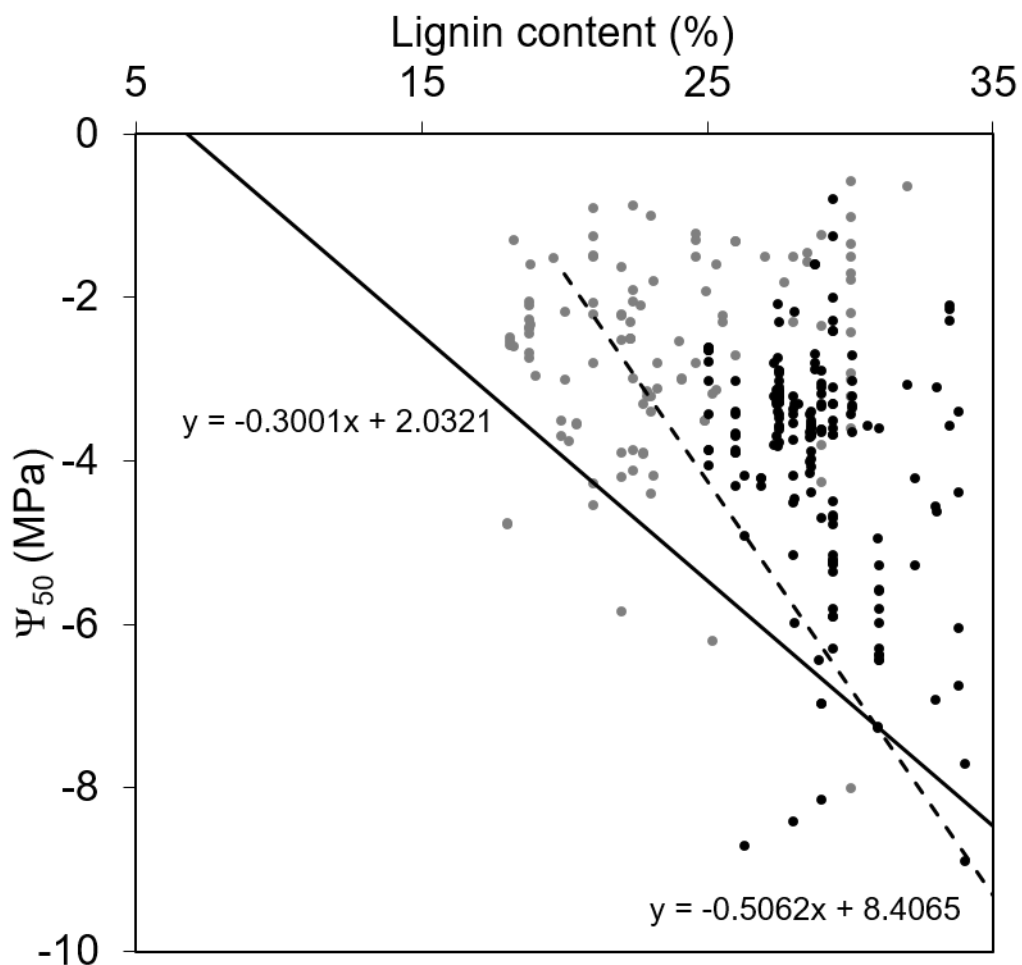
As Fig. 2 shows that the boundary relation between lignin content and Ψ_{50} was significant considering different plant groups, it is possible to speculate about herbs and grasses with low amounts of lignified tissue. The lignin content in these plants, which might be positioned in the upper left corner of Fig. 2, ranges from 1 to 15 % dry mass (Knudsen 1997, Fukushima and Hatfield 2004), and is lower than in angiosperm wood. Although few studies have been carried out on embolism resistance in herbaceous plants, it seems that they

are generally vulnerable at a water potential below -2 MPa (Tyree et al. 1986, Cochard 2002, Sperry et al. 2003). Thus, considering the boundary relationship found here (Fig. 2), when the lignin content is lower than 15%, herbaceous plants may not resist to embolism at a water potential more negative than -2 MPa. However, this hypothesis must be tested in future studies.

The different results found for gymnosperms and angiosperms might be attributed to a different wood anatomy and chemical composition. According to the data from Pettersen (1984), wood of the gymnosperms has higher lignin content than angiosperms (Gymnosperms: 29.7 ±2.8 g g^{-1}, n=100; Angiosperms: 26.1 ±5.1 g g^{-1}, N=489). Additionally, the unicellular conduits of gymnosperms (tracheids) are shorter and narrower than the multicellular vessels of angiosperms, and have the dual function of water transport and mechanical support, while vessels are specialized for conduction (Sperry et al. 2006). Such differences in terms of complexity might indicate a different strategy against embolism resistance.

Wood density also has been considered an indicator of embolism resistance (Hacke et al. 2001). To assess any significant relationship between wood density and lignin content, we used data from Pettersen (1984) for lignin content and the Global Wood Density database (Zanne et al. 2009, Chave et al. 2009). We compared data from 279 species (222 angiosperms and 57 gymnosperms) and could not find a significant relationship, analyzing the data altogether or separately (data not shown).

There are few reports examining the possible relationship between lignin content and wood density. Results obtained with transgenic hybrid aspen (*Populus* spp.) with strongly reduced sucrose synthase activity (Gerber et al. 2014) or over-expressing the transcription factor *WALLDOF* (Gerhardt et al. 2011) showed a reduction and an increase of wood density, respectively, but lignin and cellulose, the main components of the cell wall, followed the same trend, i.e., reduction and increase. The decreased wood density in the plants with reduced sucrose synthase activity was explained by a more loosely arranged structure of fibre cell wall components. Thus, wood density seems to be related to changes of all components of the cell wall and not only to lignin.

Fig. 3 a) Lignin content and Ψ_{50} of gymnosperms and angiosperms species and methods used to estimate the Ψ_{50} [AD= air-injection double end; CA= cavitron; CE= centrifuge; DH= dehydration; see review of the methods in Cochard *et al.* (2013)]. b) Mean and standard deviation of Ψ_{50} estimated by different methods. Grey and black bars represent angiosperms and gymnosperms, respectively.
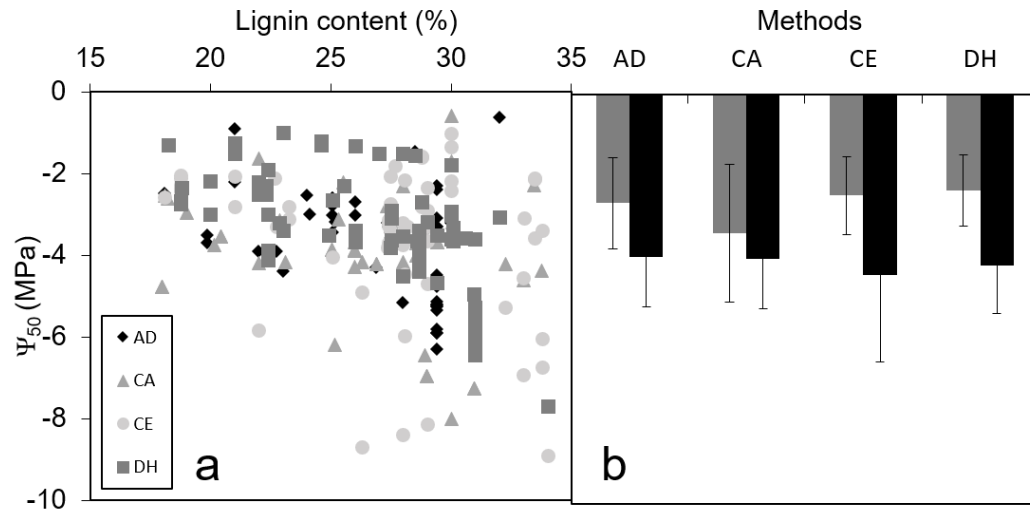
Our comparisons showed that only species with greater lignin content are more resistant to embolism, as indicated by the Ψ_{50} values. Although the number of species included in this analysis gives credibility to the relationship found, the data were taken from different sources (i.e., different plant specimens, populations, locations, subspecies, etc.). Thus, a true proof of this relationship might be obtained by increasing the number of data in a similar analysis or carrying out studies under controlled conditions with a significant and representative number of gymnosperms and angiosperms. Additionally, treatments inducing variation in the lignin content in a single species, including transgenic plants, might be another alternative.

Possible functions of different lignin

Is it possible to explain functional aspects of vessels, fibers and tracheids by the properties of their lignin composition? Although there are various detailed descriptions of lignin distribution among species (Terashima et al. 1986, 1988, Terashima and Fukushima 1988, Fukushima and Terashima 1990, 1991, Takabe et al. 1992, Wu et al. 1992, Watanabe and Fukazawa 1993, Saito et al. 2012) and even less about the natural environmental influences on lignin composition (e.g. Stackpole *et al.*, 2011), some characteristics of lignin polymers might define the tissue functionality.

In theory 16 linkages are possibly formed among H, G and S units (Baucher et al. 1998). In gymnosperms, there is a greater deposition of H units in the middle lamella and cell corners, with G units mainly deposited in the secondary wall (Fukushima and Terashima 1991). The greater lignification rate of the primary wall should increase the mechanical adhesion between adjacent cells (Niklas 1992). The higher investment in H units can be attributed to its strength, since compression wood shows large amounts of H units, both in the middle lamella and secondary wall (Fukushima and Terashima 1991), thus indicating that lignin formed by H units is more condensed (Baucher et al. 1998). This trait may increase the mechanical strength and supports the stem (Du and Yamamoto 2007). The distribution of H units can give us clues about the mechanical function of H units in gymnosperms. In addition, there is a decrease of hydraulic conductivity in compression wood (Boyce et al. 2004, Pittermann et al. 2006). On the other hand, since H units are deposited in the middle lamella of vessels (Fukushima and Terashima 1990), but in a small amount (Baucher et al. 1998), they may not play a relevant role in angiosperm plant hydraulic traits.

Lignin rich in G units is more cross-linked because more biphenyl and other carbon-carbon bonds are formed, resulting in a more rigid and hydrophobic polymer than lignin rich in S units (Koehler and Telewski 2006, Bonawitz and Chapple 2010). The relatively higher abundance of G units in conduits, and possibly more hydrophobic parts of the wall, can be a paradox since it could reduce the capillary pressure and increase the nucleation of embolism (Tyree et al. 1994). However, McCully *et al.* (2014) recently suggested that bordered pits are generally hydrophilic, composed by a hydrophilic pit chamber and hydrophobic pit border, which may become hydrophyilic or hydrophobic if the conduit is water or gas filled, respectively. Herbette *et al.* (2015) suggested the occurrence of non-condensed lignin (composed by S or G + S units) in pit membranes of hybrid poplar (*Populus tremula* X *alba*). Those polymers have free phenolic hydroxyl groups that increase the wettability and are more linear and less cross-linked by the presence of a methoxyl group than lignin rich in G units. This may result in a strong but flexible polymer (Koehler and Telewski 2006, Bonawitz and Chapple 2010). This characteristic can maximize the mechanical support function of the fibers as well as give flexibility to vessels, avoiding cell wall fractures when xylem sap is under tension (Jacobsen et al. 2005, Koehler and Telewski 2006).

Different proportions of G and S units in angiosperm vessels, as well as the total lignin content in relation to cellulose microfibrils, could modulate the hydrophobicity and affect the hydraulic properties. We showed in Fig. 4 a hypothetical model in which we estimate the potential effects of different forms of lignin in the pit membrane with respect to the air-

seeding pressure for a given pore size. Although the presence of lignin in the pit membrane may reduce the wettability and increase the vulnerability to embolism, a controlled adjustment of the deposition of lignin monomers could improve the mechanical strength of the pit membrane, while maintaining a high wettability and thus high embolism resistance. The presence of lignin might increase the young´s modulus, resulting in greater flexural rigidity of the pit membrane, which may avoid air seeding that occurs by enlargement of the pores or formation of micro cracks in the pit membrane (Tixier et al. 2014). It is also important to consider that the wettability may be affected by the type of lignin in relation to other wall components, which could be relevant for the occurrence of surface nanobubbles on hydrophobic parts of inner conduit walls.

There is evidence for the presence of lignin in the torus-margo in gymnosperms (Sachs 1963, Boyce et al. 2004) and torus-bearing pit membrane of some angiosperms species (Coleman et al. 2004, Dute et al. 2010). However, in these species the embolism resistance depends on air-seeding via the torus that seals off the pit aperture and is different from angiosperms, which relates to capillary forces in a porous membrane.

There is evidence from molecular studies that deposition of lignin in different xylem cell types is highly controlled (Ralph et al. 2004). Thus, the distinct cell functions of fibers and vessels in angiosperms, and their different S/G ratios are good indicators of a functional control. Stackpole et al. (2011) found a strongly positive relationship between latitude and S/G ratio in populations of *Eucalyptus globulus.* Although they did not identify the cause of the variation, they suggested an adaptive response to abiotic and/or biotic factors. However, as mentioned above, the tendency of an increase in S units can indicate a more elastic polymer, which influences the hydraulic as well as mechanical properties.

Fig. 5 Hypothetical model for embolism resistance considering the presence of lignin in the pit membrane. A) Pit membrane rich in syringyl, forming a lower contact angle of an air-water meniscus (α) and B) rich in guaiacyl, with wider α. C) A bubble point pressure difference (P) needed for air-seeding was calculated according to the Young-Laplace law (P = k4T.cos α /D), where k is the shape correction factor, T is the surface tension of water, α is the contact angle between the pit membrane and water and D is the pore diameter. Grey lines indicate α = 0° and black lines α = 90°. Continuous lines represent k = 1 and dashed lines k = 0.3 [see explanation to k in Schenk *et al.* (2015)]. Supposed contact angles (α) are indicated for polymers rich in S (tending to 0°) and G (tending to 90°).
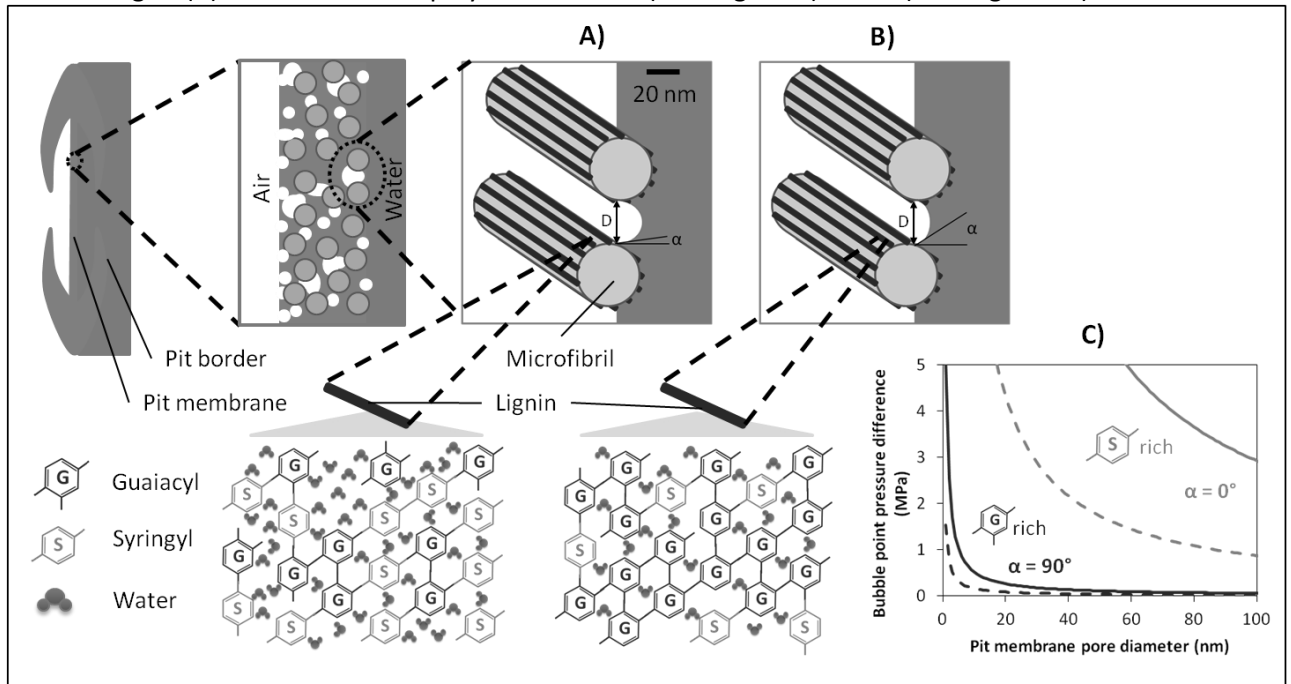
Transgenic plants

Transgenic plants with altered lignin content and/or deposition show impaired vascular system development, such as collapsed vessels, which is directly related to stunted growth shown by these plants (Anterola and Lewis 2002). There is a clear increase in vulnerability to embolism in poplar trees with reduced lignin content (Coleman et al. 2008, Voelker et al. 2011, Awad et al. 2012). These results were obtained in plants with lignin reduced by 2% to more than 50%. Although lignin has been generally related with embolism resistance, it is possible that the increase of vulnerability in transgenic plants is due to reduction of G units, affecting the vessels directly (Coleman et al. 2008). But, in others cases the lower content of S units, possibly in the fibers, also resulted in an increase of embolism vulnerability (Voelker et al. 2011). Curiously, several transgenic plants did not show altered water transport and mechanical properties, although they had increased vulnerability to embolism (Awad et al. 2012).

Transgenic plants of *A. thaliana* have been produced, containing very high amounts of H units, from 10-15-fold more than normal cell walls (Sundin et al. 2014) to lignin that is

almost exclusively composed of H units (Bonawitz et al. 2014). Under controlled conditions in growth chambers they showed very few to no collapsed vessels and although these were similar to normal cell walls, were thinner than wild plants (Bonawitz et al. 2014). Collapse of xylem conduits is very rare and unlikely to occur in the field, but the few existing observations of gymnosperms show that it was always associated with an extremely weak degree of lignification of the secondary wall and severe dehydration (Barnett 1976, Donaldson 2002). However, higher lignin content in needles from early growth stages of *P. pinaster* than adult trees (Mediavilla et al. 2014) seems to suggest that the difference in thickness to span ratio and not lignin concentration explains higher levels of xylem tracheid deformation in needles from seedlings than mature trees (Bouche et al. 2015).

Despite the success in the production of mutants with modified lignin and without apparent functional problems (Bonawitz et al. 2014, Wilkerson et al. 2014), these plants have to be tested under conditions of drought stress, where it is likely that they will have impaired growth. Although small in number, these plants do show some collapsed vessels even under controlled conditions (Bonawitz et al. 2014).

Perhaps a better understanding of the importance of structural lignin alteration in the embolism process might be obtained using T-DNA insertion mutants of *A. thaliana* available in seed stocks (Arabidopsis Biological Resource Center - https://www.arabidopsis.org/abrc/index.jsp). The inflorescence stems of these plants could be an interesting model to study embolism resistance (Tixier et al. 2013).

Conclusions

The boundary relationship between lignin content and Ψ_{50} seems to suggest that plants require a minimum amount of lignin to tolerate embolism, indicating an investment in secondary wall and an indirect relation with pit characteristics. Different proportions of lignin monomers (S/G ratio) may modulate the hydrophobicity (McCully et al. 2014, Herbette et al. 2015), and therefore the hydraulic properties of the conduits. It is possible that differential deposition of lignin occurs in response to the environment (Stackpole et al. 2011), as well as the known variation in earlywood, latewood, compression and tension wood. Further studies need to be focused on the functional consequences for growth and embolism resistance in transgenic plants with modified lignin.

References

Anderegg WRL, Klein T, Bartlett M, Sack L, Pellegrini A, Jansen S (2016) Hydraulic traits explain across-species patterns of drought-induced tree mortality. PNAS

Anterola AM, Lewis NG (2002) Trends in lignin modification: a comprehensive analysis of the effects of genetic manipulations/mutations on lignification and vascular integrity. Phytochemistry 61:221–294.

Awad H, Herbette S, Brunel N, Tixier A, Pilate G, Cochard H, Badel E (2012) No trade-off between hydraulic and mechanical properties in several transgenic poplars modified for lignins metabolism. Environ Exp Bot 77:185–195.

Bamber RK (1961) Staining reaction of the pit membrane of wood cells. Nature 4786:409–410.

Barnett JR (1976) Rings of collapsed cells in *Pinus radiata* stemwood from lysimeter-grown trees subjected to drought. New Zeal J For Sci 6:461–465.

Bauch J, Berndt H (1973) Variability of the chemical composition of pit membranes in bordered pits of gymnosperms. Wood Sci Technol 7:6–19.

Baucher M, Monties B, Montagu M Van, Boerjan W (1998) Biosynthesis and Genetic Engineering of Lignin. CRC Crit Rev Plant Sci 17:125–197.

Bonawitz ND, Chapple C (2010) The genetics of lignin biosynthesis: connecting genotype to phenotype. Annu Rev Genet 44:337–363.

Bonawitz ND, Kim JI, Tobimatsu Y, Ciesielski PN, Anderson NA, Ximenes E, Maeda J, Ralph J, Donohoe BS, Ladisch M, Chapple C (2014) Disruption of Mediator rescues the stunted growth of a lignin-deficient Arabidopsis mutant. Nature 509:376–380.

Bouche PS, Delzon S, Choat B, Badel E, Brodribb TJ, Burlett R, Cochard H, Charra-Vaskou K, Lavigne B, Li S, Mayr S, Morris H, Torres Ruiz JM, Zufferey V, Jansen S (2015) Are needles of Pinus pinaster more vulnerable to xylem embolism than branches? New insights from X-ray computed tomography. Plant Cell Environ

Bouche PS, Larter M, Domec JC, Burlett R, Gasson P, Jansen S, Delzon S (2014) A broad survey of hydraulic and mechanical safety in the xylem of conifers. J Exp Bot 65:4419–4431.

Boyce CK, Zwieniecki M a, Cody GD, Jacobsen C, Wirick S, Knoll AH, Holbrook NM (2004) Evolution of xylem lignification and hydrogel transport regulation. Proc Natl Acad Sci U S A 101:17555–17558.

Brodersen CR, McElrone AJ, Choat B, Lee EF, Shackel KA, Matthews MA (2013) In vivo visualizations of drought-induced embolism spread in *Vitis vinifera*. Plant Physiol 161:1820–1829.

Cade BS, Noon BR (2003) A gentle introduction to quantile regression for ecologists. Front Ecol Environ 1:412–420.

Cesarino I, Araújo P, Domingues Júnior AP, Mazzafera P (2012) An overview of lignin metabolism and its effect on biomass recalcitrance. Brazilian J Bot 35:303–311.

Chaffey NJ, Barnett JR, Barlow PW (1997) Cortical microtubule involvement in bordered pit formation in secondary xylem vessel elements of Aesculus hippocastanum L. (Hippocastanaceae): a correlative study using electron microscopy and indirect immunofluorescence microscopy. Protoplasma 197:64–75.

Chave J, Coomes D, Jansen S, Lewis SL, Swenson NG, Zanne AE (2009) Towards a

worldwide wood economics spectrum. Ecol Lett 12:351–366.

Choat B, Cobb AR, Jansen S (2008) Structure and function of bordered pits: new discoveries and impacts on whole-plant hydraulic function. New Phytol 177:608–625.

Choat B, Jansen S, Brodribb TJ, Cochard H, Delzon S, Bhaskar R, Bucci SJ, Feild TS, Gleason SM, Hacke UG, Jacobsen AL, Lens F, Maherali H, Martínez-Vilalta J, Mayr S, Maurizio Mencuccini, Patrick J. Mitchell, Andrea Nardini JP, Pratt RB, Sperry JS, Westoby M, Wright IJ, Zanne AE (2012) Global convergence in the vulnerability of forests to drought. Nature 491:752–755.

Cochard H (2002) Xylem embolism and drought-induced stomatal closure in maize. Planta 215:466–471.

Cochard H, Badel E, Herbette S, Delzon S, Choat B, Jansen S (2013) Methods for measuring plant vulnerability to cavitation: a critical review. J Exp Bot 64:4779–4791.

Cochard H, Barigah ST, Kleinhentz M, Eshel A (2008) Is xylem cavitation resistance a relevant criterion for screening drought resistance among Prunus species? J Plant Physiol 165:976–982.

Cochard H, Casella E, Mencuccini M (2007) Xylem vulnerability to cavitation varies among poplar and willow clones and correlates with yield. Tree Physiol 27:1761–1767.

Coleman CM, Prather BL, Valente MJ, Dute RR, Miller ME (2004) Torus lignification in hardwoods. IAWA J 25:435–447.

Coleman HD, Samuels AL, Guy RD, Mansfield SD (2008) Perturbed lignification impacts tree growth in hybrid poplar - A function of sink strength, vascular integrity, and photosynthetic assimilation. Plant Physiol 148:1229–1237.

Czaninski Y (1973) Observations sur une nouvelle couche pariétale dans les cellules associées aux vaisseaux du Robinier et du Sycomore. Protoplasma 219:211–219.

Delwiche CF, Graham LE, Thomson N (1989) Lignin-like compounds and Sporopollenin in Coleochaete, and algal model for land plant ancestry. Science (80-) 245:399–401.

Donaldson LA (2001) Lignification and lignin topochemistry - an ultrastructural view. Phytochemistry 57:859–873.

Donaldson LA (2002) Abnormal lignin distribution in wood from severely drought stressed *Pinus radiata* trees. IAWA J 23:161–178.

Du S, Yamamoto F (2007) An overview of the biology of reaction wood formation. J Integr Plant Biol 49:131–143.

Dute R, Patel J, Jansen S (2010) Torus-Bearing Pit Membranes in Cercocarpus. IAWA J 31:53–66.

Fengel D, Grosser D (1975) Chemische Zusammensetzung yon Nadel- und Laubhözern. HOLZ als Roh- und Werkst 33 33:32–34.

Fergus BJ, Procter AR, Scott JAN, Goring DAI (1969) The distribution of lignin in sprucewood as determined by ultraviolet microscopy. Wood Sci Technol 3:117–138.

Fineran BA (1997) Cyto- and histochemical demonstration of lignins in plant cell walls: an evaluation of the chlorine water/ethanolamine-silver nitrate method of Coppick and Fowler. Protoplasma 198:186–201.

Fromm J, Rockel B, Lautner S, Windeisen E, Wanner G (2003) Lignin distribution in wood cell walls determined by TEM and backscattered SEM techniques. J Struct Biol 143:77–84.

Fukushima RS, Hatfield RD (2004) Comparison of the acetyl bromide spectrophotometric method with other analytical lignin methods for determining lignin concentration in forage samples. J Agric Food Chem 52:3713–3720.

Fukushima K, Terashima N (1990) Heterogeneity in formation of lignin. XIII. Formation of p-hydroxyphenyl lignin in various hardwoods visualized by microautoradiography. J Wood Chem Technol 10:413–433.

Fukushima K, Terashima N (1991) Heterogeneity in formation of lignin. Part XV: formation and structure of lignin in compression wood of *Pinus thunbergii* studied by microautoradiography. Wood Sci Technol 25:371–381.

Gerber L, Zhang B, Roach M, Rende U, Gorzsás A, Kumar M, Burgert I, Niittylä T, Sundberg B (2014) Deficient sucrose synthase activity in developing wood does not specifically affect cellulose biosynthesis, but causes an overall decrease in cell wall polymers. New Phytol 203:1220–1230.

Gerhardt IR, Filippi SB, Okura V, Coutinho J, Rizzato AP, Gui K, Vessali N, Pontes JH, Cordeiro T, Silva SM, Garcia AF, Arruda P (2011) Overexpression of walldof transcription factor increases secondary wall deposition and alters carbon partitioning in poplar. BMC Proc 5:O35.

Gleason SM, Westoby M, Jansen S, Choat B, Hacke UG, Pratt RB, Bhaskar R, Brodribb TJ, Bucci SJ, Cao K, Cochard H, Delzon S, Domec J, Fan Z, Feild TS, Jacobsen AL, Johnson DM, Lens F, Maherali H, Martínez-Vilalta J, Mayr S, McCulloh KA, Mencuccini M, Mitchell PJ, Morris H, Nardini A, Pittermann J, Plavcová L, Schreiber SG, Sperry JS, Wright IJ, Zanne AE (2015) Weak tradeoff between xylem safety and xylem-specific hydraulic efficiency across the world's woody plant species. New Phytol

Grabber JH (2005) How do lignin composition, structure, and cross-linking affect degradability? A review of cell wall model studies. Crop Sci 45:820–831.

Hacke UG, Sperry JS, Pockman WT, Davis SD, McCulloh KA (2001) Trends in wood density and structure are linked to prevention of xylem implosion by negative pressure. Oecologia 126:457–461.

Herbette S, Bouchet B, Brunel N, Bonnin E, Cochard H, Guillon F (2015) Immunolabelling of intervessel pits for polysaccharides and lignin helps in understanding their hydraulic properties in Populus tremula × alba. Ann Bot 115:187–199.

Jacobsen AL, Agenbag L, Esler KJ, Pratt RB, Ewers FW, Davis SD (2007) Xylem density, biomechanics and anatomical traits correlate with water stress in 17 evergreen shrub species of the Mediterranean-type climate region of South Africa. J Ecol 95:171–183.

Jacobsen AL, Ewers FW, Pratt RB, Paddock III WA, Davis SD (2005) Do xylem fibers affect vessel cavitation resistance? Plant Physiol 139:546–556.

Jansen S, Choat B, Pletsers A (2009) Morphological variation of intervessel pit membranes and implications to xylem function in angiosperms. Am J Bot 96:409–419.

Jansen S, Schenk HJ (2015) On the ascent of sap in the presence of bubbles. Am J Bot 102:1561–1563.

Kedrov GB (2013) Scalariform tracheids in secondary xylem of woody dicotyledons: distribution, function and evolutionary significance. Wulfenia 20:43–54.

Knudsen KEB (1997) Carbohydrate and lignin contents of plant materials used in animal feeding. Anim Feed Sci Technol 67:319–338.

Koehler L, Telewski FW (2006) Biomechanics and transgenic wood. Am J Bot 93:1433–

1438.

Laschimke R (1989) Investigation of the wetting behaviour of natural lignin - a contribution to the cohesion theory of water transport in plants. Thermochim Acta 151:35–56.

Lens F, Tixier A, Cochard HH, Sperry JS, Jansen S, Herbette S (2013) Embolism resistance as a key mechanism to understand adaptive plant strategies. Curr Opin Plant Biol 16:287–292.

Li S, Lens F, Espino S, Karimi Z, Klepsch M, Schenk HJ, Schmitt M, Schuldt B, Jansen S (2016) Intervessel pit membrane thickness as a key determinant of embolism resistance in angiosperm xylem. IAWA J

Martínez-Cabrera HI, Jochen Schenk H, Cevallos-Ferriz SRS, Jones CS, Martínez-Cabrera HI, Schenk HJ, Cevallos-Ferriz SRS, Jones CS (2011) Integration of vessel traits, wood density, and height in angiosperm shrubs and trees. Am J Bot 98:915–922.

Martone PT, Estevez JM, Lu F, Ruel K, Denny MW, Somerville C, Ralph J (2009) Discovery of Lignin in Seaweed Reveals Convergent Evolution of Cell-Wall Architecture. Curr Biol 19:169–175.

McCully M, Canny M, Baker A, Miller C (2014) Some properties of the walls of metaxylem vessels of maize roots, including tests of the wettability of their lumenal wall surfaces. Ann Bot 113:977–989.

Mediavilla S, Herranz M, Gonzalez-Zurdo P, Escudero A (2014) Ontogenetic transition in leaf traits: a new cost associated with the increase in leaf longevity. J Plant Ecol 7:567–575.

Morris H, Plavcová L, Cvecko P, Fichtler E, Gillingham MAF, Martínez-Cabrera HI, McGlinn DJ, Wheeler E, Zheng J, Ziemińska K, Jansen S (2016) A global analysis of parenchyma tissue fractions in secondary xylem of seed plants. New Phytol 209:1553–1565.

Niklas K (1992) Plant biomechanics: an engineering approach to plant form and function. University of Chicago Press, Chicago.

O'Brien TP (1981) The primary xylem. In: J.R. Barnett (ed) Xylem Cell Development. Castle House, Kent, pp 14–46.

Pettersen RC (1984) The chemical composition of wood. In: Rowell RM (ed) The chemistry of solid wood. American Chemical Society, Washington, DC, pp 57–126.

Pittermann J (2010) The evolution of water transport in plants: an integrated approach. Geobiology 8:112–39.

Pittermann J, Sperry JS, Wheeler JK, Hacke UG, Sikkema EH (2006) Mechanical reinforcement of tracheids compromises the hydraulic efficiency of conifer xylem. Plant, Cell Environ 29:1618–1628.

Pivovaroff AL, Sack L, Santiago LS (2014) Coordination of stem and leaf hydraulic conductance in southern California shrubs: a test of the hydraulic segmentation hypothesis. New Phytol 203:842–850.

Popper Z a, Michel G, Hervé C, Domozych DS, Willats WGT, Tuohy MG, Kloareg B, Stengel DB (2011) Evolution and diversity of plant cell walls: from algae to flowering plants. Annu Rev Plant Biol 62:567–590.

Pratt RB, Jacobsen AL, Ewers FW, Davis SD (2007) Relationships among xylem transport, biomechanics and storage in stems and roots of nine Rhamnaceae species of the

California chaparral. New Phytol 174:787–798.

Raes J, Rohde A, Christensen JH, Van de Peer Y, Boerjan W (2003) Genome-wide characterization of the lignification toolbox in Arabidopsis. Plant Physiol 133:1051–1071.

Ralph J, Lundquist K, Brunow G, Lu F, Kim H, Schatz PF, Marita JM, Hatfield RD, Ralph SA, Christensen JH, Boerjan W (2004) Lignins: Natural polymers from oxidative coupling of 4-hydroxyphenyl- propanoids. Phytochem Rev 3:29–60.

Sachs IB (1963) Torus of the bordered-pit membrane in conifers. Nature 198:906–907.

Saito K, Watanabe Y, Shirakawa M, Matsushita Y, Imai T, Koike T, Sano Y, Funada R, Fukazawa K, Fukushima K (2012) Direct mapping of morphological distribution of syringyl and guaiacyl lignin in the xylem of maple by time-of-flight secondary ion mass spectrometry. Plant J 69:542–552.

Sano Y, Fukuzawa K (1994) Structural variations and secondary changes in pit membranes in *Fraxinus mandshurica* var. japonica. IAWA J 15:283–291.

Schenk HJ, Steppe K, Jansen S (2015) Nanobubbles: a new paradigm for air-seeding in xylem. Trends Plant Sci 20:199–205.

Schmitz N, Koch G, Schmitt U, Beeckman H, Koedam N (2008) Intervessel pit structure and histochemistry of two mangrove species as revealed by cellular UV microspectrophotometry and electron microscopy: intraspecific variation and functional significance. Microsc Microanal 14:387–397.

Sperry JJS, Hacke UG, Pittermann J (2006) Size and function in conifer tracheids and angiosperm vessels. Am J Bot 93:1490–1500.

Sperry JS, Stiller V, Hacke UG (2003) Xylem Hydraulics and the Soil–Plant–Atmosphere Continuum: Opportunities and Unresolved Issues. Agron J 95:1362–1370.

Sperry JS, Tyree MT (1988) Mechanism of water stress-induced xylem embolism. Plant Physiol 88:581–587.

Stackpole DJ, Vaillancourt RE, Alves A, Rodrigues J, Potts BM (2011) Genetic Variation in the Chemical Components of Eucalyptus globulus Wood. G3 Genes, Genomes, Genet 1:151–159.

Sundin L, Vanholme R, Geerinck J, Goeminne G, Höfer R, Kim H, Ralph J, Boerjan W, Hofer R, Kim H, Ralph J, Boerjan W (2014) Mutation of the inducible ARABIDOPSIS THALIANA CYTOCHROME P450 REDUCTASE2 alters lignin composition and improves saccharification. Plant Physiol 166:1956–71.

Takabe K, Miyauchi S, Tsunoda R, Fukazawa K (1992) Distribution of guaiacyl and syringyl lignins in Japanese beech (*Fagus crenata*) variation within an annual ring. IAWA J 13:105–112.

Terashima N, Fukushima K (1988) Heterogeneity in formation of lignin XI: An autoradiographic study of the heterogeneous formation and structure of pine lignin. Wood Sci Technol 22:259–270.

Terashima N, Fukushima K, And ST, Takabe K, Tsuchiya S, Takabe K (1986) Heterogeneity in formation of lignin. VII. An autoradiographic study on the formation of guaiacyl and syringyl lignin in poplar. J Wood Chem Technol 6:495–504.

Terashima N, Fukushima K, Sano Y (1988) Heterogeneity in formation of lignin X. Visualization of lignification process in differentiating xylem of Pine by

microautoradiography. Holzforschung 42:347–350.

Tixier A, Cochard H, Badel E, Dusotoit-Coucaud A, Jansen S, Herbette S (2013) Arabidopsis thaliana as a model species for xylem hydraulics: does size matter? J Exp Bot 68:2295–2305.

Tixier A, Herbette S, Jansen S, Capron M, Tordjeman P, Cochard H, Badel E (2014) Modelling the mechanical behaviour of pit membranes in bordered pits with respect to cavitation resistance in angiosperms. Ann Bot 114:325–334.

Tyree M, Davis S, Cochard H (1994) Biophysical perspectives of xylem evolution: is there a tradeoff of hydraulic efficiency for vulnerability to dysfunction? IAWA J 15:335–360.

Tyree MT, Fiscus EL, Wullschleger SD, Dixon MA (1986) Detection of xylem cavitation in corn under field conditions. Plant Physiol 82:597–599.

Tyree M, Sperry J (1989) Vulnerability of xylem to cavitation and embolism. Annu Rev Plant Biol 40:19–38.

Vanholme R, Demedts B, Morreel K, Ralph J, Boerjan W (2010) Lignin biosynthesis and structure. Plant Physiol 153:895–905.

Voelker SL, Lachenbruch B, Meinzer FC, Kitin P, Strauss SH (2011) Transgenic poplars with reduced lignin show impaired xylem conductivity, growth efficiency and survival. Plant, Cell Environ 34:655–68.

Wagner A, Tobimatsu Y, Phillips L, Flint H, Geddes B, Lu F, Ralph J (2015) Syringyl lignin production in conifers: Proof of concept in a Pine tracheary element system. Proc Natl Acad Sci 112:6218–6223.

Watanabe Y, Fukazawa K (1993) Lignin heterogeneity of the cell walls on the genus Acer. Res Bull Coll Exp For Univ 50:349–389.

Wilkerson CG, Mansfield SD, Lu F, Withers S, Park J-YJ-Y, Karlen SD, Gonzales-Vigil E, Padmakshan D, Unda F, Rencoret J, Ralph J (2014) Monolignol ferulate transferase introduces chemically labile linkages into the lignin backbone. Science (80-) 344:90–93.

Wu J, Fukazawa K, Ohtani J (1992) Distribution of syringyl and guaiacyl lignins in hardwoods in relation to habitat and porosity form in wood. Holzforschung 46:181–185.

Zanne AE, Lopez-Gonzalez G, Coomes DA, Ilic J, Jansen S, Lewis SL, Miller RB, Swenson NG, Wiemann MC, Chave J (2009) Data from: Towards a worldwide wood economics spectrum. Ecol Lett

Zanne AE, Westoby M, Falster DS, Ackerly DD, Loarie SR, Arnold SEJ, Coomes DA (2010) Angiosperm wood structure: Global patterns in vessel anatomy and their relation to wood density and potential conductivity. Am J Bot 97:207–215.

Ziemińska K, Butler DW, Gleason SM, Wright IJ, Westoby M (2013) Fibre wall and lumen fractions drive wood density variation across 24 Australian angiosperms. AoB Plants 5:1–14.

Zimmermann MH (1983) Xylem structure and the ascent of sap. Springer-Verlag.

Zwieniecki MA, Secchi F (2015) Threats to xylem hydraulic function of trees under 'new climate normal' conditions. Plant, Cell Environ 38:1713–1724.

Considerações finais

A deficiência de métodos tem sido o grande desafio para se compreender o transporte de água nas plantas, devido às grandes tensões que ocorrem no xilema bem como das microscópicas ou nanoscópicas estruturas que compõem o sistema vascular. O domínio de técnicas, desenvolvimento de aparatos e métodos, compôs a maior parte dos trabalhos aqui apresentados, porém também permitiu a abertura de interessantes possibilidades de estudo no campo da hidráulica de plantas. Acreditamos que os modelos detalhados no capítulo 3, sobre lignina e embolia, possam ser explorados mais detalhadamente, a partir dos métodos aqui desenvolvidos, em trabalhos futuros.

IB

DECLARAÇÃO

Em observância ao **§5º do Artigo 1º da Informação CCPG-UNICAMP/001/15**, referente a Bioética e Biossegurança, declaro que o conteúdo de minha Tese de Doutorado, intitulada *"Embolismo em plantas: novas técnicas de medição e a relação com a lignificação do xilema"*, desenvolvida no Programa de Pós-Graduação em Biologia Vegetal do Instituto de Biologia da Unicamp, não versa sobre pesquisa envolvendo seres humanos, animais ou temas afetos a Biossegurança.

Assinatura: _____
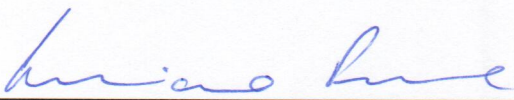Nome do(a) aluno(a): Luciano Pereira

Assinatura: _____
Nome do(a) orientador(a): Paulo Mazzafera

Data: 20/04/2016

Profa. Dra. Rachel Meneguello
Presidente
Comissão Central de Pós-Graduação
Declaração

As cópias de artigos de minha autoria ou de minha co-autoria, já publicados ou submetidos para publicação em revistas científicas ou anais de congressos sujeitos a arbitragem, que constam da minha Dissertação/Tese de Mestrado/Doutorado, intitulada **Embolismo em plantas: novas técnicas de medição e a relação com a lignificação do xilema**, não infringem os dispositivos da Lei n.° 9.610/98, nem o direito autoral de qualquer editora.

Campinas, 20 de abril de 2016

Assinatura : _____

Nome do(a) autor(a): **Luciano Pereira**
RG n.° 32338063-3

Assinatura : _____

Nome do(a) orientador(a): **Paulo Mazzafera**
RG n.° 8336840-1